Spring 4-16-2014

Analysis of Cellular Responses to Heavy Metal-induced Stress in Saccharomyces cerevisiae

Pei-ju Chin

ANALYSIS OF CELLULAR RESPONSES TO HEAVY METAL-INDUCED STRESS IN *Saccharomyces cerevisiae*

by

PEI-JU CHIN

Under the Direction of Dr. John Edgar Houghton

ABSTRACT

Chronic exposure of heavy metals is highly correlated with the epidemic of degenerative disease, nephrotoxicity, cancers and aging, while the acute response of cells to the same heavy metals provides some nuanced insights into how cells are able to handle environmental insults, and perhaps characterize specific triggers of the process, itself. Some heavy metals, such as copper, trigger an immediate accumulation of reactive oxygen species (ROS), which impair vital cellular functions by oxidative stresses; which can lead to the onset of programmed cell death, or apoptosis, which becomes an inevitable fate once the damage is too disseminative to be recovered. Other heavy metals, such as cadmium, appear to trigger similar apoptotic responses in the cell –even before ROS increases to unmanageable levels. In either instance, however, before undergoing apoptosis, there are two cellular defensive mechanisms that are able to eliminate the metal-induced oxidative stresses: 1) the neutralization of anti-oxidants, and 2) the removal of the

harmful substances through a series of self-cleaning mechanisms. We have used *Saccharomyces cerevisiae*, or baker's yeast, as a model organism to demonstrate the response of cells to the presence of heavy metals. In so doing, we highlight pertinent aspects of the metabolic transcriptome response of these unicellular organisms to the presence of these metals, such as changes in expression of genes involved in the pentose phosphate pathway (PPP), which facilitates the reduction of oxidative glutathione, or induction of the genes most commonly associated with autophagy. These findings serve to indicate the protective mechanisms that are triggered upon metal exposures in yeast. Curiously, we also discovered that the autophagic response may be duplicitous, in that while the autophagic process can be cyto-protective it can also enhance the self-destructive mechanisms of the apoptotic response, indeed it is appears to be a requisite part of that response. Whether or not the cells respond to the cellular stress by autophagy or apoptosis appears to be "decided" by whether or not a full-blown autophagic response to cellular stressors (which can be independently induced by the drug, rapamycin) is initiated before the same autophagic process is able to trigger activation of a caspase-induced apoptosis. In addition, in order to monitor the autophagic process more carefully, we have developed a cytometric methodology to assess the autophagy flow, that is less labor-intensive and more dynamic than the traditional Western blot-based method. In so doing we have been able to decipher the factors of cell fate decision with heavy metal-induced oxidative stress in *S. cerevisiae*.

INDEX WORDS: Apoptosis, Autophagy, Metal Toxicity, Yeast

ANALYSIS OF CELLULAR RESPONSES TO HEAVY METAL-INDUCED STRESS IN *Saccharomyces cerevisiae*

by

PEI-JU CHIN

A Dissertation Submitted in Partial Fulfillment of the Requirements for the Degree of

Doctor of Philosophy

in the College of Arts and Sciences

Georgia State University

2014

ANALYSIS OF CELLULAR RESPONSES TO HEAVY METAL-INDUCED STRESS IN *Saccharomyces cerevisiae*

by

PEI-JU CHIN

Committee Chair: John E. Houghton

Committee: Susanna F. Greer

Irene T. Weber

Electronic Version Approved:

Office of Graduate Studies

College of Arts and Sciences

Georgia State University

May 2014

DEDICATION

I delicate this work to my lovely wife, Hsuan Liu, for her endless support, understanding and patience, as well as her meticulous role as a wonderful companion.

To my parents, Mr. Ben-Hwei Chin and Mrs. Chiu-Lan Huang for selflessly letting their only son to leave them for pursuing his dream.

To my older sister, Ms. Shu-Yin Chin, for being a good listener at every depressed night.

To my parents-in-law, Mr. Chih-Yue Liu and Mrs. Hsiu-Chu Yu, for their kindness which warms my heart whenever I am exhausted.

To all of my friends in Atlanta for having fun together whenever I need to relax and recharge myself.

To all of you who are devoting your treasurable life to science.

ACKNOWLEDGEMENTS

I would like to thank my mentor, Dr. John Houghton, for exciting my creativity and showing no negativism about my ideas during our discussions, even though few of them are truly impractical and nonsensical. Dr. John Houghton is patient with me for being a nice audience, catching my faults and suggesting the directions in every conversation.

I would also like to thank my committee members- Dr. Susanna Greer and Dr. Irene Weber for their valuable advises, as well as their patience and perspicacity when I bring several pitfalls which seem to be unsolvable. I also thank Dr. Julia Hilliard for helping my preliminary work, and Dr. Zehava Eichenbaum for enlightening my doctoral career.

I am much grateful for having our Lab alumni and colleagues- Dr. Amrita Nargund, Dr. Anupama Shanmuganathan, Rupa Koduru, Abhishikta Madireddy, Chelsea Hagan and Yi Peng during my Ph.D student career. Thank you for giving me such a sweet memory and friendship.

The experiments couldn't be accomplished without the excellent technical support from Debby Walthall, Ping Jiang, Sonja R. Young and Gemeia Cameron and Dr. Hyuk-Kyu Seoh, who are the invaluable members in Advanced Biotechnology Core (ABC).

This work cannot be accomplished without the funding support from the Molecular Basis of Disease Fellowship at Georgia State University.

TABLE OF CONTENTS

LIST OF TABLES

LIST OF FIGURES

GENERAL INTRODUCTION

Why study heavy metal toxicity?

Heavy metals are widely utilized in society to sustain some of the living standards of the modern world. The mining and production of heavy metals and their derivatives are being increased annually to satisfy downstream electrochemistry industries (1). Unfortunately, inadequate regulation of the recycling programs have led to a number of accidental, heavy metal exposures that have given rise to major environmental issues that ultimately threaten public health (2, 3). The long-term exposure to heavy metals has been shown to be concordant with several cancers, nervous disorders and chronic affections (4-7). One metal in particular, Cadmium, has resulted in one of the most infamous pandemics, Itai-Itai (pain-pain) disease, in Japan back in 1945. The release of cadmium from the zinc mining activity to Jinzu River caused the epidemic for the people who consumed the water (8). The disease is named by the symptom of patients who suffered from the degeneration of bones and joints, and the kidney failure, or nephrotoxicity, is commonly found in the last phase of disease progress. Another heavy metal, copper, is an essential trace element in organisms. Several Cu-containing metalloproteins participate in vital functions such as hemocyanins, plastocyanin or ceruloplasmin, which carries oxygen in the blood of most molluscs, serves as an electron transporter in photosynthesis in plants, or facilitates the iron metabolism in humans. Chronic copper toxicity is rarely found since copper is metabolized by the liver and excreted via bile in healthy individuals. However, patients with Wilson's Disease preserve recessive mutation of ATP7B, which gives rise to a defect in copper transportation from liver to the bloodstream. As a result, the excess copper is accumulated in the liver and causes the oxidative stress in hepatocytes (9). The reactive copper

leads to a disease state by attacking DNA and epigenetic molecules through ROS resulting from Fenton reaction (10). Moreover, the recent report has suggested that copper impairs the homeostasis of β-amyloid peptide (Aβ) in mice brain tissue (11). In aging mice, the presence of copper in brain capillary is associated with the down regulation of lipoprotein receptor-related protein 1 (LPR1), a β-amyloid peptide transporter. As a result, β-amyloid peptide is accumulated in brain tissue, and the progression of AD occurs. The conclusion is further confirmed by showing younger mice exhibit the same symptoms as elder ones by dietary copper exposure through drinking water. Therefore, any understanding of the mechanisms by which cells respond to presence of this heavy metal will hopefully highlight some of the specific dangers of this metal and provide some insight in to strategies for its remediation.

Heavy metal-induced apoptosis results from ROS accumulation

Build up of heavy metals in the cell results in the accumulation of reactive oxygen species (ROS), which causes severe damage to a number of cellular components such as lipids, proteins and genetic materials that are all susceptible to oxidative stresses. Redox-active heavy metals such as copper (Cu), chromium (Cr) and iron (Fe) directly generate hydroxyl radical (OH^-) form the less reactive species such as peroxide (H_2O_2) and superoxide (O_2^-) through Fenton's reaction (12), while redox-inactive heavy metals such as cadmium (Cd), lead (Pb) and mercury (Hg) accumulate ROS by either impairing cellular antioxidant defenses (13, 14) or by replacing the redox-active core in catalytic enzymes (15). As a result of ROS-causing damage, cells undergo the program cell death, so-called apoptosis, in order to restrain the damage which may threaten the health of hosts. Apoptosis, or programmed cell death (PCD), plays an important role in the clearance of unwanted cells. This cellular suicide pathway can be triggered when cells

suffer several irreversible damaging responses, like viral infections (16), or genetic retardations (17). This process is beneficial for multicellular hosts in that it helps to prevent the spread of toxic agents and cellular signals that might trigger an increased dispersion of the cellular response to neigbouring cells, and thus limit the response to a localized area. Apoptosis is an irreversible and tightly-controlled mechanism with a set of proteins participating in this process, and the major part is known to be involved in the redox or energy generation pathways (18, 19). **(Fig. 1)**

Heavy metal-induced response is acute (and lethal to a subset of cells in a population of S. cerevisiae

No matter whether treated by redox-active or inactive metals, the effect of exposure is acute for *S. cerevisiae*. The consequence of heavy metal exposure is dichotomous. Overall, in the survival scenario, the oxidative-defendant pathway is promptly deployed: The transcriptome of pentose phosphate pathway instantly reacts to the heavy metal-induced oxidative stress by inducing the expression of Gnd1p and Zwf1p, two key enzymes reducing NADPH from $NADP^+$ **(Fig. 2A and B).** NADPH is further utilized to regenerate reduced glutathione (GSH) from oxidized glutathione (GSSG), which is the most crucial antioxidant pool apart from the superoxide dismutase (SOD) system in cells (20). After one hour metal exposure, the incremental level of GSH indicates the acute response to against oxidative stress in *S. cerevisiae* **(Fig. 2C)**. In contrast, the death scenario can be initiated within an hour: the alteration of cell death and apoptosis-associated transcriptome, YCA1 for instance, can be observed within 30 minutes after treatment **(Fig. 3)**, and the typical character of apoptosis, such as membrane

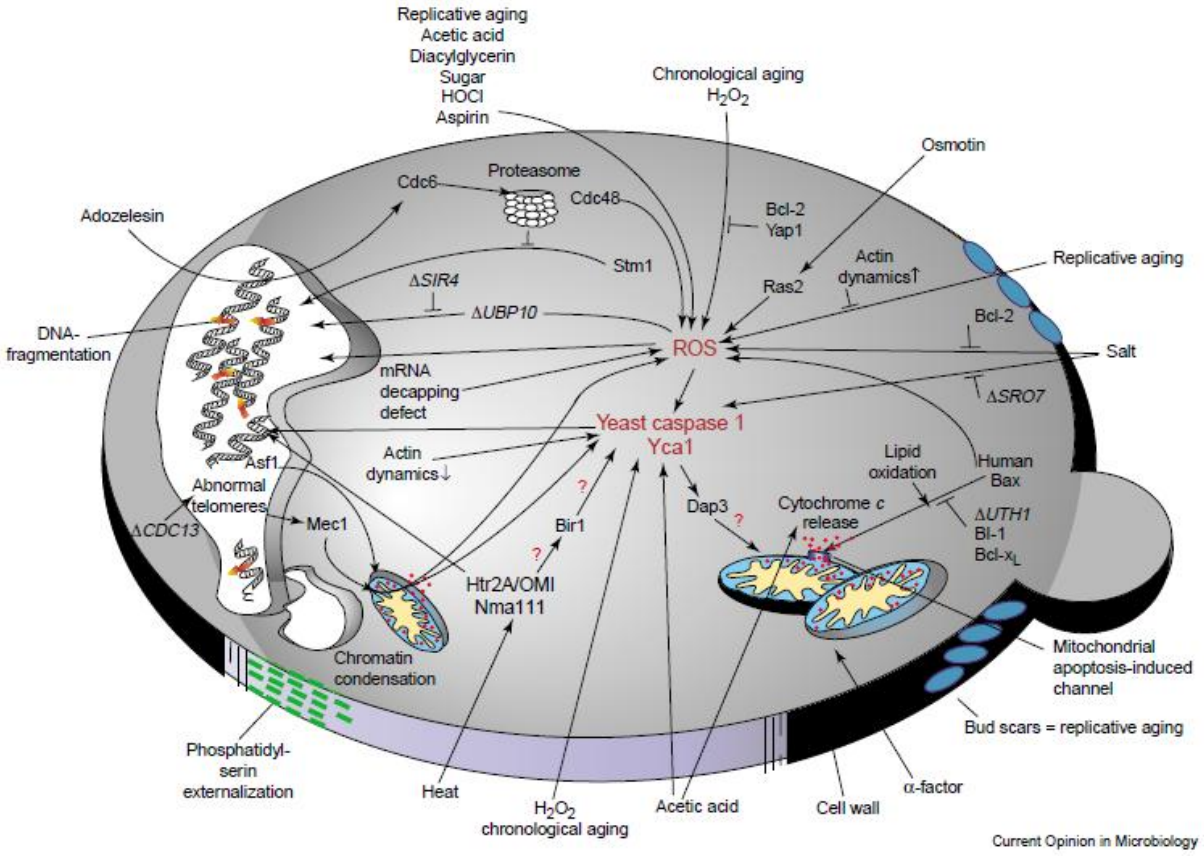

Figure 1: Stress-causing program cell death in yeast

Various internal and external stresses result in the generation of ROS, following by the activation of Yca1, which leads to the increasing permeability of mitochondrial membrane. As a result, cytochrome c is released and apoptosis is triggered (20).

(A)

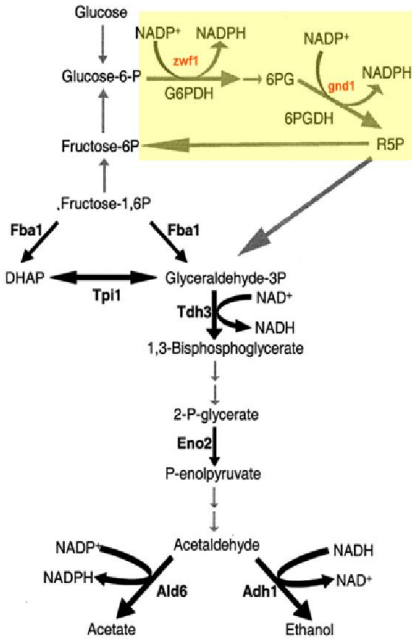
Glucose
NADP+
NADPH
zwf1
Glucose-6-P
G6PDH
6PG
gnd1
NADPH
NADP+
6PGDH
Fructose-6P
R5P
,Fructose-1,6P
Fba1
Fba1
DHAP
Tpi1
Glyceraldehyde-3P
Tdh3
NAD+
NADH
1,3-Bisphosphoglycerate
2-P-glycerate
Eno2
P-enolpyruvate
Acetaldehyde
NADP+
NADPH
Ald6
Acetate
Adh1
NADH
NAD+
Ethanol

(B)

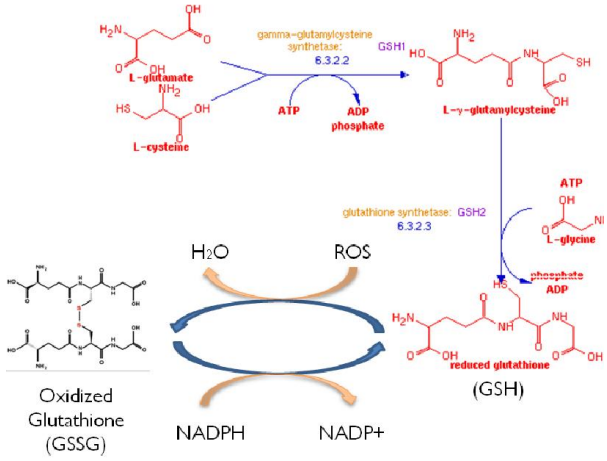
L-glutamate
L-cysteine
gamma-glutamylcysteine synthetase: GSH1
6.3.2.2
ATP
ADP phosphate
L-γ-glutamylcysteine
glutathione synthetase: GSH2
6.3.2.3
ATP
L-glycine
phosphate
ADP
reduced glutathione
(GSH)
H2O
ROS
Oxidized Glutathione (GSSG)
NADPH
NADP+

(C)

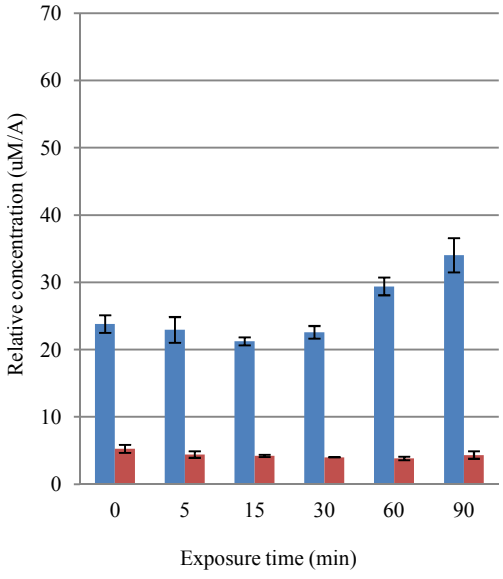
Relative concentration (uM/A)
70
60
50
40
30
20
10
0
0
5
15
30
60
90
Exposure time (min)

Figure 2: Biosynthesis of reduced glutathione (GSH) and its corresponding role in against oxidative stress.

(A) The pentose phosphate pathway (yellow shaded) is one of the major resources of NAPDH generation. Two key enzymes, Zwf1p and Gnd1p, contribute to the reduction of NADPH from NADP. **(B)** NADPH is further utilized to reduce glutathione from its oxidative form. **(C)** Reduced glutathione serves as a major anti-oxidant to against ROS stresses. Reduced glutathione (GSH) was induced upon Cd-induced oxidative stresses. *S. cerevisiae* wild-type 30 μM Cd for various time periods and assayed for cellular concentration of reduced (blue bar) and oxidative (red bar) glutathione.

(A)

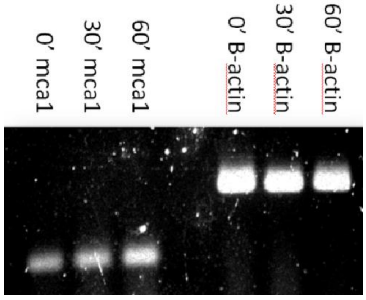

(B)

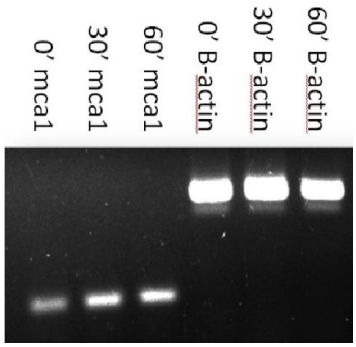

(C)

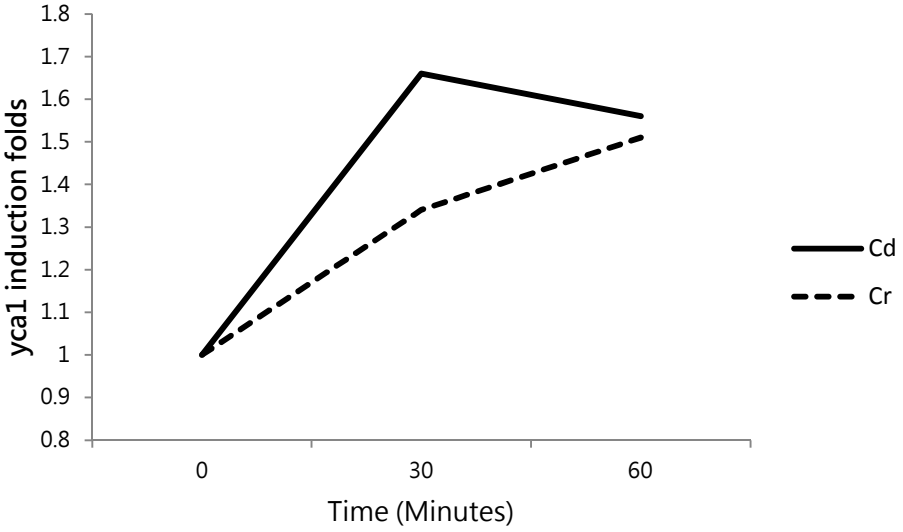

Figure 3: *YCA*1, a yeast caspase, is induced upon cadmium and chromium treatments.

The RT-PCR result of *YCA1* with 0.5mM chromium-exposed **(A)** and 30μM cadmium-exposed **(B)** yeast cell. β-actin was served as the internal control. The quantification results are shown in **Panel C**.

disintegrity, ROS accumulation, DNA fragmentation, mitochondria hyperpolarization and metacaspase activation, can be observed after one hour exposure following by three hours post-incubation (21). Conclusively, yeast cells are endued with a responsive mechanism to adapt themselves to the metal-induced stress. Meanwhile, the alternative script has been setup for the fate that the adaption has failed.

Apoptosis sustains the long-term survival in unicellular yeast

The potential benefits of apoptosis in multicellular organisms are quite diverse, as cells which undergo this form of programmed cellular demise limit the spread of this somewhat absolute cellular response to those cells that have been triggered to respond. The benefits of the response, however, to cells within a population of single-celled organisms, such as *S. cerevisiae,* are less obvious; tempting researchers to speculate on the more abstract implications of "altruism" in the natural world (22). Even so, the beneficial consequences for the survival of a population of yeast when defined group of cells are able to induce an apoptotic response have been suggested. By way of example, while the population is extending, the ammonia gradient is established with highest concentration in the center of colony where the oldest cells clustered. The elder cells undergo apoptosis and are lysed in order to provide the nutrients for the peripheral population, where younger cells stay, to survive (23). The dead-zone is more widespread in colonies with *sok2*Δ mutants, which are not able to generate ammonia gradients. (24). Another example has been shown by *S. cerevisiae yca1*Δ mutant with no caspase-3 like activity to trigger apoptosis. The *yca1*Δ population has longer life-span since it is non-apoptotic. However, the survivors lose the ability to proliferate, and eventually, the entire *yca1*Δ population becomes extinct. Moreover, through the long-term competition assay, the population size of

wild-type overwhelms that of the *yca1*Δ mutant, indicating that in the unicellular yeast preserving apoptotic potential provides an advantage in long-term for their population to revive (25). In an ironic twist, Yca1p has also been revealed as a positive survival factor that is able to regulate proteostasis in the cell by controlling the level of protein aggregation (26). *S. cerevisiae yca1*Δ expresses more stress-related proteins and apparatus such as Hsp70 family chaperone, Hsp12 and Hsp104 protein, as well as the enlargement of autophagic bodies even in the absence of any cellular stressors (27). Besides, *yca1*Δ mutants accumulate more protein aggregates, which indicate that protein "quality assurance" mechanisms within these cells has been compromised (27). Furthermore, apoptosis facilitates the sustainability of cells within a population by eliminating potentially defective organisms, which are unable to successfully mate, as mating negatively influences the onset of apoptosis (28). Apoptosis also serves as a passive tool in competition between strains. About one-quarter of *S. cerevisiae* strains harvest cytotoxin K1, K2 and K28 encoded by double strand RNA viruses (29), while they themselves are resistant to the effects of such toxins (30). During competition, these "killer yeast" release the cytotoxins in to the environment, which trigger apoptotic cascades in their "captives" and lead to their ultimate demise (31). Overall, apoptosis facilitates the maintenance of a population of cells at the expense of individual cells by providing a mechanism to eliminate defective or severely damaged cells from within the population (32), and effectively provides an intrinsic mechanism for "the survival of fittest" in a unicellular world.

Yeast as a model system to study cellular responses upon heavy metal exposure

Saccharomyces cerevisiae, also known as the budding yeast, is chosen as a model organism in our study for the advantages of not only being easy to manipulate whereas the

isogenic mutant library is available, but also the conserved mechanisms with higher eukaryotes, such as humans. This unicellular eukaryote has been well-studied, resulting in the availability of whole genome and proteome annotations (33). Most importantly, with respect to this study, a number of similarities between the apoptotic responses of budding yeast and higher eukaryotes have been reported (18), with the caspase orthologues in yeast being able to contribute to an apoptotic response pathway that is similar to that found in higher organisms (18). As such, the yeast model has been utilized to dissect the role of mitochondrial quality control associated with neurodegenerative disorders caused by apoptosis, where human neurotoxins are expressed in yeast as a host (34). The neurotoxic yeast model has been applied to discover the molecular pathology of Alzheimer Disease (AD) (35, 36), Frontotemporad Lobar Degeneration (FTLD-tau) (37, 38), Parkinson Disease (PD) (39-42), Huntington Disease (HD) (43-45), and Amyotrophic Lateral Sclerosis (ALS) (46-49), which are all caused by the abnormal cell death in neurons. Furthermore, the relative simplicity of yeast apoptosis pathway provides the computational biologists the means to decipher the human apoptosis regulation *in silico* where humanized, yeast computational model successfully recognizes the pro- and anti-apoptotic role of proteins in Bcl-2 family. Our research group has used *S. cerevisiae* as a model organism to elucidate the mechanisms of heavy metal toxicity from different aspects including the targeting of protein oxidation (19) and induction of Yca1p (caspase)-dependent apoptotic pathway (21). In this dissertation, we will expand our frontier to discuss the role of another essential cellular response, autophagy, in the response of Yca1p-dependent apoptosis under heavy metal exposure. Given that the autophagic pathway was first investigated in *S. cerevisiae* (50) and has been well studied since last decades, *S. cerevisiae* will be a decent tool to investigate the molecular mechanisms of apoptotic and autophagic responses, and the interconnection which would be achieved by a series

set of BH3-family proteins in mammalian cells (51), whereas yeast metacaspase, so-known as yeast caspase 1 (Yca1p), which lacks BH3-domain was found in our study to be an intermediate molecule between those two essential cellular events .

Why study autophagy in heavy metal-induced apoptotic yeast cells?

A singular**,** putative yeast caspase 1 (Yca1p), which preserves a number of features associated with mammalian caspase-3, has been found in yeast, and has been shown to initiate various apoptotic responses in yeast cells (52). Subsequent studies in our laboratory, however, have shown that a *yca1*Δ mutant (in which the yeast caspase has been deleted), still appears to exhibit low levels of a caspase-like enzyme activity even though the cells are no longer apoptotic (53). As a result, a number of cysteine proteases were analyzed, with one in particular, Atg4, being analyzed in-depth as to its potential for it being responsible for the additional caspase activity. Atg4 has already been well characterized, and shown to be involved in autophagy, a defense mechanism which helps the cell to overcome a number of environmental stresses (54-57). Even so, these preliminary analyses of Atg4 demonstrated that Yca1 is not cleaved either in an *atg4*Δ mutant background, (53) nor in a similarly constructed *atg6Δ* and *atg8Δ* mutants, which are collectively deficient in the preliminary steps of autophagic initialization. Cleavage of Yca1 is thought to be a critical step in the activation of the caspase. Moreover, like the *yca1*Δ mutant, the autophagic mutants are also non-apoptotic (Nargund A., unpublished data). These findings indicated that Atg4 might play a series of pleiotropic roles, beyond that of its principle role in autophagy, as a cysteine protease cleaving Atg8p in maturation process (58, 59), and may be a critical factor in the activation of Yca1p. It may even, provide the additional, putative caspase-like activity that

has been found in the *yca1*Δ mutant.

Autophagic activity is augmented in metal-induced stress.

Since Atg4 has been shown to be involved in the regulation of apoptosis and is itself an autophagy-associated enzyme, we are interested in the modulation of this enzyme's activity by investigating the autophagic transcriptome upon metal-induced stress. Our preliminary data showed that autophagy-associated genes are remarkably induced in cells upon Cd treatment, as exemplified by the 2-fold and 27-fold increases in transcriptional activities of atg14 and atg7, respectively **(Fig. 4)**. Similarly high autophagic activities and apoptotic population upon the increased exposure to Cd concentration have been reported in MES-13 cells (60), which supported some definitive interaction between the two pathways. Even so, the specific role of autophagy in the apoptotic response remains elusive (61). Thus, the major contribution of this work will be to elucidate the role of autophagy upon metal-induced stress.

Experimental Questions

Previous studies have indicated that the cellular response in yeast to the presence of heavy metals, such as cadmium and copper, are heavily dependent upon a related, central metabolic pathways (62). Firstly, the pentose phosphate pathway (PPP) transcriptome is highly induced upon heavy metal treatments. Given that PPP is one of the major resources for NADPH reduction, which further provides the reducing power for glutathione reduction, we would like to address the importance of the PPP pathway in generating anti-oxidants upon ROS stresses. Secondly, glycolytic enzymes has been shown to be the oxidation targets upon heavy metal-induced ROS stresses (62). Among those enzymes, Tdh3, a human Glyceraldehyde 3-

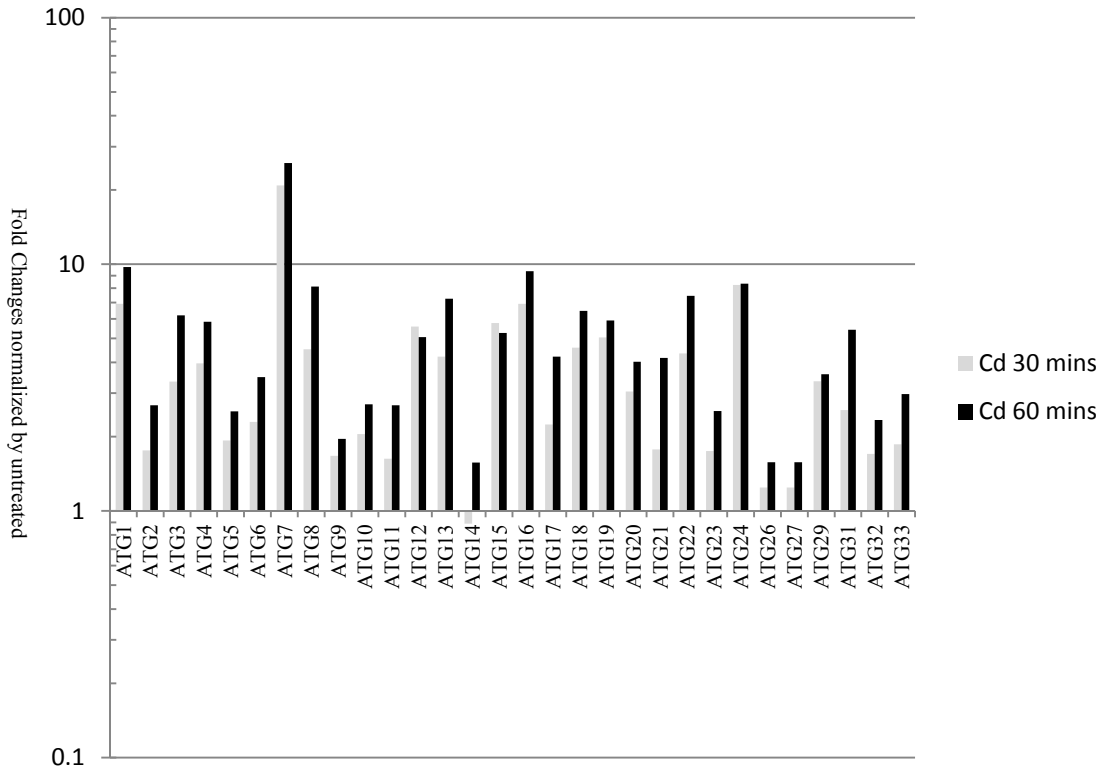

Figure 4: The expression profile of autophagy transcriptome upon cadmium treatment.

The fold change was normalized by the intensity obtained from the untreated sample.

phosphate dehydrogenase (GAPDH) orthologue, alters its conformation and trans-localizes to the nucleus upon heavy metal treatment (62). It implicates a pleomorphic nature of Tdh3 in cellular activities beyond those of its primary glycolytic metabolic role(s). Lastly, our initial findings that**; (a)** autophagy-associated genes are significantly induced upon treatment of cells , with cadmium, **(b)** Atg4 (the principal protease involved in autophagic initiation), is one of a few "cysteine proteases" that has been implicated in the activation of the yeast caspase (Yca1p), and **(c)** that Atg4-deficient yeast cells are not able to undergo metal – induced apoptosis, collectively indicate that there are significant areas of cross-talk between autophagy and apoptosis in yeast. Moreover, based on its role in maintaining homeostasis inside cells, the critical activity of autophagy is considered to be a major cyto-protective pathway. Accumulated evidence has shown that that autophagic, or Type-II cell death can further facilitates Type-I cell death (63), or can provide an alternative route for cellular response of apoptosis-compromised cells (64).

Therefore, we would like to address those questions in the following chapters:

1. Would PPP provide a major source of reduction pool generating anti-oxidants to against ROS stresses?
2. What is the role of Tdh3 playing in heavy metal-induced oxidative stresses? Would it be a signal regulator rather than a glycolytic enzyme?
3. How does autophagy mediate apoptosis (or *vice versa*) in yeast under heavy metal-induced stresses?

Significance

Chronic neuron degenerative diseases are threatening the elder society. Alzheimer's Disease and Parkinson's Disease, which result from the malfunction of memory and motor neuronal cells, mostly impact in the developed countries with the higher population of elders. In fact, about 160 billion dollars is being spent worldwide per year just for the treatments and several inestimable costs (65). Sadly, only few palliative treatments, but not radical cures, are available currently because the pathogenesis of the diseases remains opaque. In this study, we will focus on the role of the autophagic pathway as an apoptotic "modulator" in deciding whether cells are too badly damaged to survive. A clarification of the link between autophagy and apoptosis will potentially provide an alternative route to study the mechanisms that underlie cellular responses to heavy metal exposure in yeast, and by extrapolation in higher organism.

References

1. Scoullos MJ (2001) *Mercury, cadmium, lead : handbook for sustainable heavy metals policy and regulation* (Kluwer Academic Publishers, Dordrecht ; Boston) pp xviii, 525 p.

2. Hough RL*, et al.* (2004) Assessing potential risk of heavy metal exposure from consumption of home-produced vegetables by urban populations. *Environmental health perspectives* 112(2):215-221.

3. Mahaffey KR, Corneliussen PE, Jelinek CF, & Fiorino JA (1975) Heavy metal exposure from foods. *Environmental health perspectives* 12:63-69.

4. Aleksandrowicz J, Dobrowolski JW, Balechala P, & Lisiewicz J (1982) Monitoring trace elements in cells from the blood of patients with acute myeloblastic, chronic lymphocytic and chronic granulocytic leukemia. *Haematologica* 67(3):437-441.

5. Danford DE, Smith JC, Jr., & Huber AM (1982) Pica and mineral status in the mentally retarded. *Am J Clin Nutr* 35(5):958-967.

6. Penny WJ*, et al.* (1983) Relationship between trace elements, sugar consumption, and taste in Crohn's disease. *Gut* 24(4):288-292.

7. Rieder HP, Schoettli G, & Seiler H (1983) Trace elements in whole blood of multiple sclerosis. *Eur Neurol* 22(2):85-92.

8. Nogawa K, Kobayashi E, Okubo Y, & Suwazono Y (2004) Environmental cadmium exposure, adverse effects and preventive measures in Japan. *Biometals* 17(5):581-587.

9. Bull PC, Thomas GR, Rommens JM, Forbes JR, & Cox DW (1993) The Wilson disease gene is a putative copper transporting P-type ATPase similar to the Menkes gene. *Nature genetics* 5(4):327-337.

10. Linder MC (2012) The relationship of copper to DNA damage and damage prevention in humans. *Mutation research* 733(1-2):83-91.

11. Singh I*, et al.* (2013) Low levels of copper disrupt brain amyloid-beta homeostasis by altering its production and clearance. *Proc Natl Acad Sci U S A* 110(36):14771-14776.

12. Fenton HJH (1894) Oxidation of tartaric acid in presence of iron. *Journal of the Chemical Society, Transactions* 65:899-910.

13. Fortuniak A, Zadzinski R, Bilinski T, & Bartosz G (1996) Glutathione depletion in the yeast Saccharomyces cerevisiae. *Biochemistry and molecular biology international* 38(5):901-910.

14. Stohs SJ, Bagchi D, Hassoun E, & Bagchi M (2001) Oxidative mechanisms in the toxicity of chromium and cadmium ions. *Journal of environmental pathology, toxicology and oncology : official organ of the International Society for Environmental Toxicology and Cancer* 20(2):77-88.

15. Stohs SJ & Bagchi D (1995) Oxidative mechanisms in the toxicity of metal ions. *Free radical biology & medicine* 18(2):321-336.

16. Everett H & McFadden G (1999) Apoptosis: an innate immune response to virus infection. *Trends in microbiology* 7(4):160-165.

17. Hyka-Nouspikel N*, et al.* (2012) Deficient DNA damage response and cell cycle checkpoints lead to accumulation of point mutations in human embryonic stem cells. *Stem cells* 30(9):1901-1910.

18. Madeo F*, et al.* (2002) A caspase-related protease regulates apoptosis in yeast. *Molecular cell* 9(4):911-917.

19. Shanmuganathan A, Avery SV, Willetts SA, & Houghton JE (2004) Copper-induced oxidative stress in Saccharomyces cerevisiae targets enzymes of the glycolytic pathway. *FEBS letters* 556(1-3):253-259.

20. Amstad P, Moret R, & Cerutti P (1994) Glutathione peroxidase compensates for the hypersensitivity of Cu,Zn-superoxide dismutase overproducers to oxidant stress. *J Biol Chem* 269(3):1606-1609.

21. Nargund AM, Avery SV, & Houghton JE (2008) Cadmium induces a heterogeneous and caspase-dependent apoptotic response in Saccharomyces cerevisiae. *Apoptosis* 13(6):811-821.

22. Gourlay CW, Du W, & Ayscough KR (2006) Apoptosis in yeast--mechanisms and benefits to a unicellular organism. *Molecular microbiology* 62(6):1515-1521.

23. Fabrizio P*, et al.* (2004) Superoxide is a mediator of an altruistic aging program in Saccharomyces cerevisiae. *J Cell Biol* 166(7):1055-1067.

24. Vachova L & Palkova Z (2005) Physiological regulation of yeast cell death in multicellular colonies is triggered by ammonia. *J Cell Biol* 169(5):711-717.

25. Herker E*, et al.* (2004) Chronological aging leads to apoptosis in yeast. *J Cell Biol* 164(4):501-507.

26. Shrestha A & Megeney LA (2012) The non-death role of metacaspase proteases. *Frontiers in oncology* 2:78.

27. Lee RE, Brunette S, Puente LG, & Megeney LA (2010) Metacaspase Yca1 is required for clearance of insoluble protein aggregates. *Proc Natl Acad Sci U S A* 107(30):13348-13353.

28. Severin FF & Hyman AA (2002) Pheromone induces programmed cell death in S. cerevisiae. *Current biology : CB* 12(7):R233-235.

29. Starmer WT, Ganter PF, Aberdeen V, Lachance MA, & Phaff HJ (1987) The ecological role of killer yeasts in natural communities of yeasts. *Canadian journal of microbiology* 33(9):783-796.

30. Breinig F, Sendzik T, Eisfeld K, & Schmitt MJ (2006) Dissecting toxin immunity in virus-infected killer yeast uncovers an intrinsic strategy of self-protection. *Proc Natl Acad Sci U S A* 103(10):3810-3815.

31. Reiter J, Herker E, Madeo F, & Schmitt MJ (2005) Viral killer toxins induce caspase-mediated apoptosis in yeast. *J Cell Biol* 168(3):353-358.

32. Buttner S*, et al.* (2006) Why yeast cells can undergo apoptosis: death in times of peace, love, and war. *J Cell Biol* 175(4):521-525.

33. Cherry JM*, et al.* (2012) Saccharomyces Genome Database: the genomics resource of budding yeast. *Nucleic acids research* 40(Database issue):D700-705.

34. Braun RJ (2012) Mitochondrion-mediated cell death: dissecting yeast apoptosis for a better understanding of neurodegeneration. *Frontiers in oncology* 2:182.

35. D'Angelo F*, et al.* (2013) A yeast model for amyloid-beta aggregation exemplifies the role of membrane trafficking and PICALM in cytotoxicity. *Disease models & mechanisms* 6(1):206-216.

36. Treusch S*, et al.* (2011) Functional links between Abeta toxicity, endocytic trafficking, and Alzheimer's disease risk factors in yeast. *Science* 334(6060):1241-1245.

37. De Vos A*, et al.* (2011) Yeast as a model system to study tau biology. *International journal of Alzheimer's disease* 2011:428970.

38. Vanhelmont T*, et al.* (2010) Serine-409 phosphorylation and oxidative damage define aggregation of human protein tau in yeast. *FEMS yeast research* 10(8):992-1005.

39. Chesi A, Kilaru A, Fang X, Cooper AA, & Gitler AD (2012) The role of the Parkinson's disease gene PARK9 in essential cellular pathways and the manganese homeostasis network in yeast. *PloS one* 7(3):e34178.

40. Gitler AD*, et al.* (2009) Alpha-synuclein is part of a diverse and highly conserved interaction network that includes PARK9 and manganese toxicity. *Nature genetics* 41(3):308-315.

41. Skoneczna A, Micialkiewicz A, & Skoneczny M (2007) Saccharomyces cerevisiae Hsp31p, a stress response protein conferring protection against reactive oxygen species. *Free radical biology & medicine* 42(9):1409-1420.

42. Xiong Y*, et al.* (2010) GTPase activity plays a key role in the pathobiology of LRRK2. *PLoS genetics* 6(4):e1000902.

43. Mason RP & Giorgini F (2011) Modeling Huntington disease in yeast: perspectives and future directions. *Prion* 5(4):269-276.

44. Tauber E*, et al.* (2011) Functional gene expression profiling in yeast implicates translational dysfunction in mutant huntingtin toxicity. *J Biol Chem* 286(1):410-419.

45. Wang Y*, et al.* (2009) Abnormal proteins can form aggresome in yeast: aggresome-targeting signals and components of the machinery. *FASEB J* 23(2):451-463.

46. Bastow EL, Gourlay CW, & Tuite MF (2011) Using yeast models to probe the molecular basis of amyotrophic lateral sclerosis. *Biochemical Society transactions* 39(5):1482-1487.

47. Gunther MR, Vangilder R, Fang J, & Beattie DS (2004) Expression of a familial amyotrophic lateral sclerosis-associated mutant human superoxide dismutase in yeast leads to decreased mitochondrial electron transport. *Archives of biochemistry and biophysics* 431(2):207-214.

48. Johnson BS, McCaffery JM, Lindquist S, & Gitler AD (2008) A yeast TDP-43 proteinopathy model: Exploring the molecular determinants of TDP-43 aggregation and cellular toxicity. *Proc Natl Acad Sci U S A* 105(17):6439-6444.

49. Sun Z*, et al.* (2011) Molecular determinants and genetic modifiers of aggregation and toxicity for the ALS disease protein FUS/TLS. *PLoS biology* 9(4):e1000614.

50. Tsukada M & Ohsumi Y (1993) Isolation and characterization of autophagy-defective mutants of Saccharomyces cerevisiae. *FEBS letters* 333(1-2):169-174.

51. Shamas-Din A, Kale J, Leber B, & Andrews DW (2013) Mechanisms of action of Bcl-2 family proteins. *Cold Spring Harbor perspectives in biology* 5(4):a008714.

52. Madeo F*, et al.* (2004) Apoptosis in yeast. *Curr Opin Microbiol* 7(6):655-660.

53. Nargund AM (2010) Mechanism(s) of Metal-induced Apoptosis in *Saccharomyces cerevisiae*. (Georgia State University, Department of Biology).

54. Budovskaya YV, Stephan JS, Reggiori F, Klionsky DJ, & Herman PK (2004) The Ras/cAMP-dependent protein kinase signaling pathway regulates an early step of the autophagy process in Saccharomyces cerevisiae. *J Biol Chem* 279(20):20663-20671.

55. Cebollero E & Reggiori F (2009) Regulation of autophagy in yeast Saccharomyces cerevisiae. *Biochimica et biophysica acta* 1793(9):1413-1421.

56. Stephan JS, Yeh YY, Ramachandran V, Deminoff SJ, & Herman PK (2009) The Tor and PKA signaling pathways independently target the Atg1/Atg13 protein kinase complex to control autophagy. *Proc Natl Acad Sci U S A* 106(40):17049-17054.

57. Takeshige K, Baba M, Tsuboi S, Noda T, & Ohsumi Y (1992) Autophagy in yeast demonstrated with proteinase-deficient mutants and conditions for its induction. *J Cell Biol* 119(2):301-311.

58. Abeliovich H & Klionsky DJ (2001) Autophagy in yeast: mechanistic insights and physiological function. *Microbiol Mol Biol Rev* 65(3):463-479, table of contents.

59. Kiel JA (2010) Autophagy in unicellular eukaryotes. *Philos Trans R Soc Lond B Biol Sci* 365(1541):819-830.

60. Wang SH, Shih YL, Ko WC, Wei YH, & Shih CM (2008) Cadmium-induced autophagy and apoptosis are mediated by a calcium signaling pathway. *Cell Mol Life Sci* 65(22):3640-3652.

61. Maiuri MC, Zalckvar E, Kimchi A, & Kroemer G (2007) Self-eating and self-killing: crosstalk between autophagy and apoptosis. *Nat Rev Mol Cell Biol* 8(9):741-752.

62. Shanmuganathan A (2008) An analysis of glycolytic enzymes in the cellular response of metal toxicity. Doctor of Philosophy (Georgia State University).

63. Zhang M*, et al.* (2012) Autophagy and apoptosis act as partners to induce germ cell death after heat stress in mice. *PloS one* 7(7):e41412.

64. Yu L*, et al.* (2006) Autophagic programmed cell death by selective catalase degradation. *Proc Natl Acad Sci U S A* 103(13):4952-4957.

65. Wimo A, Jonsson L, & Winblad B (2006) An estimate of the worldwide prevalence and direct costs of dementia in 2003. *Dementia and geriatric cognitive disorders* 21(3):175-181.

CHAPTER 1.

THE PLEIOTROPIC ROLE OF GAPDH IN METAL-INDUCED APOPTOTIC RESPONSE OF YEAST CELLS

Pei-Ju Chin

Abstract

Apoptosis, or programmed cell death (PCD), plays an important role in cellular destruction (1). This suicide pathway is triggered when cells suffer irreversible damage such as viral infection (2), genetic retardations (3) or as we will focus on in this chapter, cellular response to heavy metal-exposure. The process is beneficial for multi-cellular hosts to minimize the potentially toxic effects of aberrant cellular functions, but is initially difficult to rationalize for single celled organisms, such as yeast. In addition to the proteins directly involved in the apoptotic response, there are additional sets of proteins that participate in this process, some of which are known to be involved in fundamental metabolic processes such as the redox or energy generation pathways (4). Indeed, a number of glycolytic proteins are induced in response to heavy metal exposure that ultimately induces an apoptotic response in these cells. One of these proteins, glyceraldehyde-3-phosphate dehydrogenase or GAPDH, is notable -not only because of its pivotal role in regulating carbon flow through the glycolytic pathway, but also for its role as an apoptotic signaling protein. GAPDH, which is normally active in the cytoplasm or attached to the outside of the mitochondrial matrix, has a pleiotropic effect in that it functions as both a glycolytic enzyme in normal cells but can shuttle in to the nucleus in response to stressors and potentially give rise to an apoptotic response.

Our studies have previously demonstrated that the transcriptional levels of GAPDH are induced in yeast cells that are exposed to Cd, and that one of the three isoforms of the enzyme, Tdh3p is specifically damaged in response to exposure to this metal (4). As a result, Tdh3p was tagged with GFP in order to trace any cellular movement of the protein in response to the presence of heavy metals. Intriguingly, the presence of the TDH3-GFP tag in otherwise wild-type cells appeared to block any and all apoptotic response to the presence of cadmium. To investigate this phenomenon further the physiological differences between wild-type cells and readily available mutant cell-lines encoding singular GFP gene fusions were analyzed by assaying their Tdh3p enzyme activity. The results of these analyses showed that there were fewer enzymatic differences between native and GFP-tagged Tdh3p than might have been expected from such a distinctive phenotype. Indeed, the data further suggest that the glycolytic activities of Tdh3p need not provide the major contribution to the apoptotic responses and that the more important role for this ubiquitous enzyme in the apoptotic response of yeast cells is its nuclear translocation. We developed a quantification method to count the Tdh3p appearance inside the apoptotic yeast cell and found higher levels of Tdh3p inside the nucleus following exposure to cadmium. The role of nuclear translocalization of Tdh3p remains an intriguing aspect of a regulated apoptotic response to metal exposure and warrants further investigations.

1.1 Introduction

While apoptosis is a fundamentally important feature of normal cellular development in multi-cellular organisms (1) this programmed cellular response pathway is also initiated when cells respond to a variety of cellular stressors and when cells incur irreversible damage resulting from viral infections (2), and genetic retardation (3). This process is considered to be beneficial

for multi-cellular organisms to prevent the damaged cells from disseminating cellular signals neighboring cells in the body when the damaged cells have been irreversibly compromised. The arguments as to why single celled organisms, such as *S. cerevisiae*, exhibit a similar potential to commit programmed cell death are more difficult to discern, the pathways and mechanisms through which they are able to do so are shared among a variety of organisms.

While there are a number of response pathways that effect the apoptotic process in yeast, a major stimulus for these responses involve, as they do in higher eukaryotes, the redox or energy generation pathways (5, 6). Indeed a number of the glycolytic enzymes are known to be induced in cells undergoing apoptosis, and it is thought that some of these enzymes play crucial signaling or regulatory roles in promoting the apoptotic response. One of these proteins, glyceraldehyde-3-phosphate dehydrogenase (GAPDH), is notable not only for of its pivotal role in glycolytic metabolism but also for its potentially regulatory roles in a variety of cellular activities. It has been shown to be involved in cell wall adhesion (7), regulation of mitochondria membrane permeability (8), transcriptional regulation (9), nuclear membrane fusion (10), telomere maintenance (11), DNA repair apparatus (12), homeostasis of metabolic oscillations (13), activation of tumor migration factors $hTAF_{II}68$ and TEC (14) and the apoptotic response in neuronal cells (15-18). The enzyme was not known to be involved in the apoptotic response until its abnormal deposit in the brain tissue from patients with neural degenerative disorders was reported. GAPDH is over-expressed in the low potassium –induced apoptotic cerebellar granule cells (19). The possible function of the nuclear GAPDH in apoptotic neural cells was disclosed, in that its presence was shown to inhibit uracil-DNA glycosylase, a major component of the DNA repair apparatus. Indeed, both the survival rate of the cell and the nuclear GAPDH activity

can be restored by introducing GAPDH antisense oligonucleotides to neutralize the enzymes over-expression (20). The relationship between GAPDH nuclear translocalization and caspase-3 activation was reported (21). By surveying the brain tissue in African-American patients with Parkinson's disease, along with age-matched controls, Tatton and his co-workers found that the increased immunoreactivity of caspase-3 and the pro-apoptotic Bax are coincident with GAPDH nuclear shuttling. Subsequently, several studies have similarly claimed that GAPDH is a pro-apoptotic protein and the presence of a nuclear form of GAPDH is a significant factor in facilitating apoptosis. Further, the Golgi apparatus, a place where protein sorting and secretion occurs, was found to contribute to the modification of GAPDH, enabling its passage into the nucleus and/or other organelles in order for it to achieve its pathological roles (22). For instance, Amyloid-β, which is abnormally precipitated in brain tissues and results in the formation of Lewy Bodies in patients with Alzheimer's Disease and Parkinson's Disease, is known to promote the formation of disulfide bonds in GAPDH and its subsequent accumulation in the nucleus (23-25). While a majority of findings have shown how GAPDH is able to facilitate the apoptotic process, some studies have also demonstrated that this enzyme can also have a negative role (26, 27). In these reports GAPDH was shown to inhibit caspase-dependent apoptosis by inducing ATG12 expression, which results in the augmentation of autophagic activities, resulting in damaged, cytochrome-c-releasing mitochondria being engulfed by autophagosomes, which effectively curtailed the apoptotic cascade. Nevertheless, the contribution of the nuclear translocation of GAPDH to the apoptotic process remains relatively unclear.

Perhaps as a consequence of its varied roles in mediating a number of cellular activities in many eukaryotes GAPDH exists in a number of different isoenzymatic forms, principally Tdh1p, Tdh2p and Tdh3p, each of which have different expression profiles and levels of glycolytic activities (28). In *S. cerevisiae*, the most abundant and most enzymatically active of these isoenzymes, Tdh3p, has also been shown to be preferentially targeted for oxidation by metal-induced stress (4, 6), which raises the probability that different isoforms of TDH may contribute differently to related aspects of nuclear induction of apoptosis than others. In yeast the presence of nuclear TDH has also been identified in potentially mediating multiple cellular responses, with the preferential translocation of one of the TDH isoenzymes, Tdh3p, into the nucleus being involved in metal-induced apoptosis (4). Shanmuganathan also found that TDH became associated with a series of different proteins upon cadmium-induced stress and concluded that these various protein complexes may be involved with TDH being able to facilitate the progression of the apoptotic response. Such selective translocation of discrete TDH isoforms would further indicate that either the specific affinity of nuclear membrane for these isoforms is modified by exposure to cadmium, or that the co-translocated proteins are perhaps able to modify the ability of specific isoforms of TDH to translocate into the nucleus.

Preliminary studies reported in this chapter further indicate that the normally stable expression of TDH (TDH protein expression is commonly used as a normalized control in numerous publications) is increased in yeast cells that have been exposed to Cd, accompanying the nuclear translocalization. As a result we hypothesize that TDH in yeast is more complex than its clearly established metabolic role in the apoptotic response (29), perhaps as a signal factor to regulate the expression or activity of pro-apoptotic genes that might be important in the apoptotic

response of the cell to heavy metals. To test this hypothesis the transcriptional levels of GAPDH were monitored in a series of microarray experiments **(Appendix A and B)**, which confirmed that TDH is induced in yeast cells exposed treated yeast cells **(Appendix H)**. We first hypothesized that the apoptotic response of cells required extra energy, and consequently, the increased expression of TDH provided a necessary boost in glycolytic pathway activity to meet increased demand (30, 31). This hypothesis was further supported by increased expression of the analysis of other glycolytically associated genes –following exposure of yeast cells to Cd; with the cluster analysis clearly showing that the genes related to the glycolytic pathway are significantly induced in apoptotic yeast cells **(Appendix H)**.

As a result of these preliminary results and the findings of Anupama Shanmuganathan we would like to determine some of the physical parameters of the metal-induced nuclear trans-localization of Tdh3p, and potentially elucidate the biological role of nuclear TDH in metal-induced apoptotic yeast cells. In so doing we would also test whether the Tdh3p deletion strain, which lacked the major TDH isoenzyme in yeast, were unable to respond to the presence of cadmium.

1.2 Materials and Methods

Strain and Medium Preparation

Saccharomyces cerevisiae BY4741 parental wild-type (*MATα his3Δ1 leu2Δ0 met15Δ0 ura3Δ0*), *tdh3*Δ isogenic mutant (Euroscarf) or TDH3-GFP fusion strain (Invitrogen) were cultured in 5mL YEPD broth [2 % (w/v) peptone (BD), 1 % (w/v) yeast extract (Difco) and 2 % (w/v) glucose (EM Industries)] overnight for making the start culture. The start culture then were

inoculated in YEPD broth and incubated at 30 ^{o}C under 225 rpm aerobic shaking. The cells mass was determined by OD600 reading. Unless specified, the harvested cells were exposed to 8 mM copper nitrate or 30 μM cadmium nitrate (Sigma-Aldrich) to trigger the apoptotic response for 1 hour, followed by being washed by YEPD medium and post-incubated in YEPD medium for additional 3 hours.

Assay of apoptotic population

The harvested yeast cells were 20X-diluted in YEPD medium and stained by dihydrorhodamine 123 (DHR123; Sigma-Aldrich) for labeling the cells accumulating ROS residues, which represents the population undergoing oxidative stresses and apoptosis. The stained cells were subjected to FACsCANTO^{TM} cytometry with PE fluorophore filter.

Total protein preparation

The cells were grown from seeding culture for overnight to OD600 = 1.8~2.5, and treated by the stress agents mentioned above. The cells were harvested by centrifuging under 5,000 xg, 3 minutes at 4 ^{o}C in JA-20 rotor (Beckman Coulter). The cells were washed by cold deionized water twice, then re-suspended in lysis cocktail containing 100 mM Tris-HCl; pH 7.4, 20 μg/mL leupeptin, 10 μg/mL pepstatin A, 0.264 mg/mL aprotinin, 1 mM PMSF and glycerol (10 % v/v). about 200 μL acid-washed glass beads were added to the mixture ,and the cells were disrupted for 30 seconds by mini beat beater-8 (BioSPEC Product) for 4 times with cooling on ice between each disruption. Total protein concentration was quantified by 2-D Quant Kit (GE Bioscience) by using the standard curve of serial-diluted BSA solution.

Confocal Microscopy of Nuclear trans-localization of Tdh3p

S. cerevisiae TDH3-GFP fusion strain was treated with 120 μM cadmium nitrate (Sigma-Aldrich) for 0 and 180 minutes. After exposure, the cells were immediately fixed by incubation in 70% ethanol for 5 minutes. The cells were washed with de-ionized water twice, and then 10 μL cell re-suspension was mixed with 10 μL DAPI-antifade solution (Invitrogen). 5 μL of stained sample was laid on the slide which was cleaned and coated by 70 % ethanol and poly-lysine solution (Sigma-Aldrich). The cell mixture was examined using a Zeiss Axioimager fluorescence microscope to validate the appropriate staining before potential nuclear trans-localization of Tdh3p was analyzed more thoroughly using a Zeiss LSM 510 confocal microscope.

SDS PAGE and Western-blotting

The protein extraction was mixed with sample loading buffer (10 % SDS, 0.1 M Tris; pH 6.8, 50 % glycerol, 0.01 % Bromophenol) and 10 mM Tris-HCl (pH 6.8). The mixture was denatured by boiling for 5 minutes before subjecting to SDS-PAGE electrophoresis under 140 V for 1.5 to 2 hours. The polyacylamide gel containing the total protein fragment was washed by deionized water then blotted to Hybrid-ECL hybridization membrane (GE Bioscience) by electro-blotting under 20V for overnight. The blotted membrane was washed by de-ionized water briefly, following by 1 hour incubation in blocking buffer containing 5 % slim milk (EMD Chemicals) and PBS with 0.1 % Tween-20 (Sigma-Aldrich). Anti-GAPDH-C-ter produced by rabbit (1:5000 titration in PBS with Tween-20) and Anti-rabbit IgG conjugated with HRP (1:5000 titration in PBS-Tween 20 and 5% slim milk) were used for primary and secondary hybridization, 1 hour for each. The membrane was washed by PBS-Tween-20 3 times for 15

minutes between each hybridization. The signal was developed by Enhanced chemiluminescence (ECL) (Amersham Bioscience) then detected by the X-ray film exposure.

Preparation of crude nuclei and cytosolic fractionation

The sample was treated and harvested by the method described above. The cell pellet was washed twice by cold de-ionized water, and re-suspended in pretreatment buffer (50 mM Tris, pH 7.5 and 30 mM DTT) then incubated at 30 ^{o}C for 15 minutes. The cells were harvested by centrifuging at 5,000 xg for 10 minutes and the pellet was re-suspended in spheroplast buffer, containing 20 mM potassium phosphate; pH 7.4, 1.2 M sorbitol and 40 mg/mL 20T zymolyase. The re-suspension was incubated at 30 ^{o}C for at least 90 minutes to digest the cell wall. The digestion process was inspected by mixing the cell suspension with 10% SDS then checking under the microscope. The ghost cells represent the removal of cell wall. The spheroplasts were gently washed twice by spheroplast buffer and re-suspended in Buffer A containing 18 % Ficoll 400 (GE Biosciences) , 10 mM Tris-HCl; pH 7.5, 20 mM potassium acetate, 5 mM magnesium acetate, 1 mM EDTA, 0.5 mM spermidine (Sigma-Aldrich) and 0.15 mM spermine (Sigma-Aldrich). Spheroplasts were disintegrated by “pestling” for at least 100 cycles. The crude nuclei fractionation was discriminated from debris sediment by spinning the supernatant at 2,988 xg, 4 ^{o}C for 5 minutes for four cycles. After the final (fourth) spin, the supernatant representing crude nucleus fraction was obtained by centrifuging at 20,199 xg, 4 ^{o}C for 30 minutes. The supernatant and pellet represents the crude cytosolic and nuclear fraction, respectively. For the sorting purpose, the crude nuclei extract was washed twice by ice-cold PBS and stained by 0.2 % (v/v) propidium iodide (PI) if necessary. The crude nuclei were assayed by FACS CANTO^{TM} flow cytometer (BD Biosciences). The supernatant was further centrifuged under 88,760 xg at 4 ^{o}C for

1 hour to obtain the pure cytosolic fraction. For nuclear protein preparation, the crude nuclear pellet was washed twice in cold PBS then lysed by nuclear lysis buffer containing 20 mM HEPES; pH 7.9, 0.4 N NaCl, 1 mM EDTA, 1 mM EGTA, 1 mM DTT, 1 mM PMSF and 1 μg/mL each of pepstatin, aprotitin and leupeptin following by agitating the suspension at 4 ^{o}C for 30 minutes and spin at 11,800 xg for 15 minutes. The supernatant represents the nuclear fractionation. The protein concentration for these two fractions was determined by 2-D Quant Kit (GE Healthcare).

Nuclear immunoprecipitation (Nuclear IP)

The intact, crude nuclei fractions of *S. cerevisiae* BY4741 wild type were pulled down by DynalBead^{TM} (Invitrogen) coated with Nsp1 antibody, which recognizes the subunit of the porin complex on the yeast nuclear membrane. The linker and primary antibody were conjugated, according to the protocol provided. The beads and crude nuclei were co-incubated at 4 ^{o}C with rotating shaker for 2 hours or overnight, followed by generic washing procedure.

Co-immunoprecipitation (Co-IP)

The Co-IP followed the instructions provided by Invitrogen. Two procedures were performed: direct and indirect method. In direct method, 100 μL DynaBead was conjugated with 20 μg of anti-GAPDH-IgG (Sigma-Aldrich), anti-TDH3Cter-IgG (GenScript) or anti-GFP-IgG (Invitrogen) at 4 ^{o}C for overnight. For the permanent crosslinking, BS3 crosslinker was used according to the instructions (Thermo-Scientific). The bead-antibody complex was washed three times by PBS, and then incubated with 200 μg protein lysate at 4 ^{o}C for 4 hours. The Co-IP product was harvested by the denaturation (boil up the beads for 5 minutes), acidic (100 mM

glycine, pH 2.8) or basic (100 mM glycine, pH 11) elution or high ionic strength (3 M KCl) elution. The pulled down product was further analyzed by SDS-PAGE and Western blot.

Molecular cloning and expression of TDH3 gene

To avoid the co-amplification of TDH1 and TDH2 isogenes, the fragment including 1 Kb up- and downstream of TDH3 was amplified in order to gain the highest heterogeneity by the primer set: Forward- CATCGTAGGTGTCTGGGTGAACAG and reverse-CATGATTTGATGGCTGTACCGATAG. This primary amplicon was served as the template to amplify the actual TDH3 gene and incorporated the BamHI/HindIII cutting sequence by the primer set: Forward- GCAGGATCCAACAAAATGGTT-AGAGTTGCTATTA and reverse-CAGAAGCTTTAAAGTAAATTCACTTAAGC-CTTGG. We then cloned the TDH3 gene into p416-GPD shuttling vector **(Fig. 5)** (32). The positive *E. coli* clones were selected by carrying ampicillin-resistant marker. The TDH3-bound vector was transformed to *S. cerevisiae* BY4741 (wild-type), *tdh3*Δ isogenic mutant and GFP-fused TDH3 strain by following the methods described in pYES2 manual from Invitrogen. The positive candidates were screened by synthetic complete (SC) media with the uracil auxotrophy. The expression of cloned-TDH3 is controlled by the TDH3-specific promoter on p416-GPD vector.

Quantitative RT-PCR

Quantitative RT-PCR technique was applied for quantifying the transcription level of TDH3 in the metal-exposed yeast cells. Total RNA treated by DNaseI was mixed with TaqMan RNA-to-CT 1-Step kit^{TM} by following the manufacture's instruction. (Applied Biosystems). The primers and TDH3-specific probe are shown: Forward primer- TCGGTAGATTGGTCATGAGAATTG,

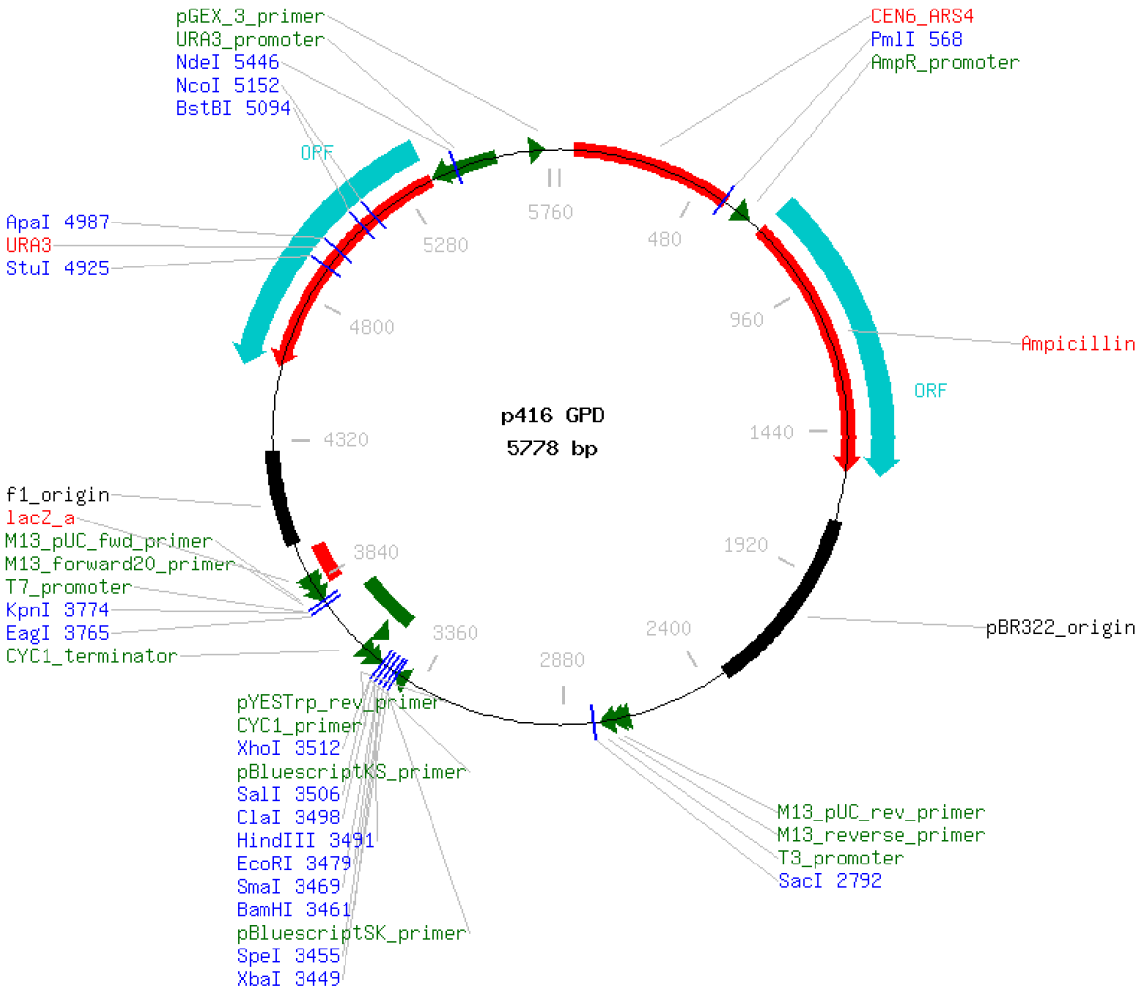

Figure 5: p416GPD (ATCC 87360) Vector Map

p416GPD is a shuttle vector harboring prokaryotic (pBR322 origin) and eukaryotic (CEN6_ARS4) replication origin. The low copy number, replication clones were selected by the ampicillin resistance, and uracil auxotroph in *E. coli* TOP10 and *S. cerevisiae* BY4741, respectively. The TDH3 amplicon with *Bam*HI (5') and *Hind*III (3') sticky ends was inserted to the multiple cloning site, which is in the downstream of eukaryotic GAPDH promoter.

reverse primer-TGAATGGGTCG-TTCAAAGCA, TaqMan probe-FAM-TGTCTAGACCAAACGTCGAA-NFQ. Amplification plots were performed by following standardized thermocycler protocols using the 7500 Fast Real-Time PCR System (Applied Biosystems): 48 ^{o}C, 30 minutes for reverse transcription, 95^{o}C, 10 minutes for denature, followed by 40 cycles of 15 seconds at 95 ^{o}C and 1 minute at 55 ^{o}C. The signal was acquired at the last step. The instrument was set to the 9600 emulation mode to increase the sensitivity.

Alcohol dehydrogenase (ADH) and glyceraldehyde-3-phosphate dehydrogenase (GAPDH) enzymatic assay

The yeast total protein, cytosolic and nuclear fractionation were assayed for ADH and GAPDH enzymatic activity. ADH activity was test by following the protocol provided by Bergmeyer et. al. (33). Briefly, the cell extract was mixed with the assay buffer containing 100 mM Tris-HCl, pH 8.3 and 2mM NAD^{+}. The reaction was started by adding 0.8 M ethanol. The GAPDH activity was measured by following the protocol provided by McAlister et. al. (28). The cell extract was mixed with the assay buffer containing 0.1M potassium phosphate; pH 7.4, 1 mM NAD^{+}, 10 mM EDTA and 0.1 mM DTT. Both ADH and GAPDH activity were measured by the increment of A340, which represents the absorbance wavelength of reduced NAD^{+}, or NADH.

1.3 Results

TDH3-deficient yeast cells are non-apoptotic which may not be due to the depletion of glycolytic activity

There are three GAPDH isoenzymes in yeast cells; Tdh1p, Tdh2p and Tdh3p with Tdh3p being the predominant form of GAPDH. Nevertheless all of these isoenzymes exhibit ~95% similarity with each other and catalyze the same critical reaction in the glycolytic pathway accordingly. Previous work in the laboratory determined that Tdh3p was preferentially fragmented in yeast cells upon exposure to heavy metals such as cadmium and copper (4). As a consequence, we have focused on the molecular aspects of Tdh3p in metal-induced apoptotic response. Preliminary data shows that TDH3 mutant is non-apoptotic upon Cd treatment **(Fig. 6)**. These findings were consistent with our hypothesis that a viable glycolytic pathway is critical to maintain cellular energy and reducing power that could mitigate any apoptotic potential. Moreover previous results in the laboratory (4) had also suggested that GAPDH movement in to the nucleus occurred upon exposure to heavy metals, indicating that this transference may be involved in the cellular response to the presence of heavy metals. Consequently, the movement of GAPDH in to the nucleus was also analyzed using green fluorescent protein (GFP)-tagged TDH3 (TDH3-GFP), which was constructed to trace the cellular movement of Tdh3p into the nucleus. Curiously, this strain was found to be non-apoptotic **(Fig. 6)**.

This finding reaffirmed the importance of GAPDH (or more specifically for this study, Tdh3p) in the cellular response of yeast to Cd. Not only is the presence of GAPDH critical for apoptosis to occur, but potentially an unmodified Tdh3p is also required for achieving the metal-induced apoptotic response. In order to test whether the glycolytic activity itself is the major contributor in this pro-apoptotic role, we assayed the enzymatic activity between wild-type and TDH3-GFP fusion strain exposed to Cd treatment but no significant difference was discovered

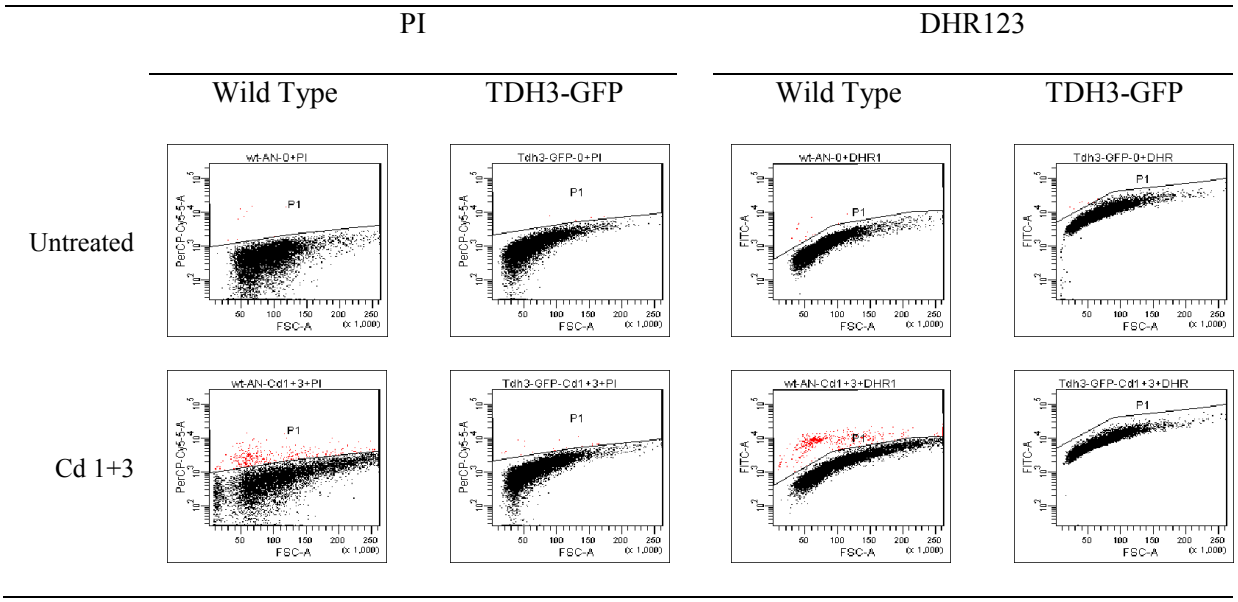

Figure 6: *S. cerevisiae* TDH3-GFP strain, like TDH3 mutant, is non-apoptotic upon cadmium treatment.

S. cerevisiae wild type and TDH3-GFP strain was treated with 30 μM Cd, and the effects of this exposure compared to cells that had not been exposed. The samples were stained with propidium iodine (PI) and DHR123 to label the cells with losing membrane integrity and ROS accumulation. The corresponding percentage of labeled cells are noted accordingly.

(Fig. 7). The cells carrying the TDH3-GFP fusion demonstrated either a negligible reduction or even higher activity which indicates that the GFP tag itself does not interfere with overall enzyme activity and that the tagged protein must contribute to apoptosis silencing in some other way. In this aspect, Tdh3p could facilitate the apoptosis responses through other pleiotypic roles rather than its glycolytic activity.

Nuclear translocalization of Tdh3p was found in Cd-treated yeast cells

The nuclear translocalization of GAPDH of apoptotic yeast was found in the previous study showing Tdh3p to be present in the nuclear fraction. To confirm that, TDH3-GFP strain was used to trace this shuttling upon Cd treatment by epifluorescence or confocal microscopy **(Fig. 8)**. The result shows that Tdh3p did indeed translocate in to nuclei of yeast cells exposed to cadmium.

Nevertheless, the microscopy-based method is not quantifiable to confirm the degree of nuclear translocation of Tdh3p upon cellular exposure to cadmium, nor did it prove to be entirely conclusive as to whether the nuclear translocation was significantly different between cells treated with Cd or not. To overcome this concern we developed a cytometric method to count the appearance of nuclear Tdh3p obtained from crude nuclear extracts. Briefly, the co-localization of TDH3-GFP and nuclei is identified once both the green (GFP) and red (PI labeled inside the nuclei) fluorescence are detected by flow cytometry for each “event”, which would be the individual nuclei in this case. Along similar lines, nuclei without TDH3-GFP would only fluoresce red, and the TDH3-GFP without localization would not be detected as there would be no boundaries able to concentrate the GFP molecules enough that they would be able to emit a

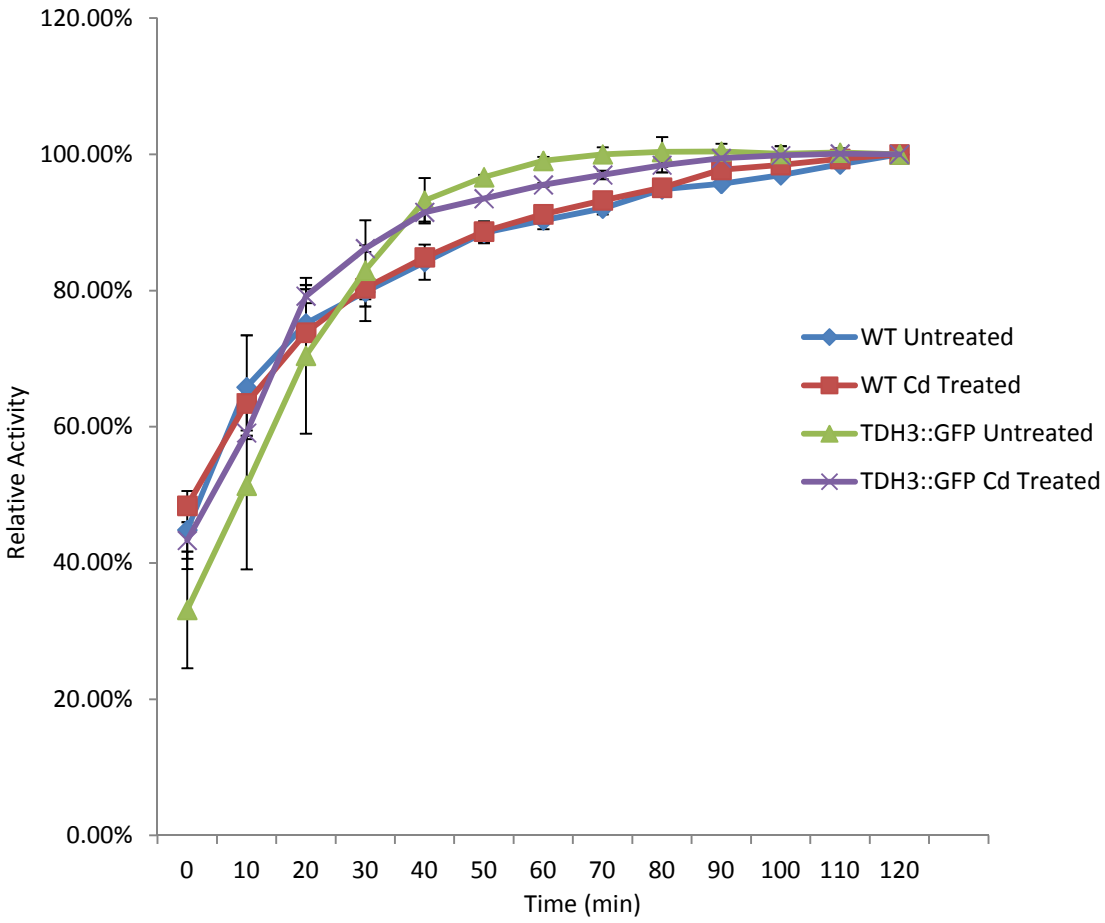

Figure 7: The enzymatic activity of wild type and GFP-tagged Tdh3p.

Using appropriate controls, *S. cerevisiae* wild type and TDH3-GFP strain were treated with 30 µM Cd and GAPDH activity was measured. Neither Cd exposure nor GFP tagging substantially impacts its glycolytic activity.

A B C

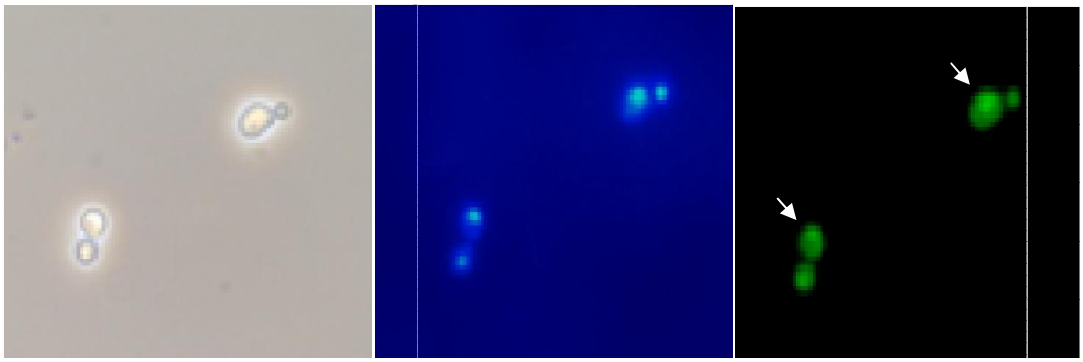

Figure 8: Confocal fluorescence microscopy image of *S. cerevisiae* TDH3-GFP fusion construct.

S. cerevisiae TDH3-GFP strain was treated with Cd. The sample was fixed on the slide coated by poly-lysine and imaged under assigned filters: **(A)** Visible light, **(B)** DAPI filter for the nuclei staining and **(C)** GFP filter. Arrow indicates the Tdh3p nuclear trans-localization in apoptotic yeast cell where DAPI and GFP signal are overlapped.

viable signal. We first evaluated the performance of this method for being quantifiable: The crude nuclear fraction, harvested from *S. cerevisiae* wild type and TDH3-GFP fusion strains, were stained with propidium iodine (PI) to label the nuclei, and the mixtures with the various proportion of GFP-labeled and PI-labeled nuclei obtained from TDH3-GFP and wild type crude nuclei extracts were subjected to cytometric analysis. Given that the ratio between PI-GFP double labeled and GFP single labeled nuclei would be known for each test condition (R_I), by comparing this value with the outcome of PI-GFP/GFP ratio assayed by flow cytometry (R_M), a concordance between the input proportions and output populations could be observed **(Fig. 9)**.

The results of this preliminary experiment indicated that the method was quantifiable, and potentially suitable to study the Tdh3p nuclear translocation in a concentration- dependent manner. In this concentration-dependent analysis (**Fig. 10**), cells were exposed to increasing concentrations of cadmium and the co-localization of nuclei expressing both PI and GFP (Tdh3p-GFP) was seen to increase up to 2-fold as the concentration of cadmium increased, which indicated that there is an discernible increase in the concentration of nuclear-translocated Tdh3p, and that this increase is associated with increased exposure to Cd, showing a potential direct correlation between potential the increased presence of Tdh3p in the nucleus and the apoptotic response of the cells to an increased exposure to cadmium.

GAPDH shows different enzymatic activities when present in either cytosolic or nuclear fractions.

Since incremental Cd exposure tended to augment the observed nuclear translocation of Tdh3p, and building on previous findings that Tdh3 has already been shown to translocate into

R_I (TDH3-GFP vs WT)	Diagram of quadrant	R_M (TDH3-GFP vs WT)
1:1 (1.00)	 Tube: 1 Population #Events %Parent %Total All Events 10,000 #### 100.0 PI + 6,062 60.6 60.6 PI+/GFP+ 2,851 28.5 28.5 unstained 748 7.5 7.5 GFP+ 339 3.4 3.4	1.0
1:0.8 (1.25)	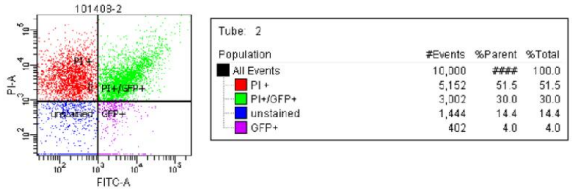 Tube: 2 Population #Events %Parent %Total All Events 10,000 #### 100.0 PI + 5,152 51.5 51.5 PI+/GFP+ 3,002 30.0 30.0 unstained 1,444 14.4 14.4 GFP+ 402 4.0 4.0	1.23
1:0.6 (1.67)	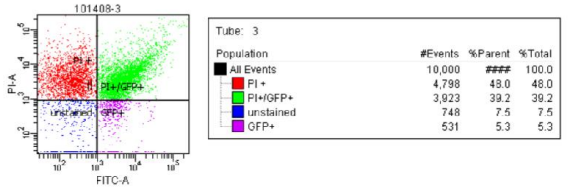 Tube: 3 Population #Events %Parent %Total All Events 10,000 #### 100.0 PI + 4,798 48.0 48.0 PI+/GFP+ 3,923 39.2 39.2 unstained 748 7.5 7.5 GFP+ 531 5.3 5.3	1.74
1:0.4 (2.50)	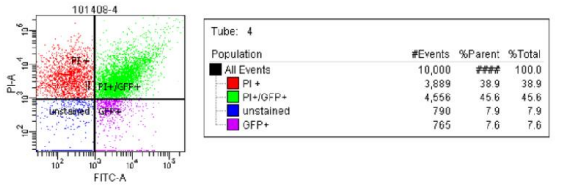 Tube: 4 Population #Events %Parent %Total All Events 10,000 #### 100.0 PI + 3,889 38.9 38.9 PI+/GFP+ 4,556 45.6 45.6 unstained 790 7.9 7.9 GFP+ 765 7.6 7.6	2.49
1:0.2 (5.00)	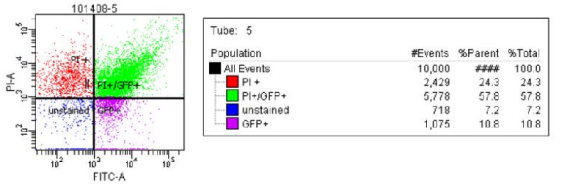 Tube: 5 Population #Events %Parent %Total All Events 10,000 #### 100.0 PI + 2,429 24.3 24.3 PI+/GFP+ 5,778 57.8 57.8 unstained 718 7.2 7.2 GFP+ 1,075 10.8 10.8	5.06
1:0.0 (∞)	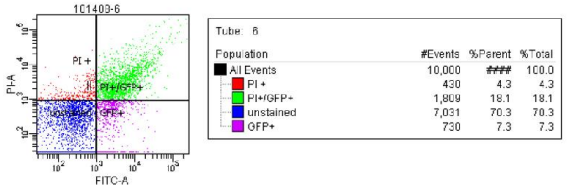 Tube: 6 Population #Events %Parent %Total All Events 10,000 #### 100.0 PI + 430 4.3 4.3 PI+/GFP+ 1,809 18.1 18.1 unstained 7,031 70.3 70.3 GFP+ 730 7.3 7.3	9.00

Figure 9: The performance evaluation of the cytometer-based nuclei sorting.

The nuclear fraction harvested from S. cerevisiae wild-type (WT) and TDH3-GFP fusion strains were stained with propidium iodine (PI). The various mixtures, along with their indicated titration of stained nuclei (R_I) were then subjected to flow cytometry to differentiate among the various heterogeneous populations of nuclei obtained from TDH3-GFP and WT cells. The sub-populations of each quadrant (from upper left to bottom left, in clockwise direction: PI only, PI and GFP, GFP only and unstained) were quantified. The measured ratio (R_M) between PI+GFP and PI only was normalized by the reading of mixture containing the identical proportion of TDH3-GFP (PI+GFP stained) and wild type (PI-stained only) nuclei (R_I = 1:1). The normalized R_M was comparable with the ratio of original input (R_I), which indicates that this cytometric method is sensitive enough to differentiate among the various populations of dual and single and double-stained nuclei.

[Cd] (μM)	Diagram of quadrant	R_{Trans}
0	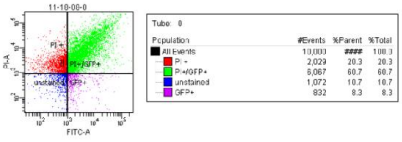	1.00
30	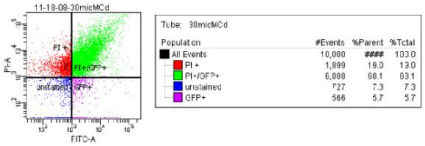	1.29
60		0.99
120		2.21

Figure 10: The cytometry-based assay of Tdh3p nuclear trans-localization

The nuclear fractionation of *S. cerevisiae* TDH3-GFP fusion strain treated with incrementally increasing concentrations of Cd were stained by propidium iodine (PI). The event number of green (upper-right) and red (upper-left) quadrant, which represents the co-staining of GFP and PI (Tdh3p nuclear localization) and PI-stained only (nuclei without Tdh3p), was used to evaluate the ratio of trans-localization (R_{Trans} equals green divided by red), which indicates the degree of nuclei harvested Tdh3p. The R_{Trans} of each treated sample was normalized against the ratio obtained from untreated samples.

the nucleus and alter its conformation as a result of heavy metal-induced stress (4), we intended to further investigate whether the glycolytic activity of Tdh3p can be altered by its relocation. Even though the enzymatic assay cannot specifically be excluded from the activities contributed by the other two isozymes (Tdh1p and Tdh2p), the crude nuclei fractionation showed less GAPDH activities than the cytosolic **(Fig. 11)**. While such attenuated activity may be due to the conformational change, post-translational modification and/or co-factors/proteins binding during the nuclear translocation of Tdh3p from the cystosol, the decreased activity is consistent with some degree of conformational change in Tdh3p structure upon its translocation in to the nucleus.

Nuclear IP is not accessible in this stage

As concluded in the previous section, obtaining a high degree of purity of nuclear Tdh3p is helpful to evaluate some of the essential differences between the cytosolic and nuclear forms of the Tdh3p in metal-treated yeast cells. Such a determination would go a long way to answer some of the more fundamental questions as to the possible role of Tdh3p in metal-induced apoptotic yeast cells. The crude nuclear preparation protocol that has been used often in this study is unable to remove much of the cytosolic contamination of the nuclear fraction, which tends to blur any interpretation as to the role that nuclear Tdh3p may play as a result of its translocation, since Tdh3p is a highly expressed, crucial metabolic enzyme. Shanmuganathan previously shown that such cytosolic contamination is a major concern with the crude nuclei fraction extracted using Ficoll gradients (4). In an effort to determine the extent to which the nuclear fraction is contaminated with cytosolic proteins, the enzymatic activity of alcohol dehydrogenase (ADH) was used. ADH is often used in the literature as a cytosolic marker due to

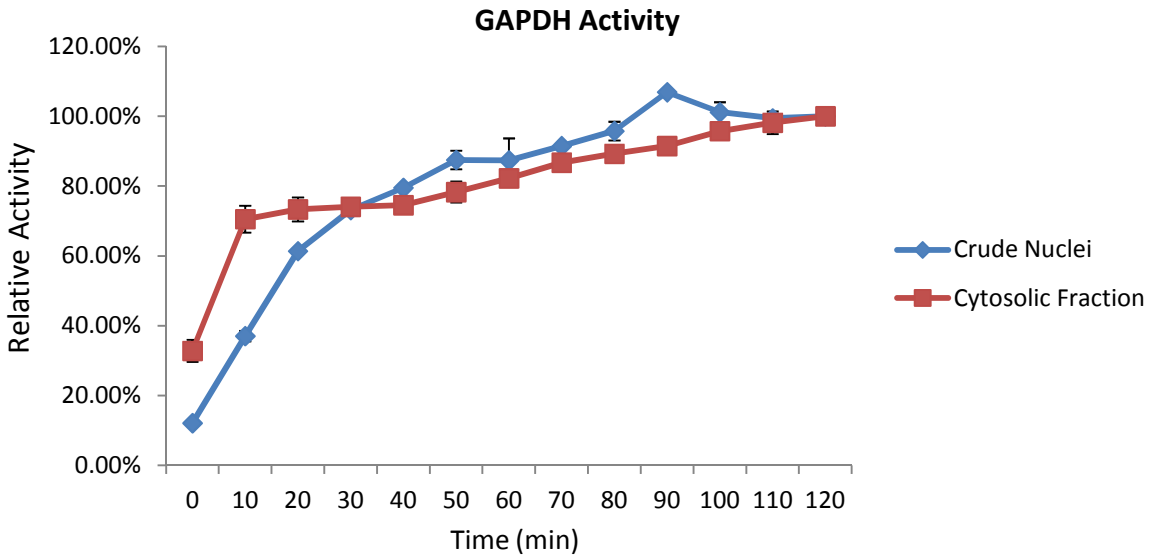

Figure 11: The distinct enzymatic activity of GAPDH assayed from the crude nuclei and cytosolic fractionation.

The crude nuclear and cytosolic fractionations of *S. cerevisiae* wild-type without Cd treatment were harvested for GAPDH enzymatic activity assay. The activity was adjusted by the protein concentration and represented by two independent tests.

its exclusive existence within the cytosol. In all the nuclear fractions that were obtained, ADH was always present, demonstrating the limitations of the Ficoll-based method in that these fractionation steps merely remove a majority, but not all cytosolic components from nuclear extract **(Fig. 12)**. Therefore, a better technique that further refines nuclei extraction is necessary to acquiring high levels of cytosolic free, nuclear Tdh3p. In an attempt to address this concern we took an alternative approach to separate nuclei by immunoprecipitation (Nuclear IP) with the magnetic beads conjugated by anti-Nsp1P-IgG instead of simply purifying pure nuclei from the heterogeneous cell lysate. Nsp1p is a porin subunit located on nuclear membranes and which commonly serves as a target for nuclei immunostaining. Crude nuclei were incubated with conjugated beads for 24 hours then lysed. Unfortunately, only heavy and light chains of anti-mouse IgG were detected in nuclear IP product in the absence of 118 KDa Nsp1p fragment, where the crude nuclei fractionation showed the signal **(Fig. 13)**. This indicated that the Nsp1p antibodies were successfully conjugated to the IP bead matrix and were able to recognize the Nsp1p in the crude nuclear fractionation. The attempted purification method ultimately proved to be unsuccessful, however, as it failed to pull down any nuclei from the lysate mixture.

Presence of cloned Tdh3p was unable to restore apoptotic potential to *tdh3Δ* cells

In an attempt to confirm the essential role of a fully functioning Tdh3p in the yeast cells' ability to produce an apoptotic response to heavy metal exposure, it was decided to transform *tdh3Δ* cells with a vector containing a TDH3 gene with the expectation that the newly transformed cells would reacquire their native apoptotic potential. A TDH3-bound shuttle vector (p416-TDH3) was constructed (Materials and Methods) and introduced in to the *tdh3Δ* isogenic yeast mutant cells Transformation of the TDH3 mutant strain was validated using a combination (A)

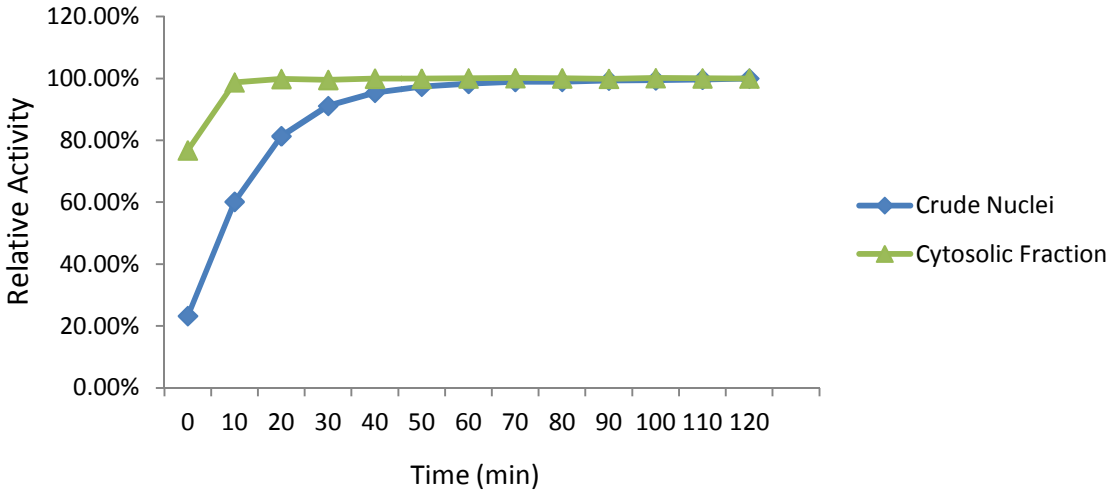

(B)

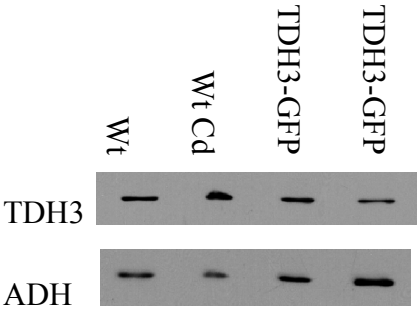

Figure 12: The cytosolic contamination suggested by the presence of ADH in the crude nuclear fraction preparation.

The ADH enzymatic activity **(A)**, as well as the protein expression **(B)**, exists in both the crude nuclear and cytosolic fractionation after performing the crude nuclei fractionation, which indicates the cytosolic contamination of crude nuclei fractionation. Wt: wild type, TDH3-GFP: GFP-tagged TDH3 strain, Cd: cells were treated by Cd.

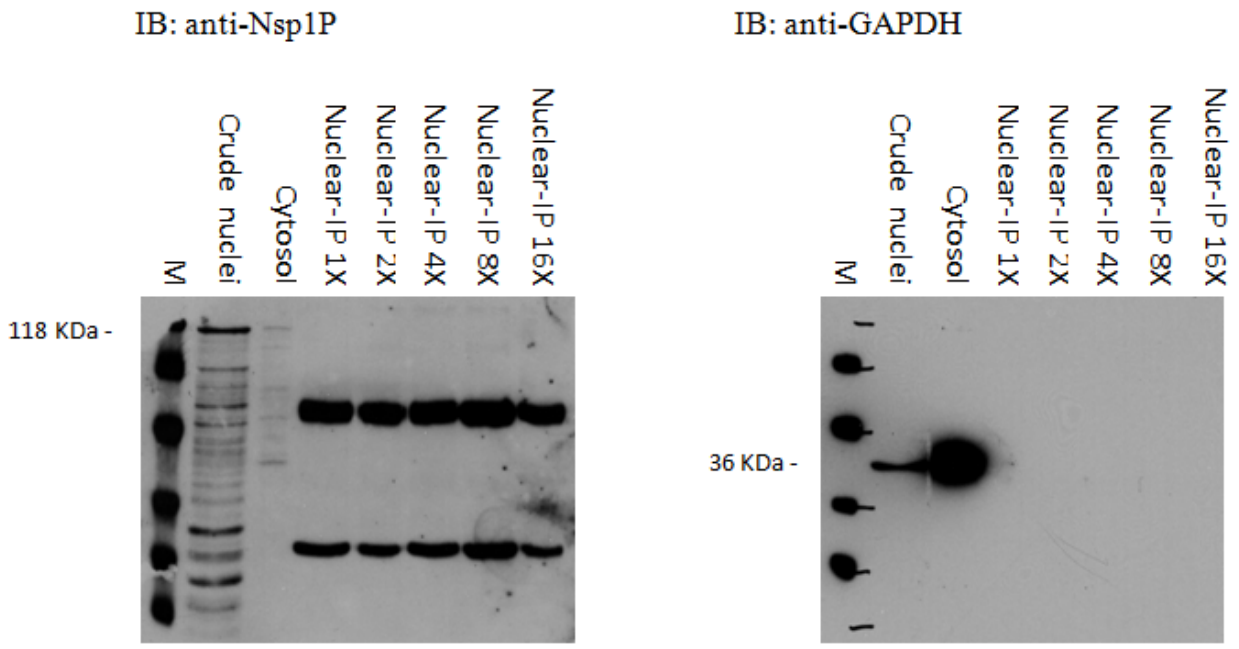

Figure 13: Nsp1p Nuclear-IP is unable to pull down pure nuclei from crude fractionation.

Nsp1p (MW=118KDa) was not present in Nuclear-IP product while no apparent cross-contamination was detected by GAPDH-probed immunoblot. M: protein size marker. Crude nuclei: crude nuclear fractionation. Cytosol: cytosolic fractionation. Nuclear-IP: nuclear IP products diluted from 1 to 16-fold. The size of Nsp1P and GAPDH is shown.

of both quantitative RT-PCR using TDH3-specific primers, designed for this purpose **(Fig. 14A)**- as well as by the detection of increased GAPDH **(Fig. 14B and C)**. As the complementation assays demonstrate, full GAPDH enzyme capability was restored to *tdh3Δ* mutants that had been transformed with vectors bearing the TDH3 gene, but not with just the vector alone. Intriguingly, neither the *tdh3Δ* strain nor its TDH3 transformants demonstrated any significant sign of apoptosis -as defined by DHR123, an indicator of the presence of ROS **(Fig. 15M and N)**, which has previously been shown to be equivalent to an apoptotic response in cells exposed to cadmium. While a relatively small ROS response was observed in a subset of the exposed population of *tdh3Δ* mutant cells that had been transformed with the TDH3-bound vector the levels were equivalent to cells transformed with vector alone **(Fig. 15F and H)**. In an attempt to ensure that there was truly no recovery of apoptotic response the Cd exposure time and concentration were increased above the normal time and concentration to 2 hours and 120 μM, respectively, but to no avail **(Fig. 15)**. Curiously, all cells that had been transformed with the TDH3-GFP appeared to demonstrate excessive potential to promote ROS, regardless of their exposure to cadmium. However, these results are considered to be artifacts of crosstalk in wavelength detection of the cytometers that were unable to distinguish between red (DHR123) and green (GFP) fluorophores. Aside from the result of these TDH3-GFP transformants, all other control experiments yielded expected results, with wild-type cells exhibiting appropriate levels of apoptosis upon Cd treatment, whether or not they had been transformed with vector or vector and TDH3 gene. These data indicate that, while the vector-borne TDH3 expression did not interfere with the normal cadmium-dependent apoptotic response of the wild-type cells (unlike the original transformation of the TDH3-GFP mutant shown in **Fig. 6**), the presence of the vector-encoded TDH3 failed to recover the ability to maintain an apoptotic response when the

(A)

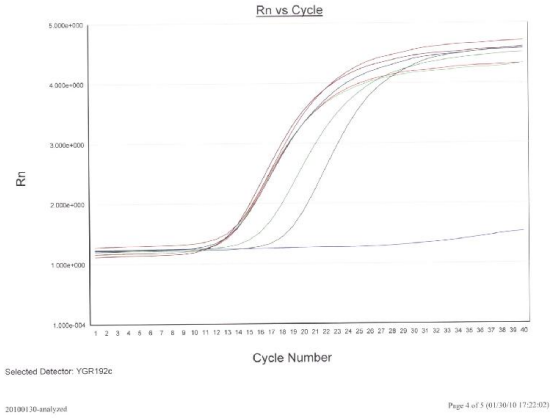
Rn vs Cycle
Rn
Cycle Number
Selected Detector: YGR192c
20180130-analyzed

(B)

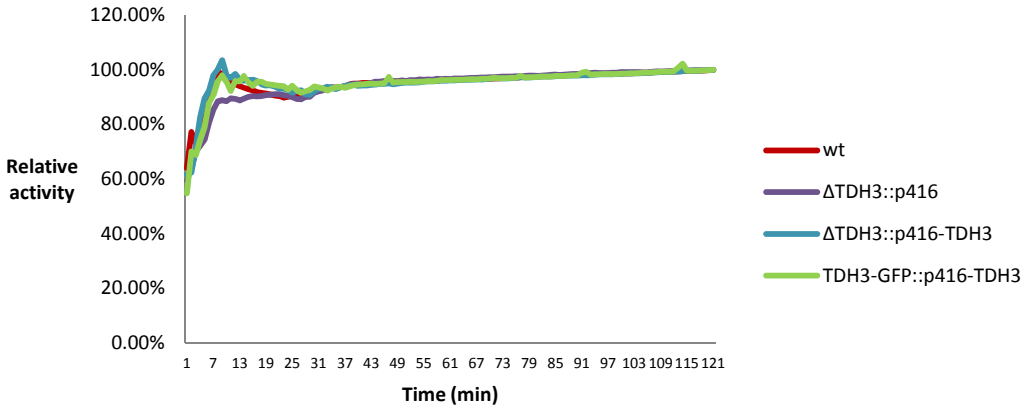
120.00%
100.00%
80.00%
60.00%
40.00%
20.00%
0.00%
Relative activity
1 7 13 19 25 31 37 43 49 55 61 67 73 79 85 91 97 103 109 115 121
Time (min)
wt
ΔTDH3::p416
ΔTDH3::p416-TDH3
TDH3-GFP::p416-TDH3

(C)

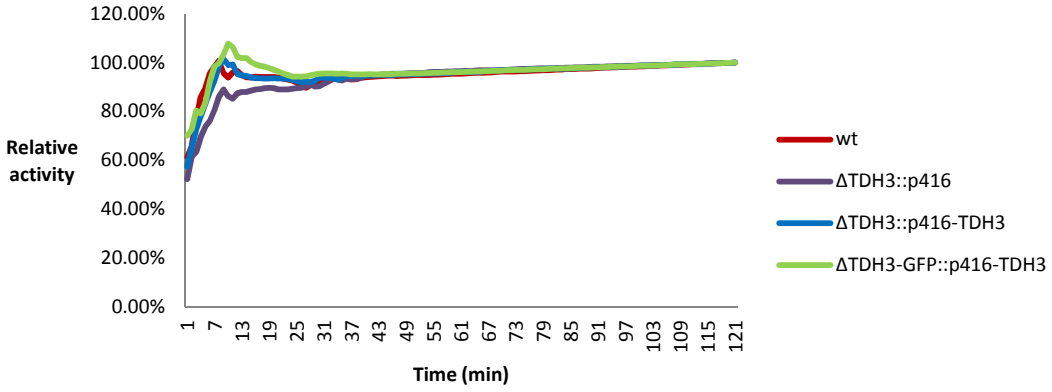
120.00%
100.00%
80.00%
60.00%
40.00%
20.00%
0.00%
Relative activity
1 7 13 19 25 31 37 43 49 55 61 67 73 79 85 91 97 103 109 115 121
Time (min)
wt
ΔTDH3::p416
ΔTDH3::p416-TDH3
ΔTDH3-GFP::p416-TDH3

Figure 14: The complementary test shows functional Tdh3p in *tdh3*Δ hosts.

(A) Transcriptional expression of TDH3 in wild type, TDH3 isogenic mutant and GFP-fused TDH3 strain upon 120 μM Cd treatment for 2 hours plus 2 hours post-incubation. Wild type and TDH3 isogenic mutant without complementation serve as a positive and negative control, which shows the specificity of TDH3 TaqMan probe. Furthermore, the complementary TDH3 was able to express and function since *tdh3*Δ::p416-TDH3 exhibits higher GAPDH enzymatic activity than the untransformed host, independent of whether the cells were untreated **(B)** or treated with cadmium **(C)**.

Strain	120 uM Cd 0+0		120uM Cd 2+2	
wt with p416	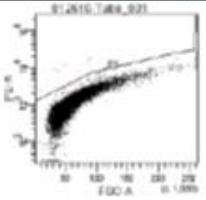	a.	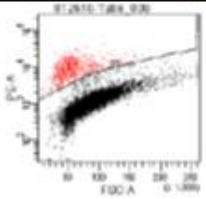	b.
Wt with p416::TDH3	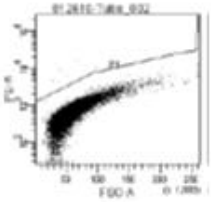	c.	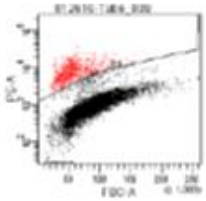	d.
ΔTDH3 with p416	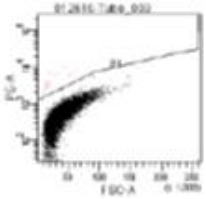	e.	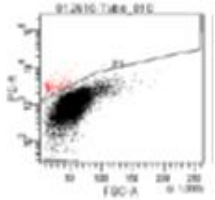	f.
ΔTDH3 with p416::TDH3	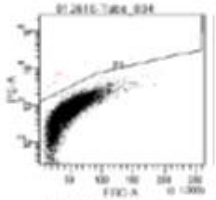	g.	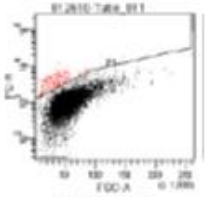	h.
GFP-fused TDH3 With p416	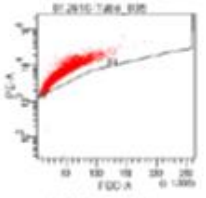	i.	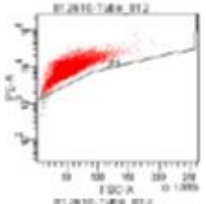	j.
GFP-fused TDH3 With p416::TDH3	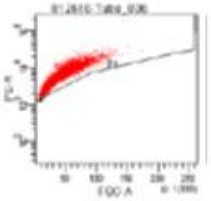	k.	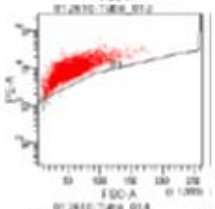	l.
wt	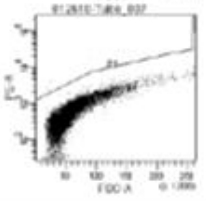	m.	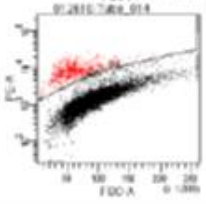	n.

Figure 15: Complementary TDH3 failed to recover *tdh3Δ* from being non-apoptotic after Cd treatment.

The p416::TDH3 construct was transformed to *tdh3Δ* and TDH3-GFP strain to test whether these two complemented strains regained the apoptotic response upon prolonged and intensive Cd treatment. The apoptotic activity was monitored by DHR123, which detects the presence of ROS. The population above the threshold in GFP-TDH3 fusion strain is presumably not due to excessive apoptotic responses, but rather to detection overlap between green and red emission. Fluorescent emissions as the gating criteria had been fixed to determine threshold values for wild type and *tdh3Δ* mutants for consistency. Overall, the expression of cloned Tdh3p was unable restore the apoptotic potential in mutants.

cells were exposed to even excessive amounts of cadmium. In light of these and previous experiments these findings would suggest that chromosomally regulated and transcribed TDH3 is necessary for the cell to mount an apoptotic response to heavy metals. As to what particular aspect of this chromosomal expression is pertinent to the apoptotic phenotype, additional experiments (beyond the scope of this dissertation) using yeast recombination genetics of the TDH3 gene will be necessary.

1.4 Discussion

Glyceraldehyde-3-phosphate dehydrogenase GAPDH (annotated as Tdhp in yeast) is a key enzyme in metabolic pathways. It has also been shown to play many other roles in a variety of organisms beyond that of its fundamental role in glycolysis (see Introduction in this chapter and General Discussion). In higher eukaryotes, the modification of GAPDH is highly associated with the pathogenesis of neurodegenerative disorders. The heparin-induced GAPDH aggregation and amyloid fibrillation acts as a scaffold to incorporate the unfolded α-synuclein into Lewy bodies and reduces the α-synuclein toxicity to neuronal tissues.(34). In contrast, S-nitrosylated GAPDH is responsible for the progression of Alzheimer's Disease, presumably due to the impeded glycolytic activity resulted from the S-nitrosylated catalytic residues, or the cell death-caused interaction with E3-ubiquitin ligase Siah1 (35). In our previous study, Tdh3p, one of the Tdhp isozymes, is one of the metabolic enzymes which is susceptible to oxidative damage upon the metal-induced stress (4). With the observation that the aerobic respiration by using glucose as the carbon source was necessary for triggering apoptotic response after metal treatment (36), we hypothesized that glycolytic pathway is required for metal-induced apoptosis. Curiously, we were able to demonstrate not only that the *tdh3Δ,* but also wild-type cells that contain a TDH3-

GFP fusion effectively lose their potential to undergo apoptosis when exposed to various levels of heavy metals, indicating that Tdh3p plays beyond its glycolytic role in apoptotic response. To confirm that this decreased apoptotic response in cells containing the GFP-tagged Tdh3p was not solely due to a change in its principle, enzymatic role, we assayed the GAPDH activity in wild-type cells and in wild-type cells containing the GFP-tagged Tdh3p. Interestingly, the cells encoding the fusion enzyme showed remarkably similar enzymatic activity to their wild-type counterparts, indicating that the non-apoptotic characteristic in these GFP-tagged cells is unlikely to be due to the depletion in any glycolytic metabolic activities. By considering the pleiotropic role of eukaryotic GAPDH discussed previously, it is reasonable, therefore, to intimate that Tdh3p is potentially involved in some other more regulatory functions in the cell, possibly even as a contributor to signal transduction mechanisms of the apoptotic response -for which it is known in other cellular responses in other organisms. The inability of cells encoding the TDH3-GFP fusion to establish an apoptotic response that was not apparently due to any loss in the specific activity of the enzyme suggested an additional pleiotropic role for Tdh3p, that it was apparently unable to undertake as a fused protein. If this role involved translocation of the Tdh3p in to and out of the nucleus, the acquisition of a bulky GFP tag to the C-terminus of the protein presumably affects a number of activities depending on how the Tdh3p is able to translocate across the nuclear membrane. The GFP tag could interfere with Tdh3p being able to interaction with other proteins in the cytosol that would abrogate translocation across the nuclear membrane, or, once inside the nucleus, the addition of the GFP may interfere with nuclear factor(s) which would disallow it to undertake its normal pro-apoptotic activities.

The nuclear fractionation Tdh3p was crucial for understanding the non-glycolytic role of Tdh3p as a regulator in nucleus. However, regarding its global expression in cellular compartments (28), the cytosolic contamination of Tdh3p leading to the ambiguous implication was inevitable. In an effort to determine the level of contamination obtained using the Ficoll protocol, the abundance of alcohol dehydrogenase (ADH) in the various extracts was monitored. ADH is known to be present only in the cytosolic compartment of yeast and, as such, is widely used as a cytosolic marker to evaluate the degree of cytosolic contamination of the nuclear preparations. Moreover, it is understood that the form in which Tdhp is able to enter the nucleus is not the same form in which it is able to catalyze the dehydrogenation of glyceraldehyde-3-phosphate (37). As a result the relative enzymatic activity of nuclear Tdhp should reflect this change in structure and concomitant decrease in enzyme active. Hence, we assayed the kinetics for these two enzymes in both the cytosolic and nuclear fraction. Both enzymes showed lower activity in the nuclear fraction with little significant differences in their respective activities. As a result, we cannot yet confirm that the GAPDH activity is specific to either the cytosolic contaminant, or the nuclear fraction. In addition, the localization of ADH to the cytoplasm, alone has been challenged: In Alzheimer's disease patients, nuclear ADH is found in abnormal neuronal cells under stress (23). While the localization of ADH is highly associated with the type of carbon sources, ADH also is present in different fractions along with the supplement of glucose or ethanol (38). In *Candida tropicalis*, for example, ADH has been shown to be present in the microsomal, mitochondrial and peroxisomal fractions, presumably to facilitate fatty acid metabolism (39). As a result, the localization of ADH appears to be highly dependent upon on the carbon source on which the cells were grown. To summarize our findings, therefore, notwithstanding the insufficiencies of the purification protocols used, both Adhp and Tdhp

potentially appear in both the cytosolic and nuclear fractions. To analyze further the importance of nuclear translocation of Tdh3p in response to heavy metal exposure either a greater degree of purity in obtaining nuclear fractions is required, or a more definitively cytosolic protein marker(s) needs to be found.

To overcome the inevitable contamination of cytosolic Tdh3p following the protocol described above, the idea of "nuclei-sorting" was proposed by reviewing related studies (40). In so doing, any requirement for pure nuclear fraction was removed since cytosolic Tdh3p, or non-nuclear, co-localized Tdh3p, is unable to form the compartment that is necessary to harbor the fluorescent dye and be detected through flow cytometry. Preliminary evaluation does show that this methodology would appear to be adequate to differentiate between the nuclear populations labeled with different fluorophore **(Fig. 9)**. As a consequence, the sample obtained from the TDH3-GFP encoding cells was treated with incremental increases of Cd. Curiously, the relative number of Tdh3p-localized nuclei increased with increasing Cd concentration **(Fig. 10)**. These findings do suggest that the addition of GFP tag on generic Tdh3p had no effect on its nuclear shuttling, and the nuclear Tdh3p is indeed an important factor in the Cd-induced response. Whether or not the level of translocation was sufficient to yield optimal cellular response, or the GFP tag affected the generic function of nuclear Tdh3p, however, has not yet been established and would require further, more quantitative analysis. Moreover, as discussed in the introduction, the intracellular translocation of GAPDH is determined by the metabolic or physiological response to external effects (41, 42). Thus, it is possible that the presence of GAPDH, or rather Tdhp, in the nucleus is potentially an artifact of the different cellular fractionation techniques that have been performed. Consequently, even though this uncertainty needs greater resolution in

the future work, and more sensitive and discriminating techniques can be brought to bear to detect and analyze trans-localized proteins.

As of the uncertainties described above, we decided to ensure the role of Tdh3p in apoptotic response by complementary test. The transcription of TDH3 was found in *tdh3*Δ strain carrying wild type TDH3 fragment carried by p416 shuttling vector **(Fig. 14A)**, but the apoptotic character was still not apparent in cells upon treatment with Cd **(Fig. 15G and H)**. We cannot completely rule out the possibility that Tdh3p expression was impeded in translational level even though the TDH3-complemented stain showed higher GAPDH activity than uncomplemented one. However, there is currently no feasible way to unambiguously monitor the translational expression of Tdh3p by immunoblot since antibodies against GAPDH cannot differentiate between Tdh3p and any of the other two isoenzymic forms as they share ~98% peptide sequence identity with each other. We initially believed that we could circumvent this problem by tagging a recognizable marker on Tdh3p, but these efforts were stymied by finding that even wild-type yeast cells become non-apoptotic following the insertion of the carboxyl terminus of Tdh3p-GFP. While such addition of GFP tag does not appear to effect the enzymatic activity, it apparently does modulate the ability of Tdhp (and in particular Tdh3p) to allow for a typical apoptotic cellular response. With respect to the recovery of GAPDH activity after complementation, it could result from a changed expression of the other two Tdh isoenzymes (Tdh1p and Tdh2p) in being able to compensate for the absence of Tdh3p. At this stage, we can only be assured of the decreased transcriptional expression of the TDH3 gene, but not the enzymatic activity of GAPDH in the complementary *tdh3*Δ strain.

In this chapter, we have been able to demonstrate conclusively that Tdh3p is involved in the heavy metal-induced response of *S. cerevisiae* to the presence of cadmium. The *tdh3*Δ and TDH3-GFP fusion strain were non-apoptotic indicating that the native form of Tdh3p, not simply the GAPDH activity, is required for the cells to undertake their normal metal-induced apoptotic response. In addition, while trying to quantify the translocation of Tdh3p into the nucleus we have been able to demonstrate that that the translocation of Tdh3p into the nucleus upon the Cd exposure is part of the cellular response to the heavy metal, cadmium, with Tdh3p potentially acting as a signal protein rather than a glycolytic enzyme. Even though the detailed pro-apoptotic role of Tdh3p still needs additional clarification, the association of Tdh3p and its translocation into the nucleus upon increased temporal exposure to Cd has been accomplished.

References

1. Alberts B (2008) Molecular biology of the cell. Chapter 18 Apoptosis: Programmed Cell Death Eliminates Unwanted Cells, ed Alberts BJ, Alexander; Lewis, Julian; Raff, Martin; Roberts, Keith; Walter, Peter (Garland Science, New York), 5th Ed, p 1115.

2. Everett H & McFadden G (1999) Apoptosis: an innate immune response to virus infection. *Trends in microbiology* 7(4):160-165.

3. Hyka-Nouspikel N*, et al.* (2012) Deficient DNA damage response and cell cycle checkpoints lead to accumulation of point mutations in human embryonic stem cells. *Stem cells* 30(9):1901-1910.

4. Shanmuganathan A (2008) An Analysis of Glycolytic Enzymes in the Cellular Response to Metal Toxicity. PhD (Georgia State University).

5. Madeo F*, et al.* (2004) Apoptosis in yeast. *Curr Opin Microbiol* 7(6):655-660.

6. Shanmuganathan A, Avery SV, Willetts SA, & Houghton JE (2004) Copper-induced oxidative stress in Saccharomyces cerevisiae targets enzymes of the glycolytic pathway. *FEBS Lett* 556(1-3):253-259.

7. Barbosa MS*, et al.* (2006) Glyceraldehyde-3-phosphate dehydrogenase of Paracoccidioides brasiliensis is a cell surface protein involved in fungal adhesion to extracellular matrix proteins and interaction with cells. *Infect Immun* 74(1):382-389.

8. Tarze A*, et al.* (2007) GAPDH, a novel regulator of the pro-apoptotic mitochondrial membrane permeabilization. *Oncogene* 26(18):2606-2620.

9. Zheng L, Roeder RG, & Luo Y (2003) S phase activation of the histone H2B promoter by OCA-S, a coactivator complex that contains GAPDH as a key component. *Cell* 114(2):255-266.

10. Nakagawa T*, et al.* (2003) Participation of a fusogenic protein, glyceraldehyde-3-phosphate dehydrogenase, in nuclear membrane assembly. *The Journal of biological chemistry* 278(22):20395-20404.

11. Sundararaj KP*, et al.* (2004) Rapid shortening of telomere length in response to ceramide involves the inhibition of telomere binding activity of nuclear glyceraldehyde-3-phosphate dehydrogenase. *The Journal of biological chemistry* 279(7):6152-6162.

12. Krynetski EY, Krynetskaia NF, Bianchi ME, & Evans WE (2003) A nuclear protein complex containing high mobility group proteins B1 and B2, heat shock cognate protein 70, ERp60, and glyceraldehyde-3-phosphate dehydrogenase is involved in the cytotoxic response to DNA modified by incorporation of anticancer nucleoside analogues. *Cancer Res* 63(1):100-106.

13. Liu W, Wang J, Mitsui K, Shen H, & Tsurugi K (2002) Interaction of the GTS1 gene product with glyceraldehyde- 3-phosphate dehydrogenase 1 required for the maintenance of the metabolic oscillations of the yeast Saccharomyces cerevisiae. *Eur J Biochem* 269(14):3560-3569.

14. Kim S, Lee J, & Kim J (2007) Regulation of oncogenic transcription factor hTAF(II)68-TEC activity by human glyceraldehyde-3-phosphate dehydrogenase (GAPDH). *Biochem J* 404(2):197-206.

15. Hara MR*, et al.* (2006) Neuroprotection by pharmacologic blockade of the GAPDH death cascade. *Proc Natl Acad Sci U S A* 103(10):3887-3889.

16. Ishitani R*, et al.* (1996) An antisense oligodeoxynucleotide to glyceraldehyde-3-phosphate dehydrogenase blocks age-induced apoptosis of mature cerebrocortical neurons in culture. *J Pharmacol Exp Ther* 278(1):447-454.

17. Ishitani R*, et al.* (1996) Evidence that glyceraldehyde-3-phosphate dehydrogenase is involved in age-induced apoptosis in mature cerebellar neurons in culture. *J Neurochem* 66(3):928-935.

18. Sawa A, Khan AA, Hester LD, & Snyder SH (1997) Glyceraldehyde-3-phosphate dehydrogenase: nuclear translocation participates in neuronal and nonneuronal cell death. *Proc Natl Acad Sci U S A* 94(21):11669-11674.

19. Ishitani R, Sunaga K, Tanaka M, Aishita H, & Chuang DM (1997) Overexpression of glyceraldehyde-3-phosphate dehydrogenase is involved in low K+-induced apoptosis but not necrosis of cultured cerebellar granule cells. *Mol Pharmacol* 51(4):542-550.

20. Saunders PA, Chen RW, & Chuang DM (1999) Nuclear translocation of glyceraldehyde-3-phosphate dehydrogenase isoforms during neuronal apoptosis. *J Neurochem* 72(3):925-932.

21. Tatton NA (2000) Increased caspase 3 and Bax immunoreactivity accompany nuclear GAPDH translocation and neuronal apoptosis in Parkinson's disease. *Exp Neurol* 166(1):29-43.

22. Maruyama W, Oya-Ito T, Shamoto-Nagai M, Osawa T, & Naoi M (2002) Glyceraldehyde-3-phospate dehydrogenase is translocated into nuclei through Golgi apparatus during apoptosis induced by 6-hydroxydopamine in human dopaminergic SH-SY5Y cells. *Neurosci Lett* 321(1-2):29-32.

23. Cumming RC & Schubert D (2005) Amyloid-beta induces disulfide bonding and aggregation of GAPDH in Alzheimer's disease. *FASEB journal : official publication of the Federation of American Societies for Experimental Biology* 19(14):2060-2062.

24. Huang J*, et al.* (2009) Involvement of glyceraldehyde-3-phosphate dehydrogenase in rotenone-induced cell apoptosis: relevance to protein misfolding and aggregation. *Brain Res* 1279:1-8.

25. Nakajima H*, et al.* (2007) The active site cysteine of the proapoptotic protein glyceraldehyde-3-phosphate dehydrogenase is essential in oxidative stress-induced aggregation and cell death. *The Journal of biological chemistry* 282(36):26562-26574.

26. Colell A*, et al.* (2007) GAPDH and autophagy preserve survival after apoptotic cytochrome c release in the absence of caspase activation. *Cell* 129(5):983-997.

27. Rathmell JC & Kornbluth S (2007) Filling a GAP(DH) in caspase-independent cell death. *Cell* 129(5):861-863.

28. McAlister L & Holland MJ (1985) Isolation and characterization of yeast strains carrying mutations in the glyceraldehyde-3-phosphate dehydrogenase genes. *The Journal of biological chemistry* 260(28):15013-15018.

29. Chiarugi A (2005) "Simple but not simpler": toward a unified picture of energy requirements in cell death. *FASEB journal : official publication of the Federation of American Societies for Experimental Biology* 19(13):1783-1788.

30. Elmore S (2007) Apoptosis: a review of programmed cell death. *Toxicologic pathology* 35(4):495-516.

31. Freude B*, et al.* (2000) Apoptosis is initiated by myocardial ischemia and executed during reperfusion. *Journal of molecular and cellular cardiology* 32(2):197-208.

32. Mumberg D, Muller R, & Funk M (1995) Yeast vectors for the controlled expression of heterologous proteins in different genetic backgrounds. *Gene* 156(1):119-122.

33. Bergmeyer HV, Gacoehm, K. and Grassl, M. (1974) *Methods of Enzymatic Analysis* (Academic Press, New York).

34. Torres-Bugeau CM*, et al.* (2012) Characterization of heparin-induced glyceraldehyde-3-phosphate dehydrogenase early amyloid-like oligomers and their implication in alpha-synuclein aggregation. *The Journal of biological chemistry* 287(4):2398-2409.

35. Zahid S, Khan R, Oellerich M, Ahmed N, & Asif AR (2014) Differential S-nitrosylation of proteins in Alzheimer's disease. *Neuroscience* 256:126-136.

36. Nargund AM, Avery SV, & Houghton JE (2008) Cadmium induces a heterogeneous and caspase-dependent apoptotic response in Saccharomyces cerevisiae. *Apoptosis* 13(6):811-821.

37. McAlister L & Holland MJ (1985) Differential expression of the three yeast glyceraldehyde-3-phosphate dehydrogenase genes. *The Journal of biological chemistry* 260(28):15019-15027.

38. Heick HM, Willemot J, & Begin-Heick N (1969) The subcellular localization of alcohol dehydrogenase activity in baker's yeast. *Biochimica et biophysica acta* 191(3):493-501.

39. Yamada T, Nawa H, Kawamoto S, Tanaka A, & Fukui S (1980) Subcellular localization of long-chain alcohol dehydrogenase and aldehyde dehydrogenase in n-alkane-grown Candida tropicalis. *Archives of microbiology* 128(2):145-151.

40. Roberts AV (2007) The use of bead beating to prepare suspensions of nuclei for flow cytometry from fresh leaves, herbarium leaves, petals and pollen. *Cytometry. Part A : the journal of the International Society for Analytical Cytology* 71(12):1039-1044.

41. Seidler NW (2013) Compartmentation of GAPDH. *Advances in experimental medicine and biology* 985:61-101.

42. Sirover MA (2012) Subcellular dynamics of multifunctional protein regulation: mechanisms of GAPDH intracellular translocation. *Journal of cellular biochemistry* 113(7):2193-2200.

CHAPTER 2.

A SIMPLE AND RAPID METHOD TO MONITOR AUTOPHAGY IN *Saccharomyces cerevisiae* USING FLOW CYTOMETRY

Pei-Ju Chin

Abstract

Over the last few decades a number of methodologies have been developed to analyze the various parameters that modulate the autophagic process in yeast. Many of these methods, however, provide only a static evaluation of what is essentially a series of dynamic, cellular changes. Herein, we propose a quantitative, flow cytometry-based method to analyze the dynamic phases of autophagy in yeast cells, which assesses two of the major cellular characteristics of autophagy; an increase in cellular complexity and granularity within the cell. The method is relatively rapid and more direct than many of the methodologies employed to date. Moreover, while this cytometric method cannot always provide the specificity of some of the more commonly used techniques, our findings indicate that it is remarkably sensitive to the various changes in autophagic flow, and offers an inexpensive evaluation of autophagy, as well as a useful augmentation to many of the more expensive methodologies that are currently in use.

2.1 Introduction

Cellular stress in Saccharomyces cerevisiae induces a variety of responses, which often include the recycling of used and damaged cellular components to provide the metabolic and structural building blocks for the generation and maintenance of viable cellular organelles. Predominant among the different mechanisms that promote the re-utilization of these cellular components is autophagy, a "self-eating", self-regulating pathway designed to promote the organized movement of intracellular materials (marked for degradation) through a series of steps to promote their ultimate degradation in the lysosome (1). As such, autophagy has been shown to be an essential cellular response against a number of cellular stressors such as nitrogen depletion (2), starvation (3), and cellular damage resulting from mis-folded proteins (4), and has been found to play a critical role in counteracting the cellular mechanisms of apoptosis -a "self-killing" programme (5).

The autophagic pathway in *S. cerevisiae* has been well studied since it was first investigated in S. cerevisiae (6). Stress induction of the pathway triggers the sequestration of cellular components from the cytoplasm to the vacuoles via the CVT (cytoplasm to vacuole targeting) pathway (7, 8). Briefly, this cascade involves the aggregation of precursor vacuolar hydrolases aminopeptidase I (prApe1), along with intracellular contents, which associate with the single membrane vesicle called pre-autophagosomal structure (PAS). PAS further engulfs the cellular components to form a double membrane autophagosome. The maturation of this structure from PAS to autophagosome involves the activity of a series of autophagic proteins (**Fig. 16**): Atg4p, a cysteine protease cleaves Atg8p to expose its C-terminal glycine residue (9), which promotes its conjugation with Atg7p, and further modification -the acquisition of a

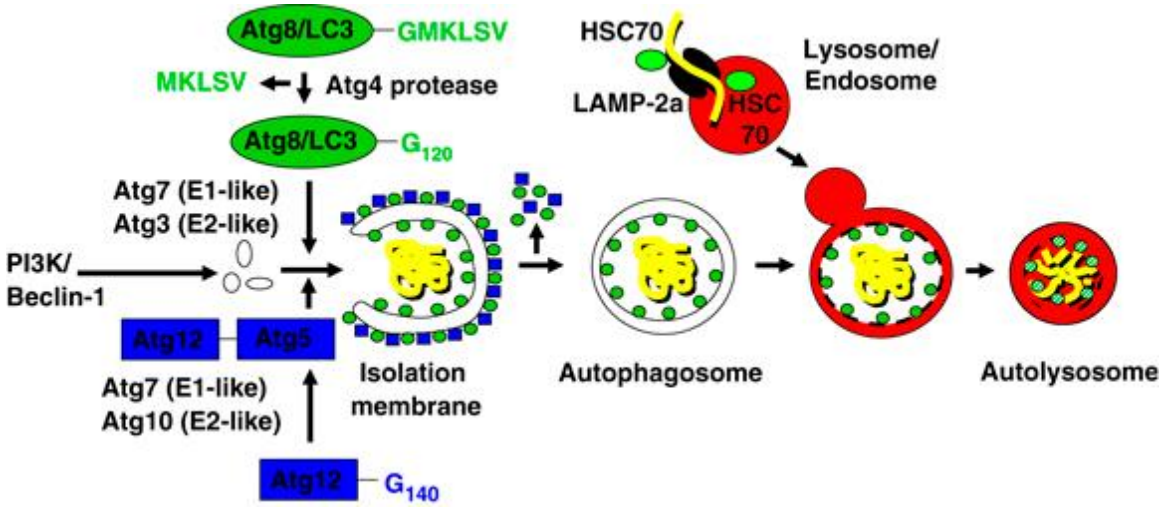

Figure 16: Atg4, Atg6 and Atg8 are involved in the maturation of autophagosome biosynthesis (12).

phosphatidylethanolamine (PE) group- through the actions of Atg3p and the Atg5p-Atg12p complex. The lipidized Atg8-PE (corresponding to the LC3-II in mammalian cells) is subsequently anchored to the PAS phagophore. This structure, along with a dimer of the Atg5p-Atg12p-Atg16p complex, is essential to enlarge the PAS and facilitate the maturation of the autophagosome (10, 11). The autophagic process is complete when the mature autophagosome fuses with the lysosome, and its contents are ultimately lysed by lysosomal enzyme and the mature prApe1p (mApe1p). Following the fusion of the autophagosome with the lysosome, the lipidized Atg8-PE is then recycled by the removal of the PE ligand, a task that is accomplished by the same protease that initiated the original activation of Atg8p, Atg4p.

The autophagic process has been shown to be highly susceptible to a number of chemicals and drugs, many of which are known to target proteins that regulate protein kinase A/cAMP signaling pathways (13-15). In this regard, rapamycin (sirolimus), an immunosuppressant drug that is commonly used for patients who have undergone an organ transplant, has been used with considerable effect to study autophagy (5, 16). Rapamycin is able to induce the autophagic response in yeast, and other systems, by inhibiting the kinase activity of the central signalling protein, Tor, which (among other things) modulates the inactivation of Atg13p. In so doing, rapamycin effectively maintains Atg13p in a hyper-phosphorylated state, allowing it to complex with Atg1p and Atg17p and trigger the vesicle nucleation of pre-autophagic structures (PAS), and ultimately augment the maturation of resulting autophagosomes (**Fig. 17A**) (5).

(A)

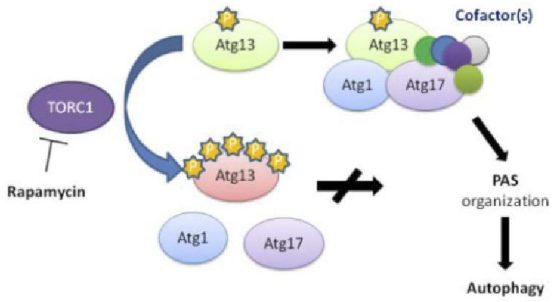

(C)

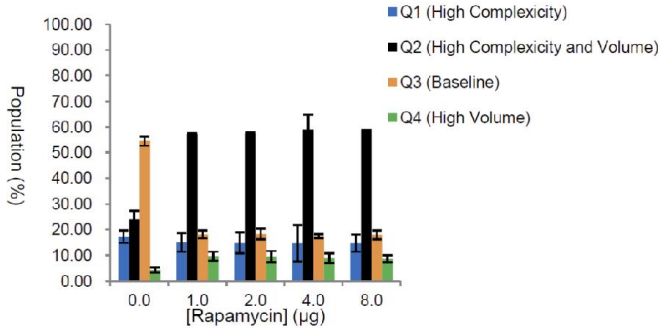

(B)

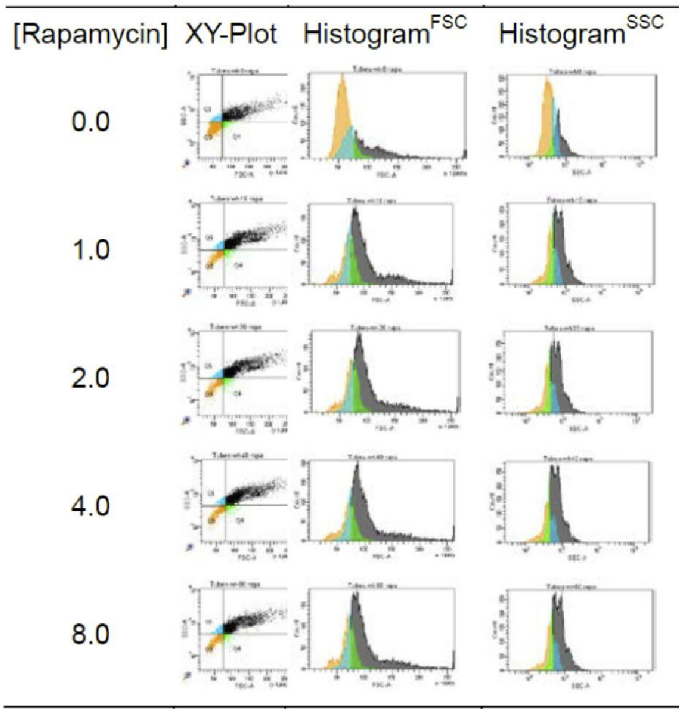

Figure 17: Rapamycin induces autophagy.

(A) A schematic showing the mechanism through which rapamycin is thought to induce autophagy in *S. cerevisae*. By inhibiting the action of the Tor1 subunit in the TORC1 complex rapamycin maintains Atg13 in a hypo-phosphorylated condition, which is able to recruit Atg1p and other downstream cofactors to initiate PAS organization, resulting in autophagy. **(B)** A series of plots showing the forward scatter (FSC) and side scatter (SSC) disposition of a population of

S. cerevisiae BY4741 wild type strain following with different concentrations of rapamycin and cytometric analysis on BD Fortessa™ flow cytometer. Gating was set according to the gravity center of population. The quadrant is designated as Q1 (blue), Q2 (black), Q3 (orange) and Q4 (green), which represent the population with high complexity, high cellular volume and complexity, low cellular volume and complexity, and high cellular volume, respectively. The quantitative analyses of these results are shown as histograms in **Panel C**.

While an understanding of autophagy has proven to be an important aspect of characterizing various cellular responses to environmental insults, there remain only a few methods available that used to monitor the different aspects of the autophagic process. Among the most commonly used methods are image-based assays; transmission electron microscopy - specifically designed to observe the formation of autophagosome or autophagic bodies directly (2), and fluorescence microscopy, in which fluorophores (such as monodansylcadaverine; MDC)(17) and acridine orange (18)) are used to specifically label autophagosomes. While the EM images afford a detailed snap-shot of the autophagic activities within a cell, the set-up and image analysis protocols are not trivial. In contrast, the use of fluorescence is simpler. However, a number of concerns have been raised as to the specificity of the fluorophores -with some indications that MDC and acridine orange, for example, have the potential to label other acidic organelles (mitochondria and lysosomes), resulting in a misrepresentation of the cellular events(16). In addition to these image-based assays, molecular-probe assays have proven to give a more quantifiable determination of the different stages of the autophagic process. These techniques primarily serve to discern the levels of autophagic proteins, such as Atg8-PE and/or Atg8 (orthologs of LC3-I and LC3-II, respectively, in the autophagic pathway of mammalian cells). Higher ratios of Atg8-PE to Atg8 indicate that the autophagic flow has been induced since Atg8-PE is mainly found in cells harboring autophagosomes (19). Even through the monitoring of critical autophagic proteins that have been immunolabelled has been commonly used, and is considered to be one of the more sensitive measures of autophagic flow, immuno- assays are time-consuming and highly labor-intensive since the crude forms of the tagged protein needs to be harvested from the treated cells. Moreover, the dynamic, temporal tracking of identical

populations of cells following different treatments is not feasible in these kinds of studies due to the requirement for the cells to be lysed.

In this study, we propose a relatively rapid and convenient method for the quantification and dynamic assessment of autophagy using flow cytometry. We demonstrate that a sub population of yeast cells undergoes a marked increase in its cellular volume and complexity when exposed to minimal concentrations of rapamycin for only an hour or so. We further demonstrate, through cell sorting technology, that the heightened levels of cell volume and cellular complexity within this sub population are commensurate with increased autophagosome formation. Furthermore, in testing some of the limitations of this relatively simple assay we demonstrate its sensitivity and reliability for detecting the autophagic response in yeast cells, and that the method compares favourably to more standard assays for detecting autophagy; including the immuno-blot analysis of Atg8-PE / Atg8 ratios and fluorescent imaging. Accordingly, we propose that this flow cytometric-based assay for autophagy provides a rapid, yet sensitive alternative to many of the more labour intensive methods that are currently employed.

2.2 Materials and Methods

Cultures, Media, and Treatments

Saccharomyces cerevisiae BY4741 parental wild type (*MATα his3Δ1 leu2Δ0 met15Δ0 ura3Δ0*) or isogenic autophagic mutants (atg4Δ, atg6Δ, and atg8Δ) were obtained from Euroscarf. The yeast cells were cultured in 5 mL YEPD broth [2 % (w/v) peptone (BD), 1 % (w/v) yeast extract (BD) and 2 % (w/v) dextrose (Sigma-Aldrich)] overnight for seeding purpose, followed by inoculating in 100 mL YEPD broth and incubated at 30 ^{o}C with 250

rpm shaking. The cells in early-log phase (OD_{600}= 1.8 ~2) were harvested and exposed to various concentration (0.0~8.0 μg) of rapamycin (Sigma-Aldrich) to induce autophagy. When necessary, the cells were treated with 30 μM cadmium nitrate (Sigma-Aldrich) for 1 hour to induce apoptosis response, followed by a washing of the cells and a 3 hours post-incubation period to allow time for any subsequent apoptotic responses to unfold.

Crude Protein Extraction

20 mL of cell culture was harvested, washed and re-suspended in 200 μL lysis buffer containing 1 % (w/v) SDS, 8 M urea, 10 mM Tris-HCl, pH 6.8, 10 mM EDTA, and Protease Inhibitor Cocktail (Roche). The cells were lysed by mechanical disruption using 500 μm acid-washed glass beads (Sigma-Aldrich). The cell debris was discarded, and the concentration of crude protein lysate was quantified by standardized, DC protein assays (BioRad)

SDS-PAGE and Western Blot

SDS-PAGE electrophoresis and Western blot techniques were applied to quantify the expression Atg8-PE / Atg8 ratio. 100 μg protein lysate dissolved in Laemmli buffer was denatured in boiled water, loaded on to a 15 % SDS-PAGE gel, and allowed to electrophoresis before being transferred to PVDF membrane (BioRad) by a routine electrical blotting protocol (20 volts for overnight). For primary probing, the customized Atg8 antiserum, harvested from rabbit (Abgent), was diluted 100 fold in PBS-0.1 % Tween-20 (PBS-T) with 5 % skim milk (EMD Biochemicals), followed by probing with anti-rabbit-IgG with HRP conjugation (Pierce) The image was developed by ECL Western Blot Substrate (Pierce) and detected by LAS-4000^{TM}

chemiluminescence imager (GE Bioscience). The intensity was quantified by MultiGauge™ version 2.3 software (FujiFilm).

Flow Cytometry and Cell Sorting

The untreated or treated cells were diluted 20-fold in YEPD medium. When necessary, the cells were stained with propidium iodine to quantify the population of cell death due to apoptosis or necrosis. The cell samples were then applied to a LSRFortessa™ cell analyzer (BD Biosciences) to quantify and differentiate the population percentage according to the cell volume and complexity, which are detected by forward and side scatter. When necessary, the non-autophagic and autophagic populations were sorted and harvested by FACSAria II™ cell sorter (BD Biosciences) based on the gating of cell complexity. Approximately forty-million cells were harvested for each population analysis in order to obtain sufficient quantity of protein lysate for immunoblot analysis.

2.3 Results

Rapamycin treatment does not result in increased cytotoxicity

In order to remove any concern that the levels of rapamycin used to induce autophagy could lead to cytotoxic events, such as apoptosis or necrosis, wild type S. cerevisiae were treated with varying concentrations of rapamycin (ranging from 0.0 ug to 8.0 μg) for up to 2 hours. After this time the cells were stained with propidium iodide (PI) to detect any apoptotic or necrotic effects of the drug (as per previous studies (20); **Fig. 18)**. No anomalous increase in PI binding was detected, even following exposure to the highest concentration of rapamycin (8.0 μg). These data indicate that rapamycin had no discernable cytotoxic effects over the range of

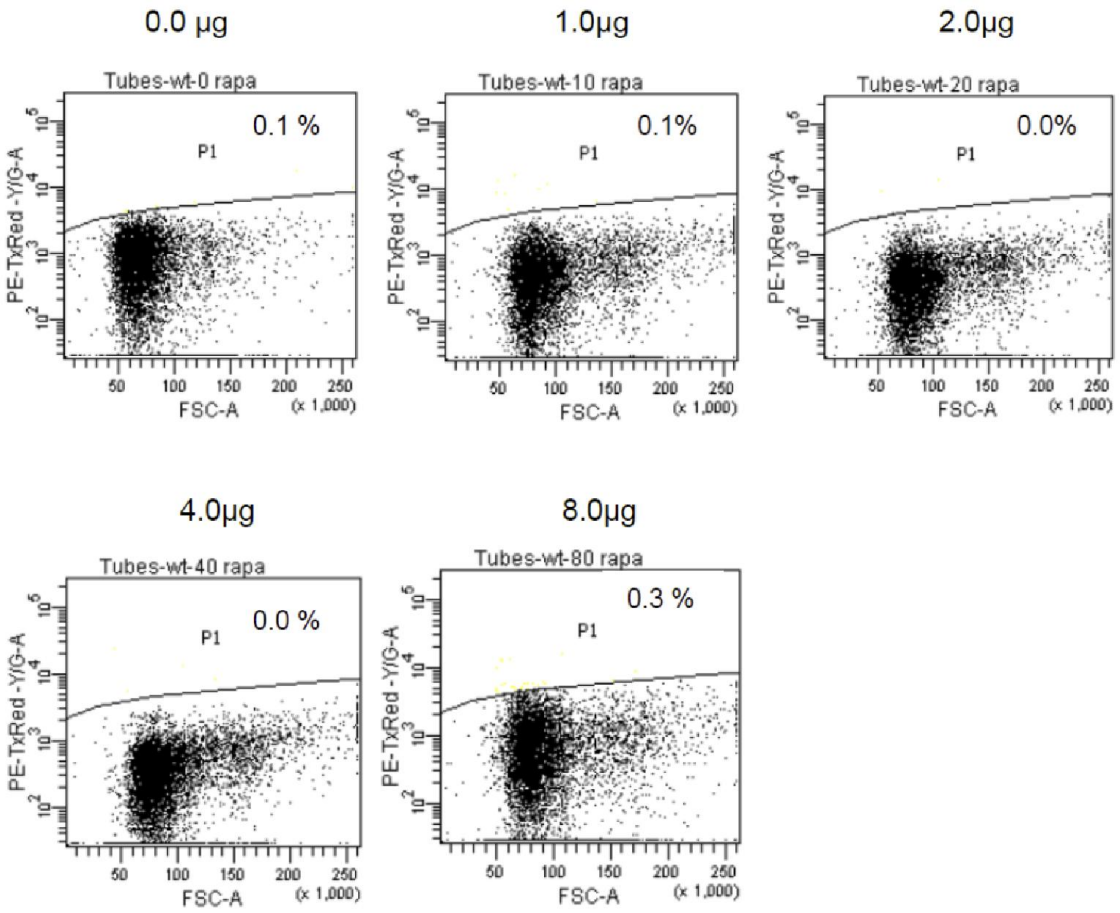

Figure 18: Rapamycin has no discernible cytotoxic effect on *S. cerevisiae.*

S. cerevisiae BY4741 wild type strain were treated with different concentration of rapamycin as indicated. The samples were stained using propidium iodine and subjected to flow cytometry to count the percentage of apoptotic or necrotic population (P1) according to previous published procedures (20).

concentrations used under the experimental conditions that were being tested. These data also demonstrated that even the addition of 1.0 μg rapamycin caused a sub population of cells to exhibit significantly greater amounts of side scatter, which would be consistent with their undergoing an increase in autophagosomal activity (**Fig. 17B and C**).

Increase in response to rapamycin associated with autophagy

As rapamycin treatment has been shown to alter the cellular volume and complexity profiles of the wild-type cell population, we further tested whether or not rapamycin was also able to alter the Atg8-PE to Atg8 ratio in a similar way. The Atg8-PE/Atg8 increased in wild-type cells upon rapamycin treatment (**Fig. 19A and B**). To confirm that this change in Atg8-PE/Atg8 was due to autophagic activity within the treated cells, the relative presence of Atg8-PE and Atg8 was also determined in two autophagic mutant strains, *atg4*Δ, *atg6*Δ, which had been treated in a similar way with rapamycin. The results depicted in **Figure 19A and B** show that the Atg8-PE to Atg8 ratio in these mutant background was significantly lower than their wild-type counterparts, indicating that the absence of either of these two, requisite autophagic genes abrogated the normal autophagic cellular response to the presence of rapamycin.

The same cell samples, along with samples from the additional *atg8*Δ mutant strain (used as labelling controls in the previous experiment), were also assayed for changes in cellular complexity in an attempt to demonstrate changes in their population profiles upon rapamycin treatment. No changes were discerned (**Fig. 20C and F**). Prior to treatment with rapamycin, the cytometric profile of cells demonstrated that the majority of cells in each strain were predominantly present in the lower left quadrant (Q3).

(A)

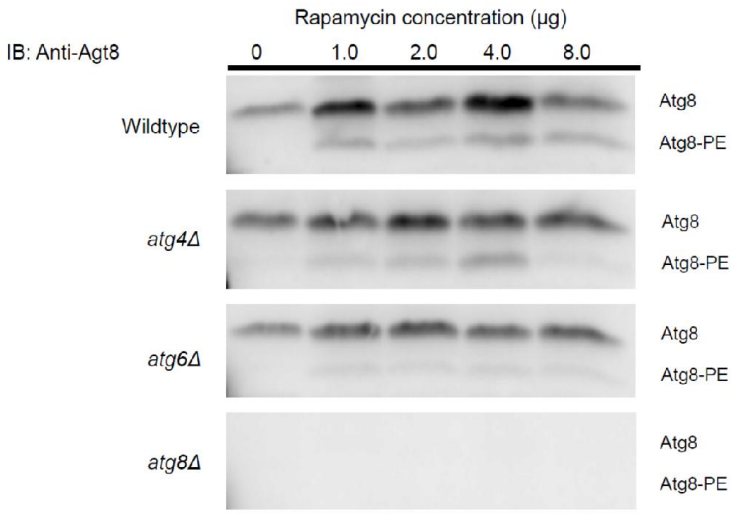

(B)

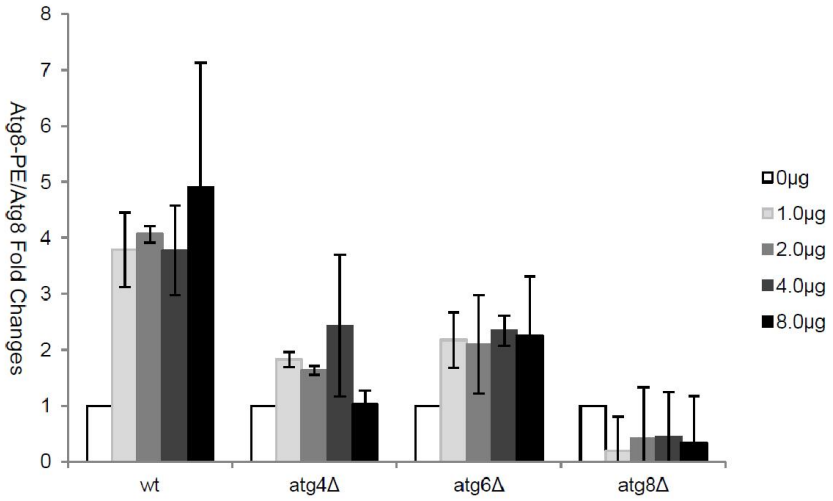

Figure 19: Atg8-PE to Atg-8 ratio was increased upon rapamycin treatment.

(A) *S. cerevisiae* wild type and autophagic mutant *atg4*Δ, *atg6*Δ, and *atg8*Δ were untreated or treated by various concentration of rapamycin as indicated. Crude protein lysate was harvested and subjected to Western blot analysis by probing with anti-Atg8 serum. **(B)** Unlike wild-type cells, none of the autophagic mutants showed any significant increase in Atg8-PE / Atg8 upon treatment with rapamycin. The results were quantified, with the data being normalized to the Atg8-PE to Atg8 ratios of untreated cells.

(A)

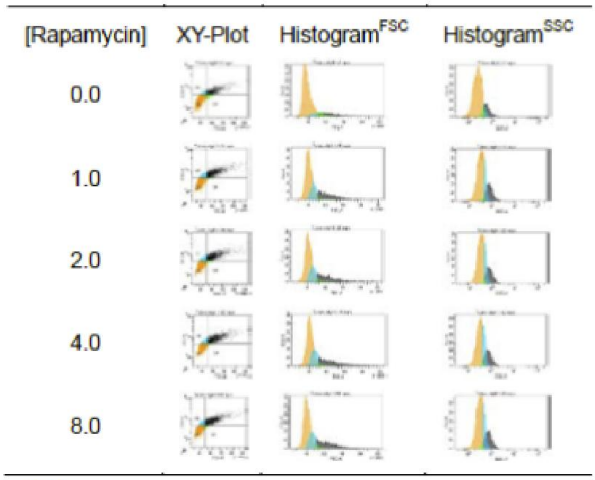
[Rapamycin]
XY-Plot
Histogram FSC
Histogram SSC
0.0
1.0
2.0
4.0
8.0

(B)

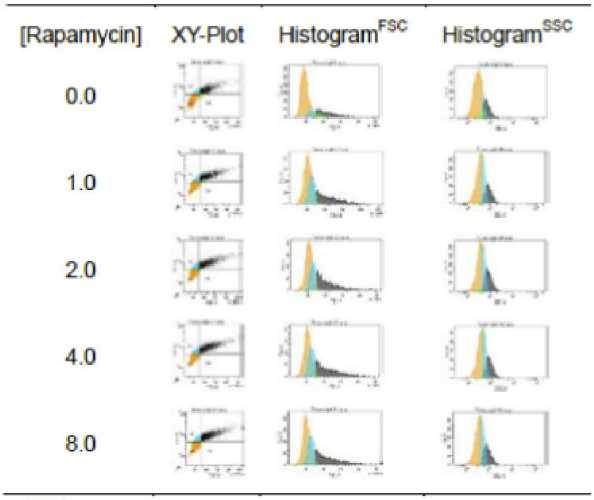
[Rapamycin]
XY-Plot
Histogram FSC
Histogram SSC
0.0
1.0
2.0
4.0
8.0

(C)

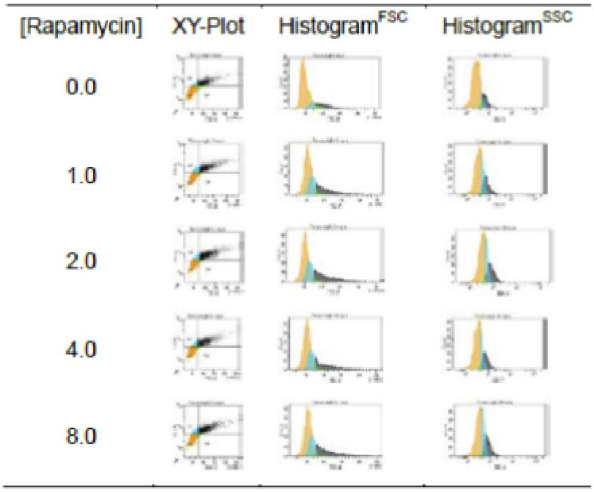
[Rapamycin]
XY-Plot
Histogram FSC
Histogram SSC
0.0
1.0
2.0
4.0
8.0

(D)

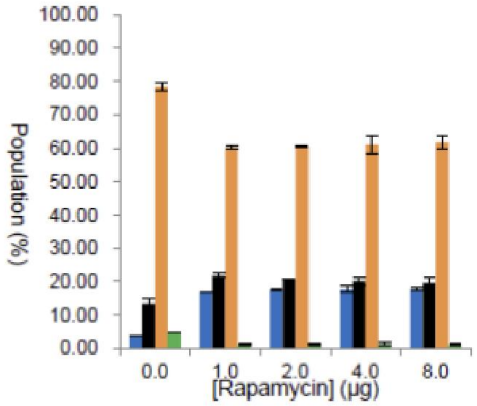
Population (%)
100.00
90.00
80.00
70.00
60.00
50.00
40.00
30.00
20.00
10.00
0.00
0.0
1.0
2.0
4.0
8.0
[Rapamycin] (µg)

(E)

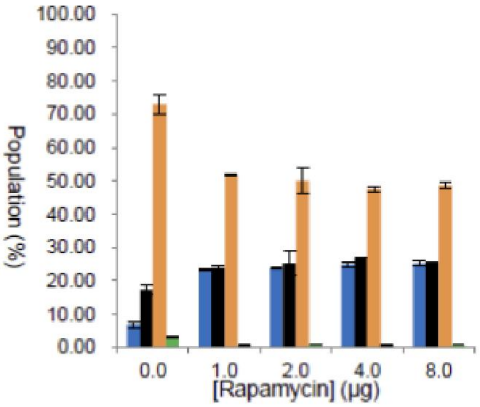
Population (%)
100.00
90.00
80.00
70.00
60.00
50.00
40.00
30.00
20.00
10.00
0.00
0.0
1.0
2.0
4.0
8.0
[Rapamycin] (µg)

(F)

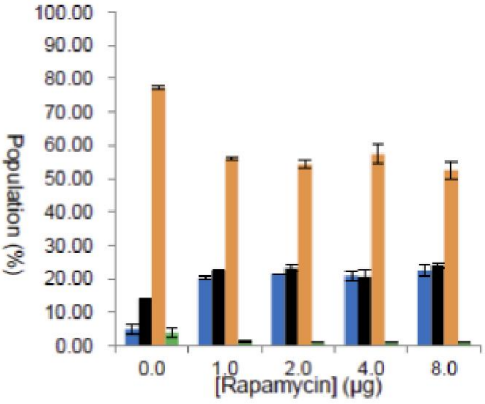
Population (%)
100.00
90.00
80.00
70.00
60.00
50.00
40.00
30.00
20.00
10.00
0.00
0.0
1.0
2.0
4.0
8.0
[Rapamycin] (µg)

Figure 20: Population heterogeneity was absent in autophagic mutants upon rapamycin treatment.

S. cerevisiae autophagic mutant strains *atg4*Δ **(Panel A)**, *atg6*Δ **(Panel B)** and *atg8*Δ **(Panel C)** were exposed to a series of different concentrations of rapamycin, as indicated. The samples were subjected to cytometric analysis using a BD Fortessa™ flow cytometry to determine the degree of forward (FSC) and side (SSC) scatter. Gating was set according to the gravity center of population. The quadrant is designated as Q1 (blue), Q2 (black), Q3 (orange) and Q4 (green), which represent the population with high complexity, high cellular volume and complexity, low cellular volume and complexity, and high cellular volume, respectively. Rapamycin had only negligible sub-effects on all autophagic mutants *atg4*Δ, *atg6*Δ and *atg8*Δ (**Panel D**, **E** and **F**, respectively) in comparison to the comparing with wild type (**Fig. 17C**).

Upon addition of rapamycin, however, a number of cells within a wild type population of cells shifted noticeably in to the upper and lower right quadrants (Q2 and Q4, respectively), presumably as a result of their higher cellular complexity and volume. Moreover, in every instance the population of cells being analyzed for SSC (a measure of cell complexity) showed a distinctive "twin peak" profile, which appeared to be diagnostic for autophagic activity with the cell. No additional peaks were apparent in similar studies undertaken on mutant cell populations where, for the most part, cells remained within the range of the normal, baseline cells (Q3) following rapamycin treatment (**Fig. 20D, E, and F**).

As an important technical aside, the separation of the cells into the discernable peaks (as represented in histograms of FSC and SSC **Fig. 17B** and **Fig. 19**) varies from cytometer to cytometer and even when using different sources of rapamycin, even yet, different lot numbers of rapamycin from the same company (data not shown). What does not appear to change, however, are the different sub populations into which the cells begin to separate over time. The results shown here are derived from the LSRFortessa^{TM} cell cytometer (BD Biosciences).

Heterogeneity of rapamycin-treated cells correlates well with subpopulations undergoing autophagy

If increased side scatter (SSC) is indeed an indication of increased cellular complexity, and rapamycin-induced autophagy results in the formation of a discernable sub population of cells that exhibits a significant increase in side scatter, it is reasonable to conclude that the sub population of cells with the greater complexity (SSC) should represent the population of cells experiencing autophagy. To test this argument directly, wild-type cells that had been treated with

4.0 μg rapamycin for 2 hours were sorted, using a FACSAria II^{TM} cell sorter (BD Biosciences) as a function of their degree of side scatter, giving rise to two pools of cells that are essentially equivalent to Q1/Q3 and Q2/Q4 in **Fig. 17C**. Each of these pools was then assayed for the presence of Atg8 and Atg8-PE**. Fig. 21A** depicts the immunoblot of these cells, along with those of the untreated and treated control samples, and shows that the preponderance of sorted cells exhibiting high levels of side scatter also possess correspondingly higher levels of Atg8-PE, while sorted cells that exhibited significantly lower levels of side scatter showed much lower levels of Atg8-PE and demonstrate ratios of Atg8 to Atg8-PE which approximate those of the untreated control samples (**Fig. 21B**). These results strongly support our contention that the degree of side scatter is an effective determinant of autophagic activity in *S. cerevisiae*.

New cytometric-based method is dynamic, but cannot discriminate between autophagy and apoptosis

To investigate whether the population shift in cellular volume/complexity and heterogeneity might prove to be a sensitive, potential marker for the dynamic evaluation of autophagic flow a time course study with 4.0 μg rapamycin exposure was set-up. The rapamycin-treated sample was harvested at a series of time points and these cells applied to cytometric-based analysis for quantification. With time processing, the Q3 quadrant representing the baseline was gradually decreased, whereas Q2, for high cellular complexity and volume, increased; meanwhile, Q1 and Q4 remained constantly (**Fig. 22A**). The gradual gain in cells within Q2 reflects a population shift from Q3. To demonstrate further that the cytometric-based method is able to differentiate autophagy from other cellular processes that also lead to enhanced cellular density, wild-type cells were exposed to varying levels of rapamycin as well as to the

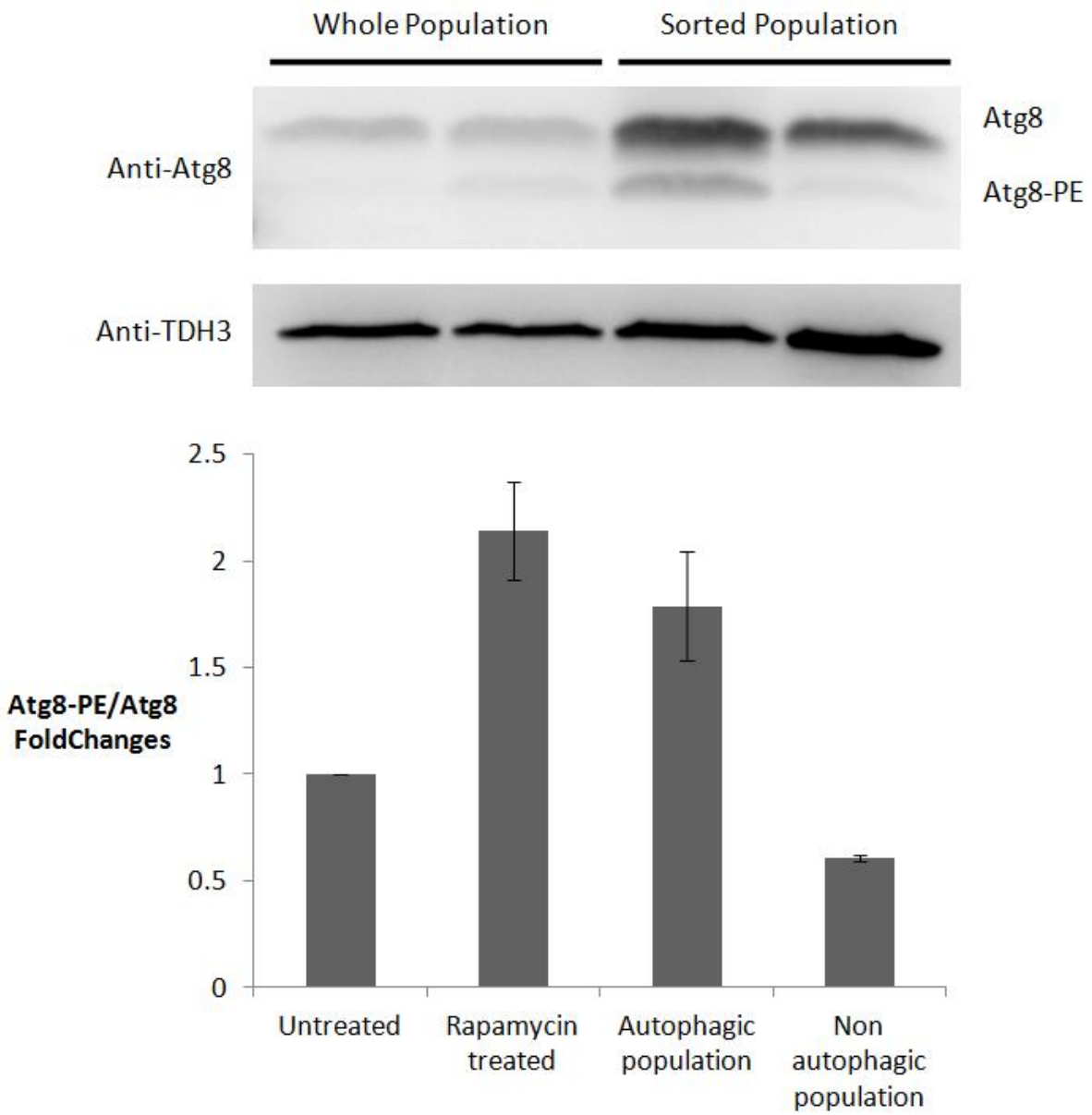

Figure 21: Population with higher complexity upon rapamycin treatment represents autophagic population.

Wild type yeast cells were treated with 4.0 µg rapamycin for 2 hours to induce autophagy. Cells were harvested and a portion of these cells were immediately sorted using a BD Aria™ cell sorter whereby the autophagic and non-autophagic populations of cells were separated as a function of SSC (cell complexity). The whole cells and sorted cells were lysed and subsequently analyzed for the Atg8-PE to Atg8 ratios. The immunoblot image is shown in the top panel, along with the same extracts treated with anti-TDH3 (GAPDH) as a blotting loading control. The results were quantified (lower panel), with the data being normalized to the Atg8-PE to Atg8 ratios of untreated cells.

(A)

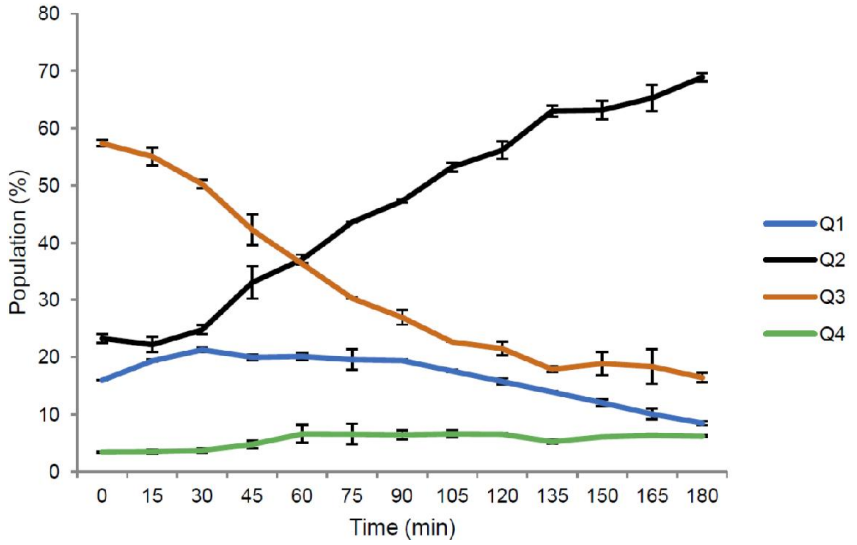

(B)

AP (%)	0.5	0.65	10.8	20.5

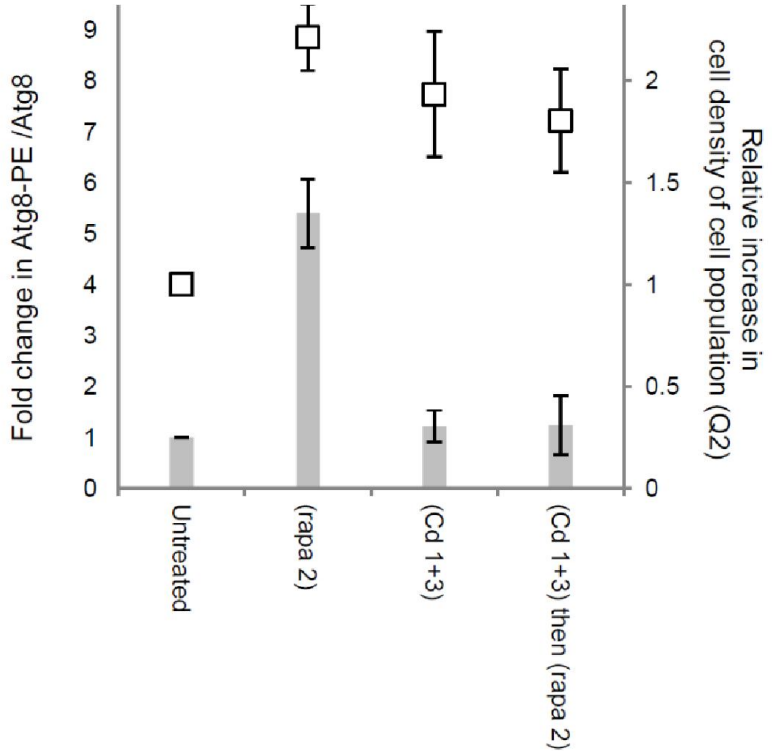

Figure 22: Comparison of the Cytometric-based technique with other method to determine temporal changes in autophagic activity as well as to discriminate between autophagy and metal-induced apoptosis.

(A) *S. cerevisiae* BY4741 wild-type cells were treated with 4.0 μg rapamycin over time for up to 180 min. Samples were harvested at 15 min intervals and subjected to cytometric-based analysis, as defined in Materials and Methods section. For each time point, the population of cells corresponding to the sub populations defined in **Figure 17B** were counted and shown. **(B)** *S. cerevisiae* BY4741 wild-type cells were assayed for the ability to exhibit rapamycin-induced autophagy and heavy metal induced apoptosis following treatment with 4.0 μg rapamycin for 2 hour. (rapa2), 30 μM $Cd(NO_3)_2$ for 1 hour followed by a 3 hours refractory period (as defined in Materials and Methods; Cd 1+3), and 30 μM $Cd(NO_3)_2$ for 1 hour, followed by a 3 hours refractory period, and then followed by treatment with 4.0 μg rapamycin for 2 hours [(Cd1+3) then (rapa2)]. All cells were harvested and assayed for autophagic activity by immunoblot (lightly shaded histograms) and flow cytometric-based method (shade squares). The corresponding apoptotic population (AP) were also assayed by addition of PI to the cells was indicated below x-axis as percentage.(20)

heavy metal, cadmium, which we have previously shown is able to induce apoptosis in *S. cerevisiae* within similar time constraints (20). Yeast cells were either left untreated, treated with rapamycin alone, or treated with 30 μM cadmium nitrate alone (**Fig. 22B**). In addition, wild-type cells were treated with cadmium followed by rapamycin (as described in Materials and Methods, **Fig. 22B**) to determine whether cells that had already triggered a metal-induced apoptotic response could also undergo autophagy, and if so, could the cytometric method be able to differentiate between the two. Autophagic flow in all cells was assessed using both immuno-blot assays for the relative presence of Atg8-PE as well flow cytometry. Upon treatment with rapamycin alone the Atg8-PE /Atg8 was shown to increase approximately 5-fold when compared to that of untreated cells (**Fig. 22** lightly shaded histograms). Upon treatment of cells with cadmium, however, it was apparent that the cytometric method was unable to differentiate between increased cellular complexity resulting from apoptotic and autophagic cellular responses, even though the Atg8-PE to Atg8 ratio clearly indicated that autophagy was not taking place at any time following heavy metal exposure.

2.4 Discussion

The autophagic process describes a series of complex events that otherwise occur (albeit at lower levels) as a function of regular, cellular activity; employing any number of enzymes and protein derivatives that are already part of the normal cellular function. It is the enhanced use of these enzymes in a coordinated increase in the formation of autophagosomes that defines the process, and which signals the autophagic cellular response to a variety of cellular insults. As such, there are few unique aspects to autophagy -other than perhaps the relative increase in the levels of Atg8-PE- that can definitively be used to characterize discernible changes in the autophagic process and thus used as specific markers. The cytometric approach that we have

tested and present in this report is one of the few methods that utilizes an effective detection of one of the more direct outcomes of the process itself, a responsive, temporal increase in cellular complexity and size. While the cytometric method could not adequately differentiate between cellular increases in complexity due to apoptosis or necrosis, for example, it is non-invasive, and these cellular responses (unlike autophagy) do have readily available, specific mechanisms to discriminate their activities. As such, a combination of simple cytometry can only augment the use of these specialized markers for the more specific determination of the different cellular responses. The method clearly comes into its own, however, when autophagy has already been shown to be the cellular response under scrutiny. The method provides a relatively rapid, non-invasive and dynamic assessment of the autophagic process that can be used by itself, or in combination with other more invasive techniques, to determine (within 30 minutes of induction) the extent to which different cells are undergoing autophagy. It is for this reason that we have outlined some of the parameters by which this method can be used.

References

1. Kiel JA (2010) Autophagy in unicellular eukaryotes. *Philos Trans R Soc Lond B Biol Sci* 365(1541):819-830.

2. Takeshige K, Baba M, Tsuboi S, Noda T, & Ohsumi Y (1992) Autophagy in yeast demonstrated with proteinase-deficient mutants and conditions for its induction. *J Cell Biol* 119(2):301-311.

3. Cebollero E & Reggiori F (2009) Regulation of autophagy in yeast Saccharomyces cerevisiae. *Biochim Biophys Acta* 1793(9):1413-1421.

4. Madeo F, Eisenberg T, & Kroemer G (2009) Autophagy for the avoidance of neurodegeneration. *Genes Dev* 23(19):2253-2259.

5. Maiuri MC, Zalckvar E, Kimchi A, & Kroemer G (2007) Self-eating and self-killing: crosstalk between autophagy and apoptosis. *Nat Rev Mol Cell Biol* 8(9):741-752.

6. Tsukada M & Ohsumi Y (1993) Isolation and characterization of autophagy-defective mutants of Saccharomyces cerevisiae. *FEBS letters* 333(1-2):169-174.

7. Klionsky DJ, Cueva R, & Yaver DS (1992) Aminopeptidase I of Saccharomyces cerevisiae is localized to the vacuole independent of the secretory pathway. *J Cell Biol* 119(2):287-299.

8. Shintani T & Klionsky DJ (2004) Cargo proteins facilitate the formation of transport vesicles in the cytoplasm to vacuole targeting pathway. *J Biol Chem* 279(29):29889-29894.

9. Kirisako T*, et al.* (2000) The reversible modification regulates the membrane-binding state of Apg8/Aut7 essential for autophagy and the cytoplasm to vacuole targeting pathway. *J Cell Biol* 151(2):263-276.

10. Kabeya Y*, et al.* (2000) LC3, a mammalian homologue of yeast Apg8p, is localized in autophagosome membranes after processing. *EMBO J* 19(21):5720-5728.

11. Kirisako T*, et al.* (1999) Formation process of autophagosome is traced with Apg8/Aut7p in yeast. *J Cell Biol* 147(2):435-446.

12. Lunemann JD & Munz C (2009) Autophagy in CD4+ T-cell immunity and tolerance. *Cell death and differentiation* 16(1):79-86.

13. Budovskaya YV, Stephan JS, Reggiori F, Klionsky DJ, & Herman PK (2004) The Ras/cAMP-dependent protein kinase signaling pathway regulates an early step of the autophagy process in Saccharomyces cerevisiae. *J Biol Chem* 279(20):20663-20671.

14. Noda T & Ohsumi Y (1998) Tor, a phosphatidylinositol kinase homologue, controls autophagy in yeast. *J Biol Chem* 273(7):3963-3966.

15. Stephan JS, Yeh YY, Ramachandran V, Deminoff SJ, & Herman PK (2009) The Tor and PKA signaling pathways independently target the Atg1/Atg13 protein kinase complex to control autophagy. *Proc Natl Acad Sci U S A* 106(40):17049-17054.

16. Klionsky DJ*, et al.* (2008) Guidelines for the use and interpretation of assays for monitoring autophagy in higher eukaryotes. *Autophagy* 4(2):151-175.

17. Biederbick A, Kern HF, & Elsasser HP (1995) Monodansylcadaverine (MDC) is a specific in vivo marker for autophagic vacuoles. *European journal of cell biology* 66(1):3-14.

18. Paglin S*, et al.* (2001) A novel response of cancer cells to radiation involves autophagy and formation of acidic vesicles. *Cancer research* 61(2):439-444.

19. Mizushima N, Yoshimori T, & Levine B (2010) Methods in mammalian autophagy research. *Cell* 140(3):313-326.

20. Nargund AM, Avery SV, & Houghton JE (2008) Cadmium induces a heterogeneous and caspase-dependent apoptotic response in Saccharomyces cerevisiae. *Apoptosis : an international journal on programmed cell death* 13(6):811-821.

CHAPTER 3.

RESCUE OR KILL? THE DUPLICITOUS ROLES OF AUTOPHAGY IN CADMIUM-INDUCED APOPTOSIS IN *Saccharomyces cerevisiae*

Pei-Ju Chin

Abstract

Autophagy is a conserved cellular mechanism to breakdown unwanted cytosolic materials. It starts with the formation of membrane vesicles, or preautophagosome structures (PAS), which engulf the cytosolic contents to be digested. The mature, double-membrane structures, so-called autophagosomes, then fuse with lysosomes to facilitate the degradation of engulfed contents; consequently, the lysed material is made available for recycling and the generation of new catabolites. Autophagy is induced in the cell under stressed conditions such as nutrient deprivation and the accumulation of dysfunctional proteins. As a result, it can be considered to be a protective mechanism. However, there is considerable debate as to the precise role of autophagy, especially when autophagic activity has been shown to correlate with programmed cell death, or apoptosis. Herein, we propose that the initial phase of autophagy is crucial in determining its duplicitous role to synergize or antagonize apoptosis. Induction of autophagy prior to cadmium-induced apoptosis, the apoptotic population was diminished. Induction of autophagy after apoptosis has already been initiated, however, serves only to facilitate apoptotic potential. Accordingly, we demonstrate that the timing of autophagic induction is a key factor to decide the role it plays.

3.1 Introduction

Autophagy, also known as "self-eating" process, is necessary to keep the cellular homeostasis upon the unsustainable resources surrounding the environment. In the nutrient-restrained condition, cells ensure their survival by degrading the redundant cellular substances such as exceed organelles or unwanted metabolites, following by recycling the essential blocks for the host to deal with such stringent environment like starvation (1), cellular damage resulting from mis-folded protein (2), or nitrogen depletion (3).

Autophagy is initiated within the cytoplasm to vacuole targeting (CVT) pathway (4, 5). Firstly, the aggregation of precursor vacuolar hydrolases aminopeptidase I (prApe1) associated with the double-membrane, nucleation of pre-autophagosomal structure (PAS) was formed, following by the engulfment of redundant substances tended to be digested. The maturation of autophagosomes from PAS requires an ubiquitin-like conjugation system associated with a series of autophagic proteins to facilitate the conjugation of Atg8 and phosphatidylethanolamine (PE) (**Chapter 2, Fig. 16**). Because Atg8-PE-anchored phagophore membranes are crucial for the maturation of autophagosome, this core machinery starts with the cleavage of the C-terminal glycine residue of Atg8p by Atg4p, a cysteine protease (6). The exposed glycine residue is conjugated by Atg7p in order to acquire the PE group through the activities of Atg3p and Atg12p-Atg5p complex (7). The lipidized Atg8-PE is subsequently anchored to the PAS phagophore. This apparatus, along with the dimerization of Atg5-Atg12-Atg16 complex, is essential to achieve the maturation of autophagosome and the docking with the lysosome machinery to form an autophagolysosome (8-10). Consequently, the intraphagosomal contents are lysed by the autophagolysosomal enzymes and matured prApe1 (mApe1) in order to

complete the autophagic cycle. The membrane-anchored Atg8-PE is dissociated from the phagophore, removed with PE ligand, and recycled by the same protease which accomplishes the activation of Atg8p in the initial step, Atg4p.

Since autophagy is associated with the recycling of non-useful metabolites, as well as eliminating damaged proteins or organelles, it is commonly considered to be a survival response to overcome stresses and facilitate the cell-surviving mechanisms. By using mouse or fruit fly as model, autophagy has also been shown to remove aggregated huntingtin, causing the neurodegenerative effects (11). The cytoprotective role of autophagy can be achieved as well by limiting the mass of ROS-generating organelles such as mitochondria, and consequently, the apoptotic response is ceased upon its induction (12). The study even suggests that autophagy even works in genomic level to resolve DNA-damage foci, and helps to stabilize chromosomes (13). In the scenario that the unfolded protein response (UPR) pathway is abolished resulting from XBP-1 deficiency, the increased autophagy activity compensates for the clearance of mutant superoxide dismutase-1 (SOD1) and prevents the progress of amyotrophic lateral sclerosis in neuronal cells (14). Autophagy is also reported to be associated with the prolonged lifespan of certain organisms: rapamycin-induced autophagy has been shown to extend the chronological life span of yeast cells (15). Upon caloric restriction, orthologues of yeast protein Atg6p and Atg7p in *Caenorhabditis elegans* have also been shown to be highly associated with the longevity. Attenuation of the synthesis of these autophagic proteins significantly reduces the life span of *C. elegans* under otherwise restricted dietary conditions (16).

Even so, there are different cellular settings that, in different scenarios, can also lead to autophagy-associated cell death, or Type-II cell death. Autophagic proteins have been reported to facilitate the neural apoptosis response in the case of lysosome dysfunction (17). In this mode, accumulation of autophagic vacuoles, resulting from the dysfunction of lysosome formation, augments caspase 3-like activity and the apoptotic response. Type-II cell death can be inhibited by introducing Atg7 shRNA, but not Beclin-1 shRNA, which suggests that Atg7 plays a unique, pro-apoptotic role in the cell death caused by the deficiency of lysosome formation. Curiously, under various conditions of stress or starvation, Atg7, along with Beclin-1, have also been shown to be cytoprotective. As the same protein (Atg7) reacts differently under differing conditions of stress, which shows that the duplicitous role of autophagy would be determined by the different types of stimuli. In addition, while caspase activity and related cell death is inhibited by the substrate, autophagy is shown to take over and contribute to the demise of the cell by the selective degradation of catalase, which eventually leads to the accumulation of reactive oxygen species (ROS) and apoptosis (18).

Crosstalk between autophagy and apoptosis has also been intensively investigated in higher eukaryotic cells. Among some of the proposed mediators of such pathways in higher eukaryotes are intercommunication of the apoptosis-regulatory proteins of Bcl-2 family of proteins, which is notably absent in yeast. Anti-apoptotic Bcl-2 or Bcl-XL (19), and pro-apoptotic Bax (20) have been shown to inhibit autophagic activities in these higher eukaryotes by directly interacting with the Bcl-2 Homology 3 (BH3) domain of Beclin-1, a yeast Atg6p orthologue. Autophagic activity can be easily resumed following the dissociation of Bcl-2 from Beclin-1, resulting in the c-Jun N-terminal kinase (JNK) dependent phosphorylation of Bcl-2

(19). Alternatively, autophagic proteins harboring BH3 domain have also been shown to possess some anti- and/or pro-apoptotic roles: Atg12, beyond its role as a conjugation enzyme involved in the maturation of the autophagosome, also shows some pro-apoptotic potential by binding with Bcl-2 through its C-terminal BH3 domain. As a result, anti-apoptotic activity of Bcl-2 is decreased (21). Atg4D (22) and Atg6 (20), two other autophagosomal-initiating enzymes which encode BH3 domains in their C-termini, also exhibit pro-apoptotic potential by facilitating the release of cytochrome *c* from mitochondria. Intriguingly, in unicellular eukaryotes such as, *Saccharomyces cerevisiae*, which can undergo both autophagic and apoptotic responses, there is a notable absence of any Bcl-2 family of proteins and the BH-like domain within Atg6p is not apparent. As such, any crosstalk between autophagy and apoptosis in unicellular yeast must be mediated through some alternative protein activities and interactions.

In this study, we demonstrate that the autophagic proteins in yeast are indeed required for the activation of Yeast Caspase 1 (Yca1p), which is the sole caspase-like protein and is responsible for initiating any caspase-dependent apoptotic programmed cell death in *S. cerevisiae*. In addition, the role of autophagy as either a rescue or killing pathway in yeast is addressed. In particular we have found that the degree of heavy metal-induced apoptotic response in yeast is highly responsive to whether autophagy or apoptosis is initiated first. To this end, preliminary results in our laboratory suggest that cadmium-induced apoptotic response is found to be severely compromised under growth conditions in which the autophagic pathway had first been activated. Conversely, autophagy further augmented the Cd-induced apoptotic response once Cd had already initiated an apoptotic response.

3.2 Materials and Methods

Cultures, Media, and Treatments

Saccharomyces cerevisiae BY4741 parental Wild Type (*MATα his3Δ1 leu2Δ0 met15Δ0 ura3Δ0*) or isogenic autophagic mutants (*yca1*Δ, *atg4*Δ, *atg6*Δ and *atg8*Δ) were obtained from Euroscarf. The yeast cells were cultured in 5mL YEPD broth [2 % (w/v) peptone (BD), 1 % (w/v) yeast extract (BD) and 2 % (w/v) dextrose (Sigma-Aldrich)] overnight for seeding purpose, followed by inoculating in 100mL YEPD broth and incubated at 30°C with 250 rpm shaking. The cells in early-log phase (OD_{600}= 1.8 ~2.5) were harvested and exposed to 4 μg of rapamycin, 30 μM cadmium nitrate or 8 mM copper nitrate (Sigma-Aldrich) to induce autophagy or apoptosis, respectively.

Total RNA Extraction

Saccharomyces cerevisiae BY4741 strain at early log phase was untreated or treated by 30 μM cadmium nitrate for 0, 30 and 60 minutes before being harvested. The cell pellet was stored at -80 °C before the mechanical disruption. The total RNA was obtained by Qiagen RNeasy™ Mini Kit according to the manufacturer's protocol. The total RNA crude extract was digested by DNase I (Qiagen) at 37 °C for 30 minutes for genomic DNA removal, followed by the inactivation at 65 °C for 10 minutes and spin column cleanup. Absence of genomic DNA contamination was confirmed by performing regular PCR, with the *Saccharomyces cerevisiae* BY4741 genomic DNA served as the positive control. Briefly, 2 μL total RNA was added to the PCR mixture containing 2 μL 10x PCR buffer, 1 μL 10 mM dNTP, 1 μL 30 μM forward and reverse primer for Yeast Caspase 1 (YCA1), 0.5 μL Taq polymerase (Qiagen) and 12.5 μL nuclease-free water (Ambion), following by the thermocycling protocol: 94 °C, 30 seconds for

denature, 30 cycles of 30 seconds at 94 ^{o}C, 30 seconds at 55 ^{o}C and 1 minute at 72 ^{o}C. The reaction mixture was then incubated at 72 ^{o}C for 10 minutes and stored at 4 ^{o}C. The amplicon was applied to 2.5 % (w/v) agarose gel for electrophoresis.

cDNA Microarray Analysis

The Affymetrix Yeast Genome 2.0^{TM} Array was applied for investigating the expressional profile of the unexposed (0 min exposure or control) and Cd-exposed (30 and 60 minutes exposure) yeast cell. Briefly, the total RNA was synthesized for the first strand cDNA by SuperScript^{TM} RT (Life Technologies), and the second strand cDNA by *E. coli* DNA polymerase I (Life Technologies). The double strand cDNA was cleaned up by Phase Lock Gels (PLG)-phenol/chloroform extraction and precipitated by ethanol. The cDNA pellet was re-suspended in RNase-free water (Ambion), following by being transcribed to biotin-labeled cRNA by RNA Transcript Labeling Kit (Affymetrix). The labeled-cRNA was cleaned up and precipitated by isopropanol, and the concentration was determined in order to adjust the starting concentration of the fragmentation. The proper amount of cRNA was fragmented by 5x RNA fragmentation buffer containing 200 mM; pH 8.1 Tris-acetate (Sigma-Aldrich), 500 mM potassium acetate (Sigma-Aldrich) and 150 mM magnesium acetate (Sigma-Aldrich). The fragmented cRNA was mixed with 20x GeneChip^{TM} Eukaryotic Hybridization Controls Kit (*bioB, bioC, bioD* and *cre*) (Affymetrix). The mixture was hybridized with the Yeast Genome 2.0 Array Chip (Affymetrix) for 16 hours. The chip was washed and stained automatically by the Fluidics Station (Affymetrix) with the fluidics program according to Yeast Genome 2.0 Array manual. The raw data was processed by GeneSpring^{TM} GX 7.3 software (Agilent) and Office Excel 2007 (Microsoft) by using β-actin as the normalization anchor.

Crude Protein Extraction

20mL of the cell culture was harvested and washed by ice-cold deionized water. The cells were re-suspended in different lysis buffers according to the purpose afterward: For Western Blot probed with Atg8 antisera, the cells were lysed with 200µl lysis buffer containing 1% (w/v) SDS, 8M urea, 10mM Tris-HCl, pH6.8, 10mM EDTA, and Complete Protease Inhibitor Cocktail (Roche), whereas Buffer M (0.5% NP-40, 20mM HEPES (pH 7.4), 84 mM KCl, 10 mM MgCl2, 0.2 mM EDTA, 0.2 mM EGTA, and 1mM DTT) (23) was used for the case of Yca1-probed Western Blot. The cells were lysed by mechanical disruption with 500 µm acid-washed glass beads (Sigma-Aldrich) for four, 30 seconds beating and cooling cycles. The cell debris was discarded, and the concentration of crude protein lysate was quantified by DC protein assay (BioRad).

SDS-PAGE and Western Blot

100 µg protein lysate dissolved in Laemmli Buffer was denatured in boiled water, loaded to 15% SDS-PAGE gel, run under 20V/cm, and transferred to PVDF membrane (BioRad) by electrical blotting (20 volts for overnight). For primary probing, the customized Atg8 (Abgent) or Yca1 (Genescript) antiserum harvested from rabbit was dilute by 100 folds in PBS with 0.1% Tween-20 (PBS-T), or 2,500 folds in TBS with 0.1% Tween-20 (TBS-T) with 5% skim milk (EMD Biochemicals), followed by probing with anti-rabbit-IgG with HRP conjugation (Pierce) The image was developed by ECL Western Blot Substrate (Pierce) and acquired by LAS-4000^{TM} chemiluminescence imager (GE Bioscience). The intensity was quantified by MultiGauge ^{TM} version 2.3 software (FujiFilm).

Crude Preparation of Crude Autophagic Vacuole

The protocol is modified from Cabrera, M et. al. (24). 100 mL of yeast culture was harvested and washed by ice-cold deionized water twice. The cell pellet was re-suspended in 2 mL pretreatment buffer (50 mM Tris, pH 7.5 and 30 mM DTT) and incubated at 30 ^{o}C for 15 minutes. The cells were span down, re-suspended in spheroplast buffer (20 mM potassium phosphate; pH 7.4, 1.2 M sorbitol, 20 mg 20T zymolyase) and incubated at 30 ^{o}C for 2 hours. The cell wall breakdown was confirmed by mixing 4 µL of cells with 4 µL deionized water or 1 % SDS on a glass slide. Ghost images under the microscope represent the progress of cell wall lysis. The spheroplasts were harvested by centrifuge at 4 ^{o}C and 5,380 xg for 3 minutes. The spheroplasts were gently re-suspended in PS buffer (10 mM PIPES/KOH; pH 6.8 and 200 mM sorbitol) containing 15 % Ficoll (*w/v*). And 200 µL PS buffer with 0.4 mg/mL DEAD-dextran was added to lyse the spheroplasts. The mixture was then incubated on ice for 5 minutes, followed by heat shock in 30 ^{o}C water bath for 2 minutes with gentle mixing at least twice. A cold shock was applied by placing the tube back on ice for 5 minutes. The breakdown spheroplasts ($\fallingdotseq$ 5 mL) were transferred to SW 41 tube (Beckman Coulter), and the step gradient was formed by slowly adding 2.5 mL of 8 % Ficoll in PS buffer, following by 2.5 mL of 4% Ficoll in PS buffer. Finally, the top of the gradient was covered with 2.5 mL PS buffer without Ficoll. Bubbles should be avoided during the entire stacking process. The tubes were placed in SW41 swing buckets and centrifuged at 100,000 xg at 4 ^{o}C for 90 minutes. The white band stacked between 0 % to 4 % Ficoll layer represents crude autophagic vacuoles. The vacuoles were harvest by centrifuging the harvested fraction at 110,000 xg at 4 ^{o}C for 30 minutes. The pellet was re-suspended in SUTEB buffer (1% (*w/v*) SDS, 8M urea, 10 mM Tris; pH 6.8, 10 M EDTA and 0.01 % (*w/v*) bromophenol blue) and subjected to SDS-PAGE analysis.

Quantification of Apoptotic Population

The harvested yeast cells were 20X-diluted in YEPD medium and stained by propidium iodine (ImmunoChemistry Technologies) for labeling the cells losing membrane integrity, which represents the population undergoing apoptosis. The plausible event of necrosis was ruled out under the control of exposure duration and concentration (25). The stained cells were subjected to BD Fortessa™ cytometry with PE-Y/GA fluorophore filter.

Monodansylcadaverine Staining for Autophagic Cells

Autophagic staining of cells was performed according to the procedure previously described. Briefly, 200 μL treated culture was harvested and washed in PBS. The cells were re-suspended in PBS with 0.1 mM monodansylcadaverine (MDC) and incubated for 10 minutes at 25 °C in the dark. Stained cells were washed in PBS four times to remove exceeding dye residue, and immediately observed under Zeiss Axioimager M2 fluorescent microscope with DAPI filter.

Expression and purification of yeast Yca1p and Atg4p in E. coli

The Yca1 and Atg4 coding sequences were amplified and incorporated with *Bgl*II or *Hind*III cutting sequences by using following primers: *BglII*YCA1-Forward: GCA-AGATCTGCATGTATCCAGGTAGTGGA. *Hind*IIIYCA1-Reverse: CAGAAGCTT-CTACATAATAAATTGCAGATTTACG. *Bgl*IIATG4-Forward: GCAAGATCTGCAT-GCAGAGGTGGCTAC. *HindIII*ATG4-Reverse: CAGAAGCTTCTAGCATTTTTCAT-CAATAGGACTG. The amplified fragments were inserted into pBAD-HisA plasmid vector with *E. coli* TOP10 as a host (Invitrogen). The expression was induced by LB medium containing 0.0002% *L*-arabinose (Sigma-Aldrich) by incubating at 16 °C for overnight. The induced *E. coli*

cells were washed and re-suspended in lysis buffer (25 mM Tris-HCl; pH 7.5, 20 % glycerol (*v/v*), 1 mM DTT, and Complete™ protease inhibitors (Roche Applied Science)) and lyzed by French Press with 800 psi pressure under low speed. The His-tagged Yca1p and Atg4p were purified by passing the lysate through HisTALON™ Gravity Columns (Clontech Laboratories). The buffer exchange and desalting were done by AmiCON™ Ultra Centrifugal Filter (Millipore) with 50 KDa cutoff size. The presences of final product was confirmed by Western blot with Anti-Xpress (Invitrogen) or customized Yca1 (Genscript), Atg4 and Atg8 (Abgent) antibodies.

Expression of Yeast Yca1p and Atg4p in Saccharomyces cerevisiae

The Yca1p and Atg4p coding sequences were amplified and incorporated with *EcoR*I or *Xba*I cutting sequences by using following primers: *EcoR*IYCA1-Forward: GC-AGAATTCTGATGTATCCAGGTAGTGGA. *Xba*IYCA1-Reverse: CAGTCTAGAC-TACATAATAAATTGCAGATTTACG. *EcoR*IATG4-Forward: GCAGAATTCTGATG-CAGAGGTGGCTAC. *Xba*IATG4-Reverse: CAGTCTAGACTAGCATTTTTCATCAA-TAGGACTG. Amplified fragments were inserted into pYES2-NT.A plasmid vector with *E. coli* DH5α as the host (Invitrogen). Plasmid DNA from the clones containing inserts was purified and transformed into *S. cerevisiae* BY4741 wild-type, *yca1*Δ or *atg4*Δ mutant according to the purpose. Briefly, the yeast competent cells were prepared by harvesting the overnight-cultured yeast cells which were diluted by YEPD medium to OD 600 = 0.4 and incubated for additional 2-4 hours in YEPD medium. The cells were washed by 40 mL of 1X TE buffer (10mM Tris; pH 7.5, 1 mM EDTA), and re-suspended in 2 mL of 1X LiAc/0.5X TE buffer (100 mM LiAc; pH 7.5, 5 mM Tris-HCl; pH7.5, 0.5 mM EDTA). The cells were incubated at room temperature for 10 minutes. Each transformation reaction contains 50 μL of cell re-suspension from the previous

step, 350 μL of 1X LiAc/40% (*v/v*) PEG-3,350/1X TE, 500 ng of pYES2-NT.A plasmid vector and 50 μg of denatured sheared salmon sperm DNA (Sigma-Aldrich). The mixture was incubated at 30 ^{o}C for 30 minutes, and then 44 μL of DMSO was added. Heat-shock was performed by incubating the mixture at 42 ^{o}C for 7 minutes. The cell pellet was harvested, washed by 1 mL of 1X TE buffer and re-suspended in 100 μL of 1X TE buffer. The cell re-suspension was poured on SC dextrose plate without uracil for selecting transformed cells compensated for uracil auxotroph.

Expression and Purification of His-tagged Atg4 and Yca1 in Saccharomyces cerevisiae

Following selection for uracil autotrophy, candidate clones were grown in SC Ura- dextrose medium for overnight. Cells were washed by 5 mL of SC Ura- galactose medium twice and diluted in SC Ura- galactose medium until OD 600 reaches 0.4. Cells were incubated at 30 ^{o}C, 250 rpm shaking for 8 to 16 hours for the induction. The induced cells were washed twice by ice-cold de-ionized water and lysed by mechanical disruption with 500 μm acid-washed glass bead (Sigma-Aldrich) with lysis buffer (50 mM sodium phosphate; pH7.4, 1 mM EDTA, 5 % (*v/v*) glycerol and Complete^{TM} Protease Inhibitors without EDTA (Roche Applied Science)). The soluble lysate was harvested by 20,000 xg centrifuge at 4 ^{o}C for 10 minutes. The His-tagged Yca1 and Atg4 protein were purified by either passing the lysate through HisTALON^{TM} Gravity Columns (Clontech) or performing batch purification by HisPur^{TM} Ni-NTA Superflow Agarose (Thermo Scientific) according to the manufacture protocol. The buffer exchange and desalting were done by using AmiCON Ultra Centrifugal Filter with 50 KDa cutoff size (Millipore). The presences of final product was confirmed by Western blot with Anti-Xpress (Invitrogen) or customized Yca1 (Genscript) and Atg4 (Abgent) antibodies.

Caspase activity assay

For each assay, 2 µL Protein lysate was added to caspase assay buffer containing 100 mM HEPES; pH 7.9, 100 mM NaCl, 0.1 % (*w/v*) CHAPS, 10 mM DTT; 10% (*v/v*) glycerol, 1 mM EDTA, 2 mM Ac-IETD-Amc (caspase-8 like) or Ac-DEVD-Amc (caspase-3,7 like) substrate (Enzo Life Sciences). The emission from cleaved substrate representing activated caspase was measured by Vector^{TM} multicolor plate reader (Perkin Elmer) with 2 hours duration. The caspase activity was determined by the increasing slope of fluorochrome.

3.3 Results

E. coli-expressed Atg4p shows no caspase activities in vitro

Our previous hypothesis claims that Atg4p, a cysteine protease, is an Yca1 activator since Yca1 activity was abated in *atg4*Δ mutant. Accordingly, ATG4 and YCA1 was cloned and purified to assay the caspase-like activities. *E. coli*-expressed Atg4p and Yca1p was expressed and purified by the methods described above, and the expression was confirmed by Western blot with anti-Xpress antibody **(Fig. 23A)**. *E. coli*-expressed Atg4 shows unexpected molecular weight (75 KDa instead of 56KDa). Even so, the purified Atg4 was tested for IETD cleavage activity. Comparing with the empty vector and wild type yeast protein lysate harvested from Cd-induced cells as negative and positive control, respectively, *E. coli*-expressed Atg4 showed insignificant difference from negative control meaning that *E. coli*-expressed Atg4 has no IETD cleavage activity *in vitro* **(Fig. 23B)**. Whether Atg4p is necessary to activate or cleave Yca1p was tested as well: By mixing the constant *E. coli*-expressed Yca1p with the *E. coli*-expressed Atg4 concentration *in vitro*, there was no cleaved fragment of Yca1p, which indicates that *E. coli*-expressed Atg4 does not cleave Yca1, or *vice versa*, *in vitro* (**Fig. 23C**).

(A)

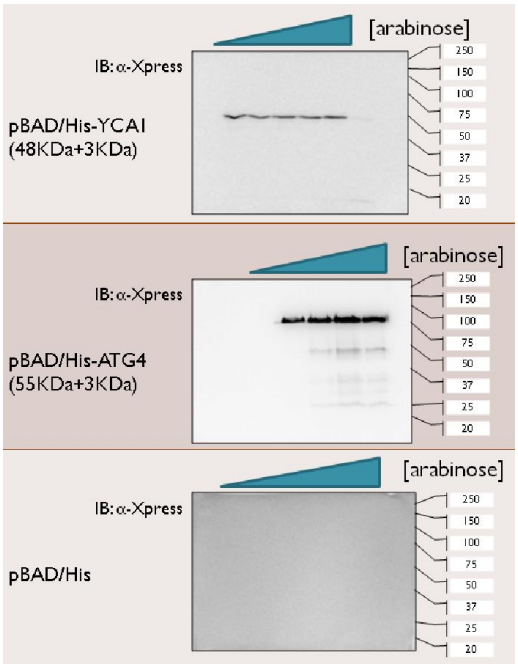
[arabinose]
IB: α-Xpress
pBAD/His-YCA1
(48KDa+3KDa)
250
150
100
75
50
37
25
20
[arabinose]
IB: α-Xpress
pBAD/His-ATG4
(55KDa+3KDa)
250
150
100
75
50
37
25
20
[arabinose]
IB: α-Xpress
pBAD/His
250
150
100
75
50
37
25
20

(B)

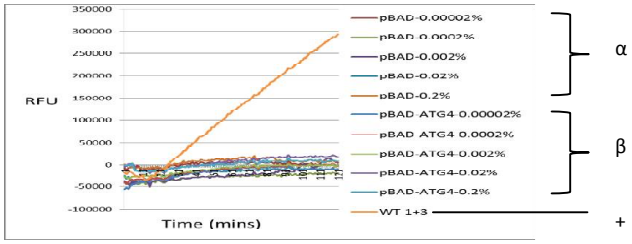
RFU
Time (mins)
pBAD-0.00002%
pBAD-0.0002%
pBAD-0.002%
pBAD-0.02%
pBAD-0.2%
pBAD-ATG4-0.00002%
pBAD-ATG4-0.0002%
pBAD-ATG4-0.002%
pBAD-ATG4-0.02%
pBAD-ATG4-0.2%
WT 1+3
α
β
+

(C)

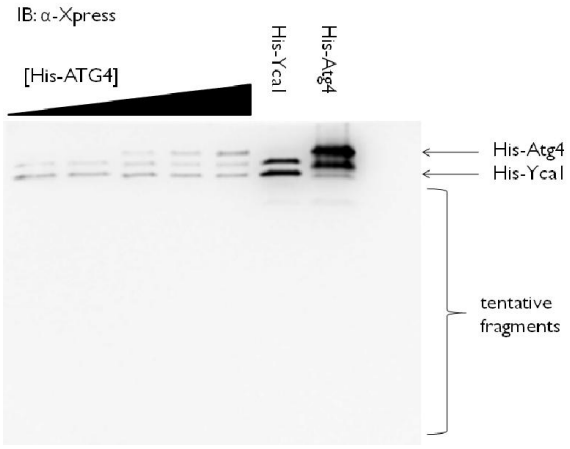
IB: α-Xpress
[His-ATG4]
His-Ycal
His-Atg4
His-Atg4
His-Ycal
tentative
fragments

(D)

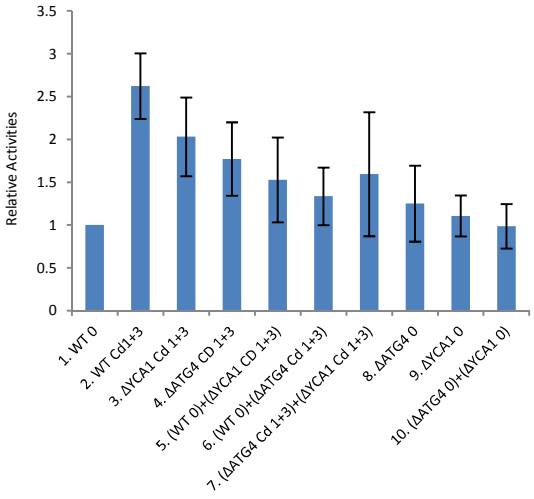
Relative Activities
3.5
3
2.5
2
1.5
1
0.5
0
1. WT 0
2. WT Cd1+3
3. ΔYCA1 Cd 1+3
4. ΔATG4 CD 1+3
5. (WT 0)+(ΔYCA1 CD 1+3)
6. (WT 0)+(ΔATG4 Cd 1+3)
7. (ΔATG4 Cd 1+3)+(ΔYCA1 Cd 1+3)
8. ΔATG4 0
9. ΔYCA1 0
10. (ΔATG4 0)+(ΔYCA1 0)

Figure 23: Purified Atg4p and cloned His-tag Atg4p exhibit neither caspase 8-like activity nor protease activity to cleave Yca1p.

(A) The *E. coli* expressed Yca1p and Atg4p were confirmed by XpressTM -probed immunoblot. The induction was done by a series titration of arabinose in order to find the optimal condition of induction. *E. coli* host harboring empty vector was served as a negative control. The expected size of expressed protein along with His-tag is shown. **(B)** *E. coli* harboring ATG4 construct (β) along with empty vector (α) was induced by various concentration of arabinose and harvested for the protein lysate for caspase 8-like (IETD) enzymatic activity assay. A series of *E. coli*-expressed Atg4, as well as the empty construct, shows no caspase 8-like activities *in vitro,* comparing with the positive activity in wild type yeast cell treated by Cd for 1 hour plus 3 hour post-incubation (+). **(C)** A series concentration (0.625, 1.25, 2.5, 5, and 10 μg) of Atg4p (expressed from *E. coli*) was co-incubated with a constant concentration (10 μg) of *E. coli*-expressed Yca1p, *in vitro*. No tentative fragmentation of Yca1p were apparent, indicating that Atg4p (when expressed in *E. coli*) has no Yca1p cleavage activity, and *vice versa*. **(D)** The different yeast strains were treated, and the protein lysates harvested and co-incubated as indicated to elucidate whether the mixture of *atg4*Δ and *yca1*Δ (Sample #7 and #10) were able to compensate for the loss of caspase-like activities that were absent in both mutants. The caspase-3,7-like activity was assayed and normalized by the activity of untreated wild-type (WT0). Atg4p may not be directly involved in the activation of Yca1p *in vivo* since the caspase-like activity of complementary groups (Sample #7 and #10) were not significant different from the negative control (Sample #3)

Since the prokaryotic expression system used for expressing eukaryotic proteins raises some concerns as to the appropriate synthesis of Atg4p (such as unexpected Atg4 molecular weight), it may be more appropriate to validate the interactions of proteins derived *in vivo* from Atg4p and Yca1p in yeast (**Fig. 23D**). The wild type, *yca1*Δ*, atg4*Δ*, atg8*Δ mutants were treated or untreated with Cd and harvested for the protein lysate. The protein lysate from Cd-treated *atg4*Δ and *yca1*Δ was mixed and assayed for caspase 3 (DEVD)-like activity. The rationale, for the use of these strains is based upon the idea that if Atg4p is essential for the Yca1p activation, mixing these two protein lysates should be able to complement for the absence of either Yca1p or Atg4p in the other, and would, therefore, restore the Yca1p activity given that *atg4Δ* and *yca1*Δ strains show no caspase 3-like activity **(Fig. 24)**. Unfortunately the Yca1 activity in each of the different mixtures was too statistically varied to yield any statistically interpretable data, although it is interesting that the Yca1 activities in all cells (even those of Yca1 mutants was always higher than un-induced cells.

Autophagy-associated genes are required for heavy metal-induced apoptosis response

Since *E. coli*-expressed Atg4p revealed no caspase-3,7 like activity, and was not able to cleaved *E. coli*-expressed Yca1 *in vitro* (**Fig. 23**), an alternative hypothesis was addressed that not only Atg4p alone, but the whole autophagic activity is critical for Yca1p activation since autophagy is a protein degradation process and the specific targeting property has been found in many studies (1, 9, 26, 27). In order to test this hypothesis, two additional autophagic mutants, *atg6*Δ and *atg8*Δ, were included in the analysis. Like Atg4p, these two proteins are responsible for the early process of autophagy pathway involved in the maturation of autophagosome. By knocking out these three proteins, the autophagy-specific protein degradation is ceased. Yet, by taking atg6Δ

(A)

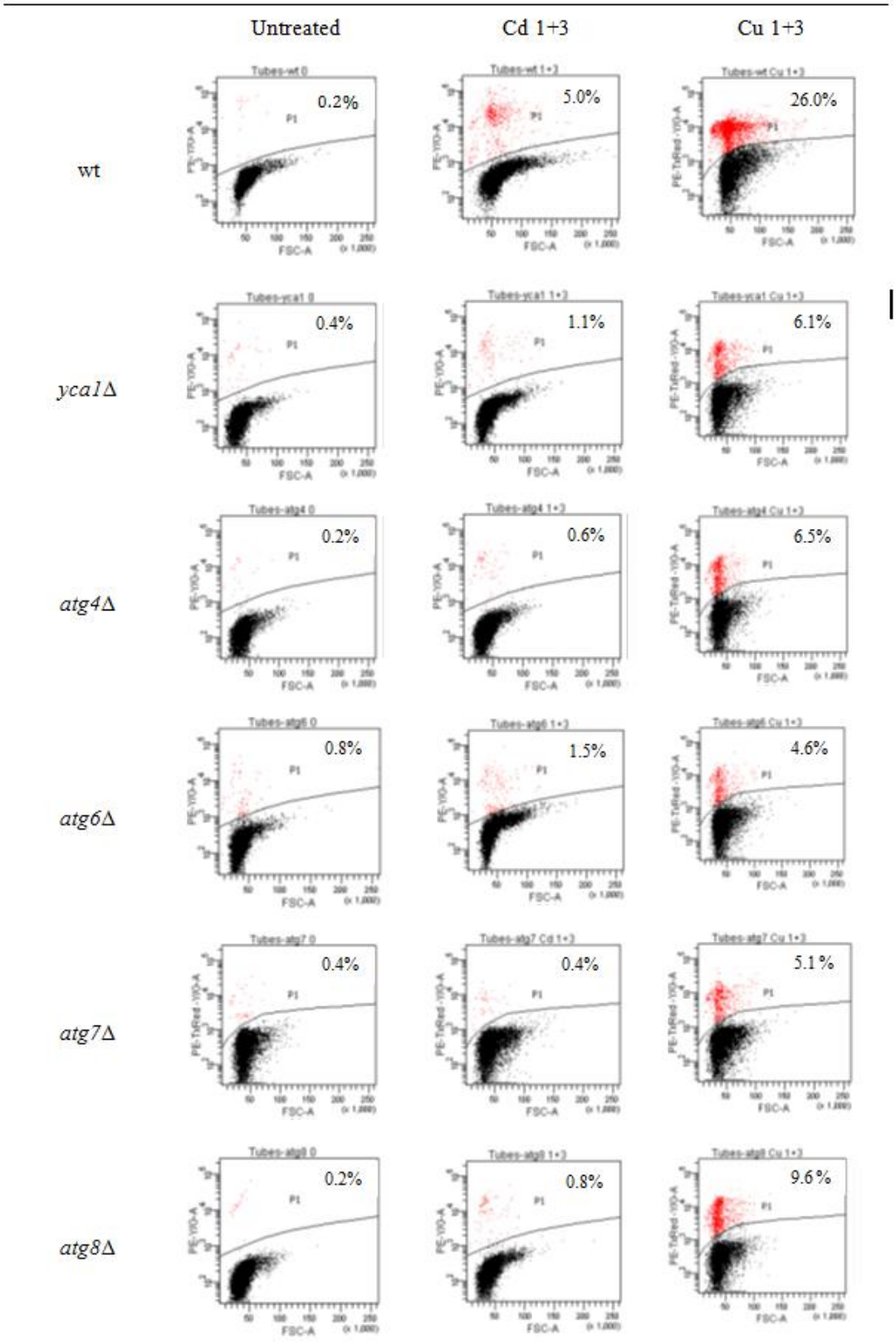
Untreated
Cd 1+3
Cu 1+3
wt
0.2%
5.0%
26.0%
yca1Δ
0.4%
1.1%
6.1%
atg4Δ
0.2%
0.6%
6.5%
atg6Δ
0.8%
1.5%
4.6%
atg7Δ
0.4%
0.4%
5.1%
atg8Δ
0.2%
0.8%
9.6%

(B)

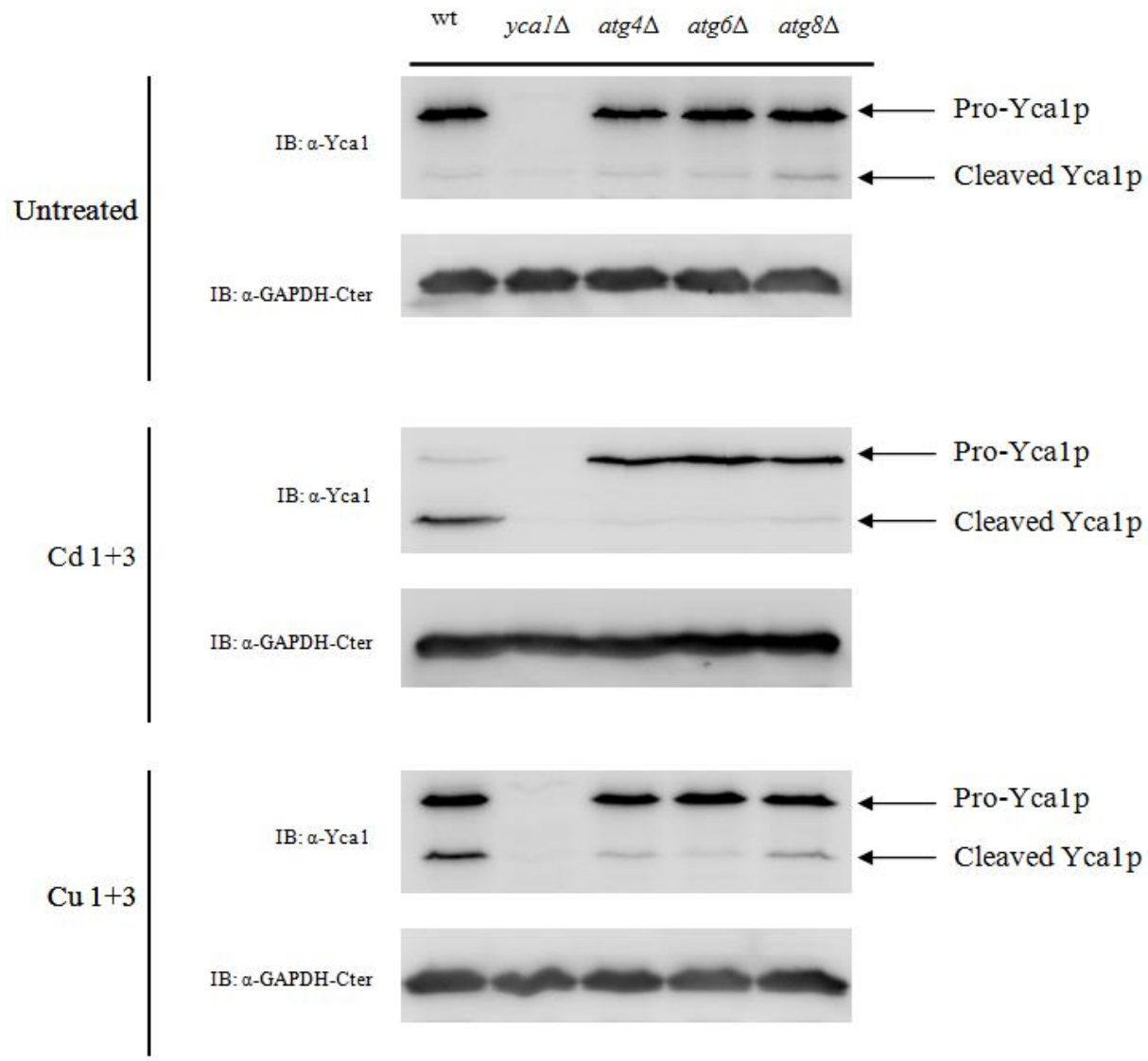

Figure 24: A number of autophagic proteins are required for apoptotic responses in yeast cells.

Apoptotic population of wild-type (wt), *yca1*Δ, *atg4*Δ, *atg6*Δ, and *atg8*Δ upon 1 hour 30 μM cadmium nitrate or 8mM copper nitrate treatment followed by 3 hours post-incubation (Cd 1+3 and Cu 1+3, respectively). Apoptotic cells with disrupted membrane integrity were stained by propidium iodine and subjected for FACS analysis **(A)**. The percentage of apoptotic cells (top right corner of each figure) indicates the PI-positive, or apoptotic population. **(B)** The same cells were treated, harvested, lysed and assayed for the presence of cleaved-Yca1p. Immunoblot with anti-GAPDH-Cter (lower blot in each assay) is used as the internal concentration control.

and atg8Δ mutants into account, they showed equivalent apoptotic population as *atg4*Δ mutant upon cadmium treatment instead of behaving like wild type or *yca1*Δ mutant (**Fig. 24A**). Moreover, like *atg4*Δ mutant treated by Cd, the cleaved-Yca1p was presented in neither *atg6Δ* nor *atg8*Δ mutants (**Fig. 24B**). Overall, it suggests that not only Atg4p, but also the integrant autophagy activity is required for Yca1p cleavage and activation.

Autophagy-associated genes are induced in cadmium-induced apoptotic yeast cells

Since initiation of autophagic proteins is required for Yca1p activation, we further performed microarray analyses to investigate the expression of autophagy-associated genes upon Cd exposure. Our previous study has shown that apoptosis-associated genes such as Yca1, an executor caspase in yeast, were induced in transcriptional level upon cadmium treatment (25). Similarly, autophagy-associated genes are significantly induced in wild-type cells upon Cd treatment, as exemplified by the 2-fold and 27-fold increase in transcriptional levels of *ATG*14 and *ATG*7, respectively (**Fig. 25**). These findings further indicate that there is a significant interconnection between apoptosis and autophagy in *S. cerevisiae*. Nevertheless, the specific role of autophagy in the apoptotic response remains inconclusive (28).

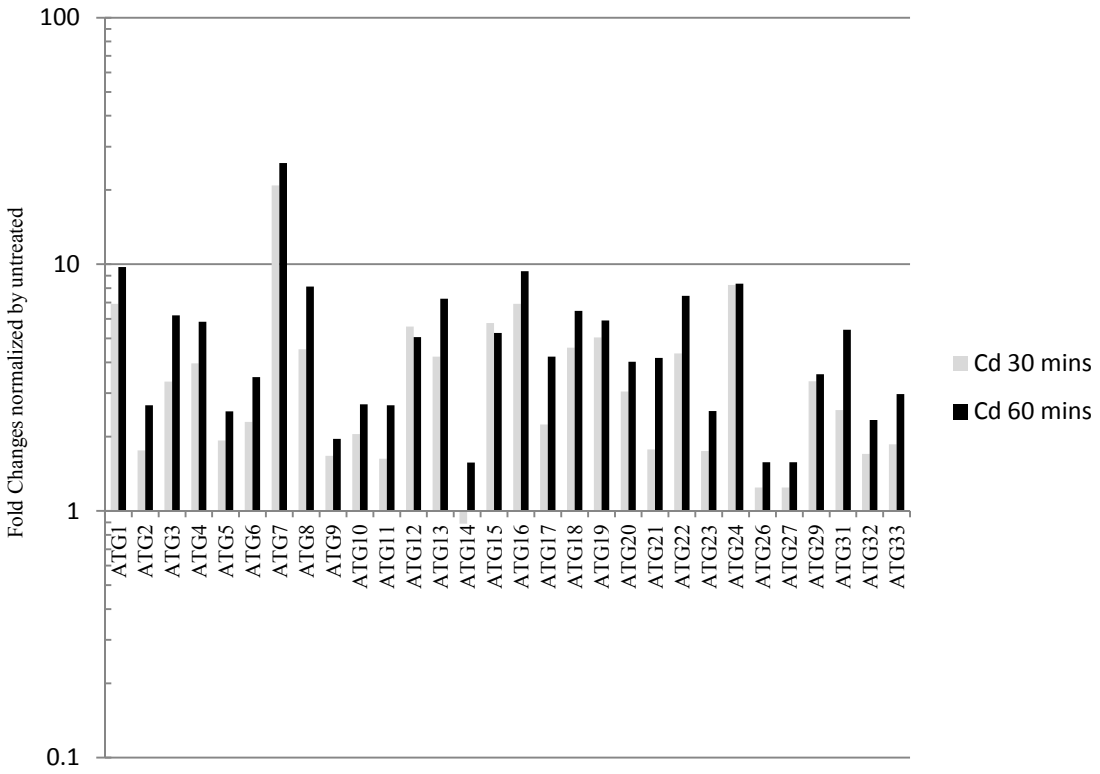

Figure 25: The expression profile of autophagy gene cluster upon Cd treatment.

The yeast cells were treated with 30 μM cadmium nitrate (Cd) for 0, 30 and 60 minutes and subjected to cDNA microarray analysis. The fold change was normalized by the intensity of obtained from the 0 time point, or untreated sample. Significantly, the genes involved in autophagy initiation such as ATG4, ATG6, ATG7 and ATG8 were highly induced upon Cd-induced stresses.

Yca1p is localized, then modified in autophagosome

Given that the Atg4p, Atg6p and Atg8p, which contribute to the initiation of autophagosome formation, are necessary for Yca1p activation, we then further tested odds that Yca1p would be modified inside autophagosome. After 24 hours Cu exposure, the co-localization of Yca1p-GFP with MDC-stained acidic vacuoles, such as autophagosomes, was found by observing the yellow puncta representing the overlapped green and red signal **(Fig. 26A)**. To further confirm this finding, *S. cerevisiae* harboring c-terminus-tagged GFP in Yca1p (Yca1-GFP) was untreated or treated by cadmium for 1 hour, followed by 3 hour post-incubation, and the crude autophagic vacuoles were purified and subjected to Western Blot analysis.

Three Ficoll layers; one between Ficoll 0%~4% (0~4%), another between 4%~8% (4~8%) and the third including the cell sediment (SD) were used to harvest proteins expressed from the YCA1-GFP strain as well as from the TDH3-GFP stains. The successful separation of proteins into each layer was confirmed by immunoblot analysis against Atg8 protein, which is involved in the initiation of autophagosome formation is, therefore, expected to be enriched in the autophagosome fractionation. The Yca1-GFP presents in autophagosomal fraction no matter whether the cells were exposed to Cu-induced stress or not **(Fig. 26B)**, and the Yca1p-GFP and autophagosome co-localization appears to be Yca1p-specific, since no GFP signal was found in the fractionation of Ficoll 0~4% layer from the same treatment of *S. cerevisiae* harboring TDH3 with c-terminus-tagged GFP **(Fig. 26C)**. Interestingly, after Cu-treatment, Yca1p-GFP tended to release from the sedimentation layer **(Fig. 26C)**, which indicates the solubility of Yca1p-GFP was increased after Cu treatment.

(A)

DIC

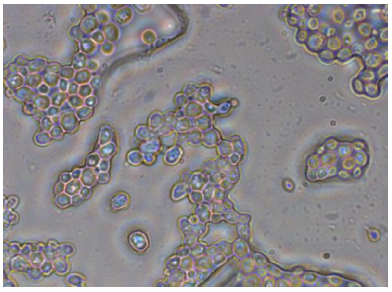

GFP

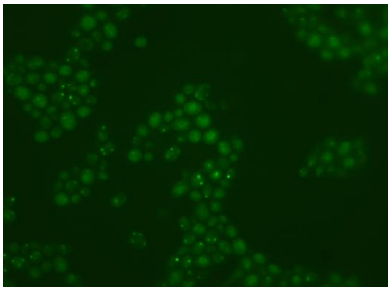

MDC

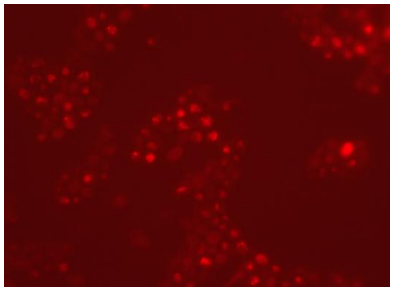

Merge

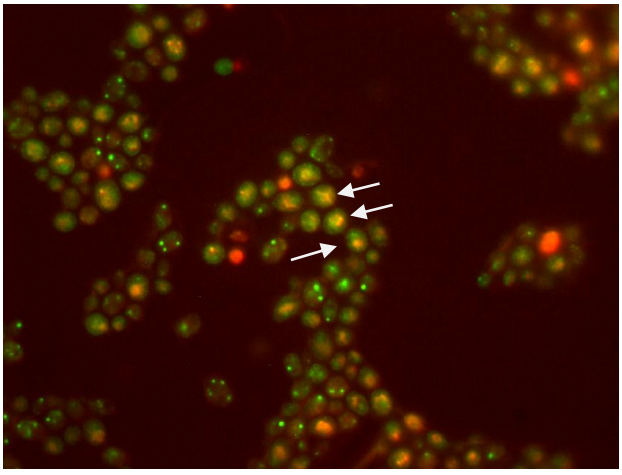

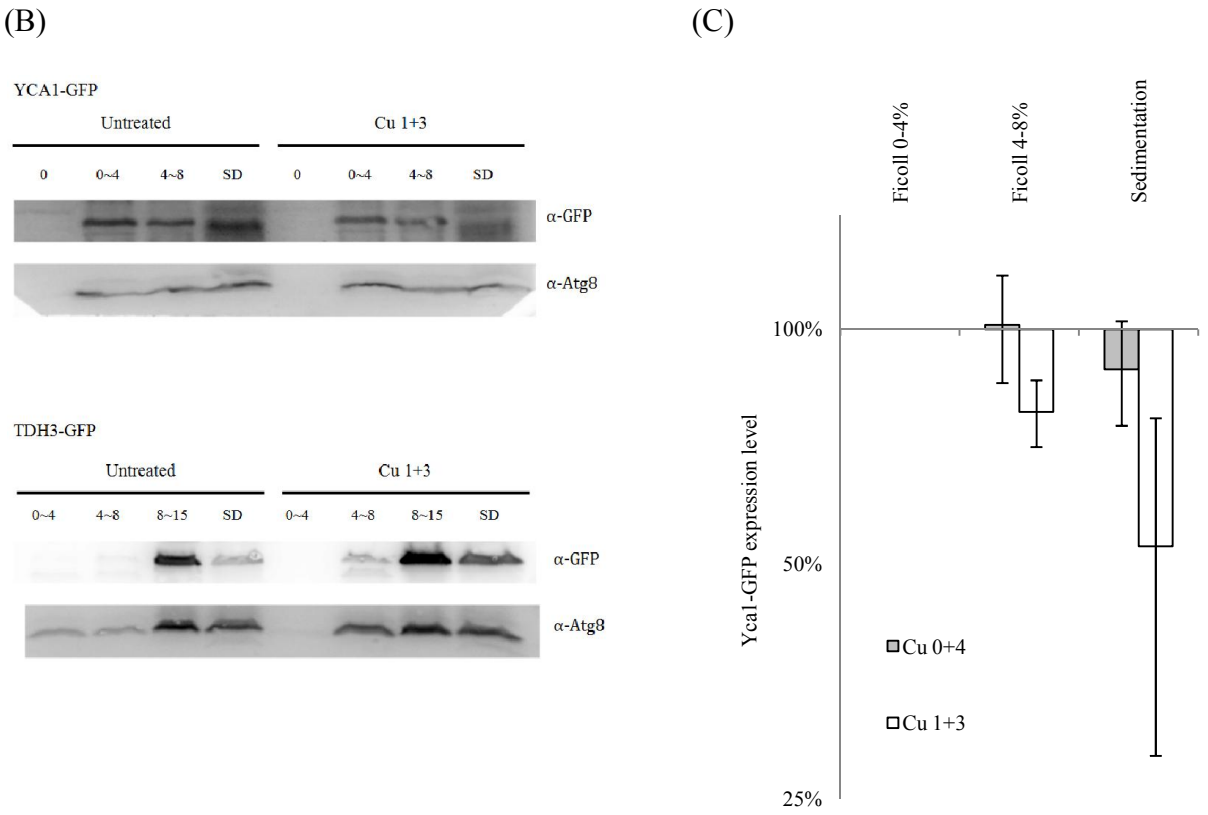

Figure 26: Yca1-GFP is presented in crude autophagic fractionation.

(A) YCA1-GFP tagged yeast strain was treated by Cu, stained by MDC and imaged by fluorescent microscopy. The white arrow indicates the colocalization of Yca1p-GFP and acidic vacuole, which is presumable to be autophagosomes. **(B)** YCA1-GFP tagged yeast strain was treated or untreated by Cu and subjected to the Ficoll fractionation. Four layers of Ficoll gradients as well as sedimentary debris (SD) were harvested as indicated, and the crude autophagic vacuoles are expected in 0~4% Ficoll fractionation. *S. cerevisiae* harboring TDH3 with c-terminal-tagged GFP was served as a control to exclude the possibility that GFP results in the co-localization. The quantification result of the blot, which is normalized by the intensity of Ficoll 0-4% signal, is shown in **(C)**.

The timing of autophagy induction is crucial in determining the role of autophagy/apoptosis in metal-stressed cells.

We previously conclude that autophagic activity is responsible for the activation of Yca1p; as a result, autophagy may facilitate apoptotic response. However, the debate exists that whether autophagy rescues cells from being apoptotic, or as an executor to facilitate the kill response. By reviewing previous findings, the diverse conclusion may result from the various cell types, the agents of autophagy induction, or simply the occasion to introduce autophagy agents. Hence, rapamycin, an immunosuppressor commonly used to induce autophagy in mammalian cells and budding yeasts, was inset at given time frame of our cadmium treatment scheme **(Table 1. and Fig. 27A)**. Surprisingly, in the setting of rapamycin prior to cadmium treatment, the apoptotic response was significantly depleted (**Fig. 27C, Treatment 3**). In contrast, apoptotic response was further enhanced if rapamycin was introduced after Cd-induced apoptosis had been ignited (**Fig. 27C, Treatment 5**). Since rapamycin *per se*, within the test concentration and exposure time, has no capability to induce apoptosis (unpublished data), the enhancement of apoptotic response is not due to rapamycin cytotoxicity. Conversely, rapamycin-induced autophagy protected the cells from being apoptotic once it was introduced prior to cadmium. Herein, rapamycin-induced autophagy demonstrates distinct effects depending on the juncture it was introduced.

(A)

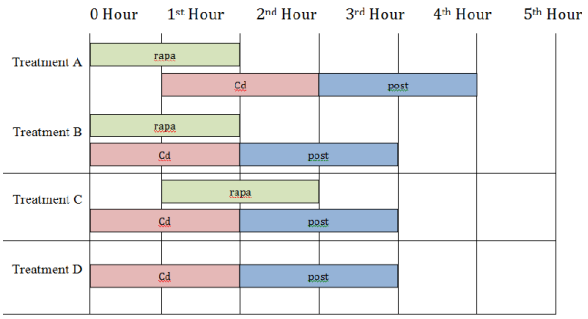

(B)

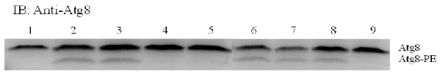

(C)

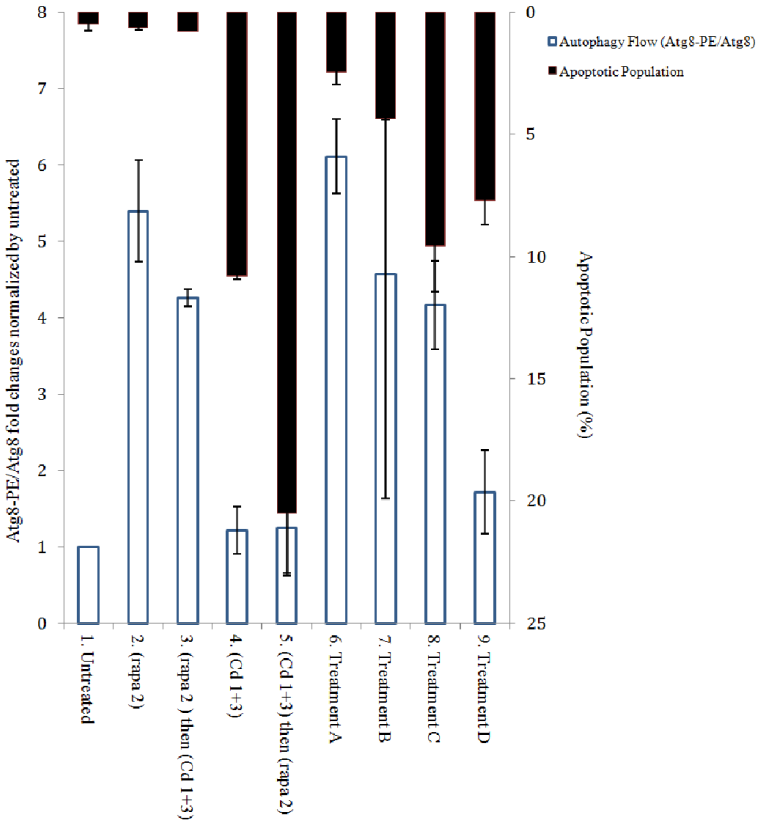

Figure 27: Quantitation of autophagic and apoptotic activities with various treatments of wild type yeast cells.

The schema of treatment A, B, C and D is shown in **(A)**. The samples were treated according to the scheme, subjected to Atg8-based Western Blot **(B)**, and measured for the Atg8-PE to Atg8 ratio (**Panel C** with open bar and Table 1). The same batch of samples was subjected to propidium iodide staining and FACS analysis in order to determine the percentage of apoptotic population (**Panel C** with closed bar).

Table 1: The treatment scheme and the corresponding autophagic flow determined by Atg8-PE to Atg8 ratio described in Figure 27.

Sample ID	Treatment	Atg8-PE/Atg8 Ratio Determined by IB
1	Untreated	0.054 ± 0.001
2	(rapa 2)	0.290 ± 0.040
3	(rapa 2) then (Cd 1+3)	0.229 ± 0.009
4	(Cd 1+3)	0.065 ± 0.017
5	(Cd 1+3) then (rapa 2)	0.067 ± 0.032
6	Treatment A	0.328 ± 0.022
7	Treatment B	0.246 ± 0.161
8	Treatment C	0.224 ± 0.034
9	Treatment D	0.092 ± 0.028

(Cd 1+3): 30 μM cadmium nitrate treatment for 1 hour, followed by 3 hours post-incubation
(rapa 2): 0.2μg/mL rapamycin treatment for 2 hours
Treatment A, B, C and D: Shown in Figure 5a.

Co-incubation of cadmium and rapamycin rescues the wild-type yeast cells from apoptosis

In previous studies, rapamycin, an autophagic inducer, has been shown to be involved in apoptosis response in two different manners: by being introduced prior to cadmium, it dramatically reduces the apoptotic population. On the other hand, it can further augment the apoptosis response after cadmium treatment (**Fig. 27C**). Thus, autophagy plays different roles to support, or suppress the yeast cells to survive based on the stage it is triggered. Since autophagy and apoptosis were introduced in separate time frames, it is curious to know the effect of introducing these two responses simultaneously. The exposure time scheme is shown in **Figure 27A**. Interestingly, by exposing the cells with cadmium and rapamycin simultaneously (Treatment B), the apoptotic population is half of the treatment of cadmium-only (Treatment D). It suggests the antagonism of apoptosis and autophagy once they were triggered simultaneously. Similarly, introducing cadmium (Treatment C)/rapamycin (Treatment A) prior to each other with one hour overlap behaved as similar as when treated in separate time periods.

Apoptosis and autophagy are antagonistic

The stage of rapamycin introduction is crucial to determine whether the wild-type cell undergoes apoptosis. Therefore, it is interested to know the autophagy flux upon various inductions of apoptosis and autophagy. The treatments are described in **Table 1**, along with the immunoblot result probed by anti-Atg8 serum shown in **Figure 27B**. By comparing with apoptosis population and autophagy flux **(Fig. 27C)**, the antagonistic trend of apoptosis and autophagy is found. In general, higher autophagy flux can be found in the treatment with autophagy prior to apoptosis, no matter whether these two responses were temporally overlapped.

Autophagy activity is coincident with apoptosis response upon cadmium treatment

Since Cd-induced apoptotic response was tremendously augmented by adding rapamycin, we further investigated the role of autophagy as a killer. The yeast parental wild-type, *yca1*Δ and *atg8*Δ were treated by Cd 1+3, harvested and co-stained with propidium iodine (PI) and monodansylcadaverine (MDC), which labels the membrane disintegration due to apoptosis and the presence of autophagolysosome, respectively. As shown in **Figure 28**, the wild-type showed most tremendous response to be apoptotic after Cd 1+3 according to PI staining. *yca1*Δ showed the moderate effect with cadmium resulting from the caspase-independent response. *atg8*Δ, as shown before, was less apoptotic due to the lack of activated Yca1p. Most importantly, no matter if parental wild-type or mutants were used, all of the cells stained by PI were co-stained with MDC as well. Since MDC labels the autophagolysosome formation, it reveals that not the few autophagic genes, but the entire autophagic pathway is necessary for triggering apoptosis response upon cadmium treatment in yeast. The crosstalk between PI and MDC can be excluded since not all MDC-stained cells were co-stained by PI.

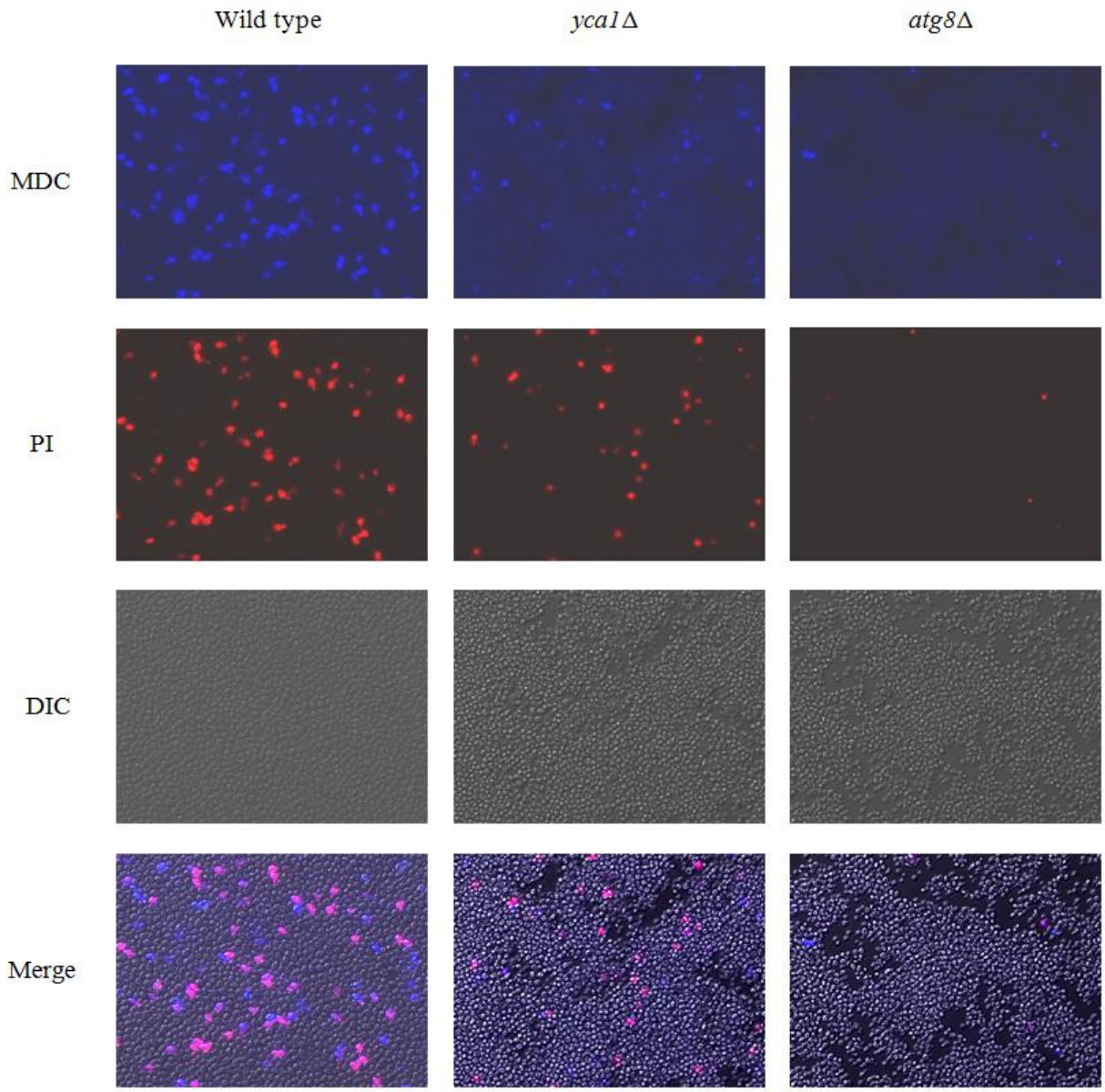

Figure 28: Autophagy facilitates the cell death upon metal-induced apoptosis has triggered.

The wild Type and indicated isogenic mutants were treated with cadmium for 1 hour plus 3 hours post-incubation, then double-stained with propidium iodide (PI) and monodansylcadaverine (MDC) to label apoptotic and autophagic cells. In wild-type, all propidium iodine-staining positive cells are coincident with MDC-staining positive, which reveals that autophagic activity is obligatory for the Cd-induced apoptotic response. Moreover, caspase-independent, autophagic cell death was exhibited by *YCA1Δ* (*mca1*, Yeast Meta Caspase 1) mutant.

3.4 Discussion

We provided the first clue of an interconnection between apoptosis and autophagy in budding yeast by undertaking microarray analysis on cells that had been subjected to a limited exposure of cadmium, known to be sufficient to trigger an apoptotic response in yeast cells (25). Among the autophagic cluster of genes, those responsible for expressing Atg7p, an E1 activating enzyme, and other autophagic activities (Atg12p and Atg8p) (29), were highly induced by 27-fold, 7-fold and 10-fold, respectively (**Fig. 25**). Considering the fact that along with *atg4Δ*, *atg6Δ* and *atg8Δ* (tested in this study), *atg7Δ* was also non-apoptotic **(Fig. 31A)**. This would suggest strongly that the autophagic process is necessary for any metal-induced apoptosis to occur. Therefore, even though some reverse interconnection between apoptosis and autophagy has previously been reported in mammalian model (30), this interaction is unidirectional inhibition of autophagy by caspase cleavage of Atg proteins, and is not a requirement for proteins in one pathway providing a permissive condition for the other to continue. Moreover, it is less likely that such a caspase-specific proteolytic activity actually occurs in *S. cerevisiae* since the conserved caspase-cleavage sites are absent in yeast Atg4p and Atg6p primary sequences. In addition, in our hands, neither purified Atg4p nor Yca1p were able to cleave themselves or the other (**Fig. 30C**). As a consequence, the findings detailed in this chapter would indicate that there is not one discrete component of autophagy necessary to trigger for Yca1p activation, but it is the formation of the autophagosome itself and the preliminary steps in its maturation that are thought to contribute to the Yca1p activation. It may well be that Atg4p (the only other related cysteine-protease relevant to both autophagy and apoptosis, and which is though to provide some additional caspase-like activity in the absence of Yca1 (31), may still contribute a trigger, but this can only occur within the relatively defined

confines of an actively maturing autophagosome. Similar findings have been reported in mammalian cells that suggest high autophagic activities and apoptotic population occur upon their increased exposure to Cd concentration (32), although under condition tested in this report Cd was unable to induce autophagy in *S. cerevisiae*.

Studies on the interactive connections between autophagy and apoptosis have become an important focus, of late, as a result of the potential protective role of autophagy against programmed cell death. Researchers have come to realize that, beyond its role as the "cell waste-disposal and recycling center", where normal autophagosomal activities have been implicated as providing a protective role (2, 12, 13, 33-35), autophagy can also be involved in cell death pathways -categorized as autophagy-dependent cell death (APC). Even so, the actual role of autophagy in these autophagy-dependent cell death pathways remains obscure. The different conclusions as to whether autophagy facilitates or acts to antagonize apoptosis, mainly results from a collection of studies that use different cell types and tissues as well as different mechanisms that are used to induce autophagy (such as starvation versus drugs). In this study, we demonstrate that there does appear to be clearly defined interaction between autophagy and apoptosis, and that it is the autophagic activity that is critical to whether or not it plays a protector or executioner role. Intriguingly, it is unlikely that yeast cells possess a cadmium-dependent autophagic pathway, because under conditions tested minimal autophagic activity was detected in Cd treated cells (**Table 1, and Fig. 27).** However, rapamycin-induced autophagy has a dramatic effect upon the fate of these exposed cells, depending on the timing of its introduction **(Fig. 27)**. It appears that autophagy can be both protective (if initiated before triggering cadmium-induced apoptosis), or it can augment the apoptotic response, if initiated after apoptosis

has been triggered **(Fig. 27C)**. The later scenario was further confirmed by the MDC-staining image **(Fig. 28)** showing that all of the PI-staining positive, or apoptotic yeast cells, were co-stained by MDC, which is thought to specifically label the autophagolysosomal activities.

Even though this apparent antagonism between autophagy and apoptosis was found in this study (**Fig. 27C)** it is possible that higher Atg8-PE to Atg8 ratio may not always be co-related with higher autophagic activities. Such increases in Atg8p cleavage may also indicate a blockage of autolysosome formation (36), or enhanced recycling of Atg8 by Atg4p, a cysteine protease. To our knowledge, however, rapamycin has not been reported to have either of these two effects.

Our previous study has shown that, even low amounts of Yca1p is not soluble in regular lysis buffer and requires the addition of non-ionized detergent, such us NP-40 or its derivatives. This would suggest that theYca1p protein may be sequestered in vacuoles, and may not be readily accessible for activation through cleavage. In order to investigate this characteristic of Yca1p further, and possibly to determine the cellular location of Yca1p in the cell, the Yca1-GFP fusion strain was treated with Cd and Cu and, thereafter, subjected to MDC staining, with the co-localization of Yca1p with acidic vacuoles was found **(Fig. 26A)**. However, this co-localization is only found following prolonged exposure to each of the metals, and is not so apparent in the shorter exposure that we have been, that is heavy metals for one hour followed by 3 hour post-incubation. Given that Yca1-GFP strain is less sensitive to cadmium or copper-induced apoptosis according to our assay, it might be reasonable to suggest that the Yca1p takes a longer time to co-localize with these acidic vacuoles. In another expect, this co-localization may be due to the

starvation of cells, in that following a 24 hours incubation, the nutrients have been depleted and the autophagy has been induced to recycle unwanted proteins to basic metabolic bricks. As a result, the localization of Yca1 in acidic vacuoles may simply indicate the starving cells lysing Yca1p protein, although the degree to which these cells have been starved has not been ascertained.

In order to further confirm the co-localization of Yca1p and autophagic vacuoles, the autophagosome fraction from copper-treated Yca1-GFP yeast cells was purified to test for the presence of Yca1. Yca1-GFP presented in the Ficoll 0~4% layer, which represents the crude autophagic fractionation **(Fig. 26B and C)**. Intriguingly, less Yca1-GFP was found in the sedimentation layer of Cu-treated yeast cells than in untreated cells. These results agreed nicely with our previous finding that activated/cleaved Yca1p is more soluble. Consequently, it is reasonable to conclude that the disappearance of Yca1-GFP from the sedimentation layer after heavy metals treatment may due to the increased solubility of Yca1-GFP, which is required for the Yca1 caspase activities. Such results serve to reinforce the argument that autophagic activity may play an essential role to increase Yca1p solubility.

In this study, we have proposed the interconnection between heavy metal-induced apoptosis and rapamycin-induced autophagy *in vivo*. Such interplay provides an insight that the autophagic activity facilitates the activation of Yca1p, a mammalian caspase-3 ortholog, possibly through the modulation of solubility to make the activated Yca1 accessible to the downstream processing machinery. The interaction of these two major cellular pathways, we would suggest, critically influences the cell fate in response to acute heavy metal toxicity.

References

1. Cebollero E & Reggiori F (2009) Regulation of autophagy in yeast Saccharomyces cerevisiae. *Biochim Biophys Acta* 1793(9):1413-1421.

2. Madeo F, Eisenberg T, & Kroemer G (2009) Autophagy for the avoidance of neurodegeneration. *Genes Dev* 23(19):2253-2259.

3. Takeshige K, Baba M, Tsuboi S, Noda T, & Ohsumi Y (1992) Autophagy in yeast demonstrated with proteinase-deficient mutants and conditions for its induction. *J Cell Biol* 119(2):301-311.

4. Klionsky DJ, Cueva R, & Yaver DS (1992) Aminopeptidase I of Saccharomyces cerevisiae is localized to the vacuole independent of the secretory pathway. *J Cell Biol* 119(2):287-299.

5. Shintani T & Klionsky DJ (2004) Cargo proteins facilitate the formation of transport vesicles in the cytoplasm to vacuole targeting pathway. *J Biol Chem* 279(29):29889-29894.

6. Kirisako T*, et al.* (2000) The reversible modification regulates the membrane-binding state of Apg8/Aut7 essential for autophagy and the cytoplasm to vacuole targeting pathway. *J Cell Biol* 151(2):263-276.

7. Ichimura Y*, et al.* (2000) A ubiquitin-like system mediates protein lipidation. *Nature* 408(6811):488-492.

8. Kabeya Y*, et al.* (2000) LC3, a mammalian homologue of yeast Apg8p, is localized in autophagosome membranes after processing. *EMBO J* 19(21):5720-5728.

9. Kiel JA (2010) Autophagy in unicellular eukaryotes. *Philos Trans R Soc Lond B Biol Sci* 365(1541):819-830.

10. Kirisako T*, et al.* (1999) Formation process of autophagosome is traced with Apg8/Aut7p in yeast. *J Cell Biol* 147(2):435-446.

11. Ravikumar B*, et al.* (2004) Inhibition of mTOR induces autophagy and reduces toxicity of polyglutamine expansions in fly and mouse models of Huntington disease. *Nature genetics* 36(6):585-595.

12. Ravikumar B, Berger Z, Vacher C, O'Kane CJ, & Rubinsztein DC (2006) Rapamycin pre-treatment protects against apoptosis. *Human molecular genetics* 15(7):1209-1216.

13. Mathew R*, et al.* (2007) Autophagy suppresses tumor progression by limiting chromosomal instability. *Genes Dev* 21(11):1367-1381.

14. Hetz C*, et al.* (2009) XBP-1 deficiency in the nervous system protects against amyotrophic lateral sclerosis by increasing autophagy. *Genes Dev* 23(19):2294-2306.

15. Alvers AL*, et al.* (2009) Autophagy is required for extension of yeast chronological life span by rapamycin. *Autophagy* 5(6):847-849.

16. Jia K & Levine B (2007) Autophagy is required for dietary restriction-mediated life span extension in C. elegans. *Autophagy* 3(6):597-599.

17. Walls KC*, et al.* (2010) Lysosome dysfunction triggers Atg7-dependent neural apoptosis. *J Biol Chem* 285(14):10497-10507.

18. Yu L*, et al.* (2006) Autophagic programmed cell death by selective catalase degradation. *Proc Natl Acad Sci U S A* 103(13):4952-4957.

19. Maiuri MC*, et al.* (2007) Functional and physical interaction between Bcl-X(L) and a BH3-like domain in Beclin-1. *EMBO J* 26(10):2527-2539.

20. Luo S & Rubinsztein DC (2010) Apoptosis blocks Beclin 1-dependent autophagosome synthesis: an effect rescued by Bcl-xL. *Cell Death Differ* 17(2):268-277.

21. Rubinstein AD, Eisenstein M, Ber Y, Bialik S, & Kimchi A (2011) The autophagy protein Atg12 associates with antiapoptotic Bcl-2 family members to promote mitochondrial apoptosis. *Molecular cell* 44(5):698-709.

22. Betin VM & Lane JD (2009) Caspase cleavage of Atg4D stimulates GABARAP-L1 processing and triggers mitochondrial targeting and apoptosis. *Journal of cell science* 122(Pt 14):2554-2566.

23. Madeo F*, et al.* (2002) A caspase-related protease regulates apoptosis in yeast. *Molecular cell* 9(4):911-917.

24. Cabrera M & Ungermann C (2008) Purification and in vitro analysis of yeast vacuoles. *Methods in enzymology* 451:177-196.

25. Nargund AM, Avery SV, & Houghton JE (2008) Cadmium induces a heterogeneous and caspase-dependent apoptotic response in Saccharomyces cerevisiae. *Apoptosis* 13(6):811-821.

26. Camougrand N*, et al.* (2003) The product of the UTH1 gene, required for Bax-induced cell death in yeast, is involved in the response to rapamycin. *Mol Microbiol* 47(2):495-506.

27. Kissova I, Deffieu M, Manon S, & Camougrand N (2004) Uth1p is involved in the autophagic degradation of mitochondria. *J Biol Chem* 279(37):39068-39074.

28. Maiuri MC, Zalckvar E, Kimchi A, & Kroemer G (2007) Self-eating and self-killing: crosstalk between autophagy and apoptosis. *Nat Rev Mol Cell Biol* 8(9):741-752.

29. Tanida I*, et al.* (1999) Apg7p/Cvt2p: A novel protein-activating enzyme essential for autophagy. *Molecular biology of the cell* 10(5):1367-1379.

30. Norman JM, Cohen GM, & Bampton ET (2010) The in vitro cleavage of the hAtg proteins by cell death proteases. *Autophagy* 6(8):1042-1056.

31. Nargund AM (2010) Mechanism(s) of Metal-induced Apoptosis in *Saccharomyces cerevisiae*. (Georgia State University, Department of Biology).

32. Wang SH, Shih YL, Ko WC, Wei YH, & Shih CM (2008) Cadmium-induced autophagy and apoptosis are mediated by a calcium signaling pathway. *Cell Mol Life Sci* 65(22):3640-3652.

33. Eisenberg T*, et al.* (2009) Induction of autophagy by spermidine promotes longevity. *Nat Cell Biol* 11(11):1305-1314.

34 Orlotti NI*, et al.* (2012) Autophagy acts as a saf-eguard mechanism against G-quadruplex ligand-mediated DNA damage. *Autophagy* 8(8):1185-1196.

35. Qu X*, et al.* (2003) Promotion of tumorigenesis by heterozygous disruption of the beclin 1 autophagy gene. *The Journal of clinical investigation* 112(12):1809-1820.

36. Mizushima N, Yoshimori T, & Levine B (2010) Methods in mammalian autophagy research. *Cell* 140(3):313-326.

ANALYSIS OF CELLULAR RESPONSES TO HEAVY METAL-INDUCED STRESS IN *Saccharomyces cerevisiae*

GENERAL DISCUSSION

The use of heavy metals in industry has become inevitable in modern society (1) and the accidental exposure, resulting from mining activities, improper disposal or halted recycling programs of expired products pose a major threat to public health. Indeed, a number of degenerative diseases and carcinomas have been epidemiologically associated with chronic heavy metal exposure (2-5). Thus, the conscientious regulation of heavy metal exposure along with the passive defense such as the medical prospection is constructive to diminish the potential pandemic associated with the liberal use of these heavy metals. *S. cerevisiae* provides a limpid and sophisticated platform to elucidate the different effects of different metal toxicities because of its simplicity and well-studied genetics and cellular metabolism. It has previously been shown that dysfunctional proteins, resulting from metal-induced damage, are a consequence of oxidative stress, which results from the accumulation of reactive oxygen species (ROS) (6). These harmful oxidative species attack and damage the organic components of the cell, and trigger multiple survival mechanisms that are able to neutralize some, if not all of their harmful effects. Such mechanisms include groups of genes whose expression and activities are coordinated as a network to establish a well-organized series of reactions, a so-called “reactome”, to overcome the undesirable effects of cellular stress such as; heat, cold, osmotic shock, nutrient depletion and oxidative stresses (7). We have previously determined some of the components of the transcriptional reactome in yeast that is initiated in response to heavy metal exposure (Appendix F, G, H and I). The genes associated with cell fate and glucose metabolism work together in

response to the heavy metal-induced reactive oxygen species (ROS) stress. Even so, the response to the presence of different heavy metals is not uniform, nor is the response of different cells within a population that has been similarly exposed to a single heavy metal. One such overtly variable response within population of cells to an acute exposure to various heavy metals, such as cadmium, copper and chromium is that a subset of the cells (5 - 20 %) is shown to undergo cell suicide, or apoptosis. As a consequence, we believe, more solid conclusions could be obtained as to the response mechanisms of cells to heavy metals by sorting the sub-population of cells that appear to behave differently from the others and subjecting these cells to transcriptome analysis, independently. In this way, the transcriptome of cell fate decisions upon heavy metal-induced stresses will be clarified. Investigating the translatome of cells exposed to these same heavy metals could further expand these studies. Our preliminary studies along these lines showed that when wild-type yeast are transiently exposed to heavy metals, the treated and untreated cells do exhibit quite different proteomic profiles (data not shown). We believe that it would be useful to determine the metabolic consequences of their different protein expression. Previous studies have also shown the retardation of protein synthesis resulting from stalled ribosomes on targeted mRNAs in response to various kinds of stress. The targeted mRNAs (along with their stalled ribosomes) are stored in P-bodies and provide an ample resource of stored proteins that become readily available for translation once the stress factors are removed from the immediate environment (8, 9). It would be interesting to know whether the heightened expression of certain proteins in the metal-stressed yeast relates to proteins that are eventually synthesized from these P-bodies.

As the first-line defensive mechanism, the transcriptome of pentose phosphate pathway

(PPP) was induced to generate the reducing power for glutathione, which was demonstrated by discovering the prompt increase of GSH to GSSG ratio upon Cd treatment while lower reduced-glutathione (GSH) level was discovered in *gnd1*Δ mutant with defective PPP. In contrast, Zwf1p deficiency had no effect to reduce oxidized glutathione (GSSG) (appendix). Given that Zwf1p and Gnd1p convert the identical molecule of NADPH from NADP, this distinction would be resulted from the enzymatic activity. Therefore, it would be curious to assay the activity of Gnd1p and Zwf1p from wild type yeast cells upon heavy metal treatments to elucidate the redox contribution between those two enzymes majorly contributing to the pool of reducing power.

Even though the results of the research described in Chapter 1 are not entirely conclusive, the relationship between apoptotic and glycolytic pathway has been clearly shown. Previous studies in the laboratory have indicated that the apoptotic response of cells exposed to heavy metals is highly dependent on the carbon source and resulting type of respiration that the cells are undertaking. Importantly, cells growing in the absence of a fermentable sugar in the medium, such as glucose, demonstrated a marked reduction in their apoptotic response, which was diminished by the heavy metal treatments without the addition of glucose in the medium (10). Moreover, the glycolytic enzymes Tdh3p tended to be oxidized, fragmented and reduced its enzymatic activities upon exposure to these heavy metal stressors, and the *tdh3*Δ mutant is entirely non-apoptotic (11). Consequently, we inferred that glycolytic activity is required to facilitate the apoptotic response which would be energy-demanding. This assumption was supported by a study, which revealed that the pro-apoptotic BAD protein is de-phosphorylated upon glucose deprivation, and therefore, ceases the apoptotic response (12). In this scenario, the cellular dephosphorylation, resulting from low energy state, would also interfere in the

checkpoint enzymes within apoptotic cascade. However, this assumption was shown to be ambiguous when the strain expressing the C-terminally GFP-tagged Tdh3p preserved equivalent wild-type Tdh3p enzyme activity, but was found to be non-apoptotic (Chapter 1). We then focused on the potential, pleiotropic role of Tdh3 and its function as a signal factor, rather than simply as the glycolytic enzyme by attempting to show the nuclear localization of Tdh3p-GFP in apoptotic yeast cells. Several studies in higher eukaryotes, and some preliminary work in our laboratory by Anupama Shanmuganathan (11) have indicated a unique regulatory role for a nuclear form of GAPDH (see Introduction in Chapter 1). Even though our original hypothesis had been negated by the complementation test showing that the compensation of extrinsic TDH3 in *tdh3*Δ mutant was unable to allow the cells to recover their apoptotic activities, the role of Tdh isozymes in heavy metal-induced apoptotic response is far from clear given that other two isoforms, Tdh1p and Tdh2p, may compensate the effect of Tdh3p deprivation. Moreover, unlike the dominant expression of Tdh3p in normal conditions, Tdh1p is dominantly expressed at stationary phase in the absence of glucose while the expression of Tdh2p was found to be repressed in cells undergoing heat shock stress (13). As a consequence, we cannot neglect the different GAPDH isozymes, and the role that Tdh1p and Tdh2p potentially play in metal-stressed yeast cells when the Tdh3p activities are defective.

Beyond its glycolytic role, other researchers have proposed that GAPDH can also function as an epigenetic modulator to contribute to any apoptotic responses by interacting with several epigenetic components. By way of example, GAPDH may contribute to the apoptotic response by interacting directly with Su(var)3-9, Enhancer of zeste, Trithorax (SET) protein. SET, as an epigenetic modulator, methylates histone H3 lysine 27 (H3K27me) by its histone

methyltransferase (HMT) activity, and consequently result in the silencing of genes **(Fig. 29 Path A)**(14). In other aspects, SET inhibits the caspase-independent apoptosis by sequestering Granzyme A (GzmA) activity, which cleavages procaspases or DNases to an active form **(Fig. 29 Path A)** (15-17). This could suggest that the activity of GzmA would be indirectly controlled by GAPDH. Besides, SET regulates the cell cycle under the control of GAPDH: Cyclin B-cdk1 binding with SET reduces its kinase activity and retards the cell cycle. As an antagonistic factor, GAPDH interacts with the carboxyl-terminal of SET and reduces its affinity with Cyclin B-cdk1 molecules (**Fig. 29 Path A**; (18)).

As an example, associated with epigenetic control, GAPDH regulates the transcription of histone H2B subunit: Histone complexes wrapping around the DNA strand influence the chromatin conformation either to be more compact (heterochromatin) or more loosely bound (euchromatin). Post-translational modifications imposed on histones, such as methylation and acetylation, crucially determine the resulting conformation of the resulting chromatin structure. It is through these histone modifications that genes with identical genetic content and arrangements can be expressed differently under differing conditions. Epigenetically-regulated gene expression is crucial to any number of critical cellular functions; in spermigenesis (19), embryogenesis (20), tumorigenesis (21) and, more pertinently to this writing, certain kinds of apoptotic responses. Among the various kinds of epigenetic modifications, Histone subunit H2B is known to facilitate chromatin condensation, which is one of the typical characteristics associated with an apoptotic response (22, 23). It is known, for example, that in yeast, phosphorylation of H2B serine 10

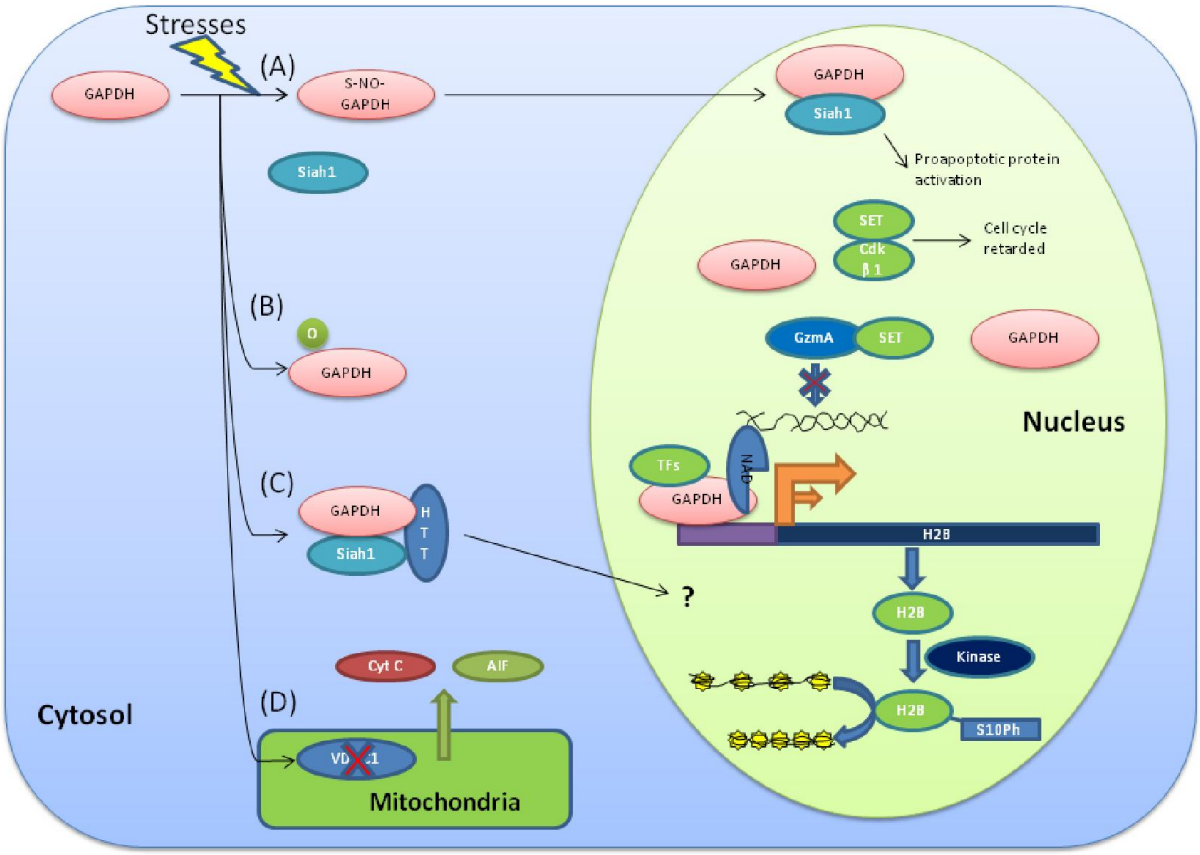

Figure 29: Summary of the pathological role of GAPDH in higher eukaryotic organisms.

GAPDH contributes cell death mechanism by multiple aspects. **(A)** In nucleus, GAPDH facilitates the stabilization and nuclear transportation of Siah1, which is required for proapoptotic protein activation(27, 28). Moreover, the co-transportation of Huntingtin with GAPDH-Siah1 is found in patients with Huntington Disease **(C)** (29). GAPDH may involve in cell cycle regulation by competing cyclin B-cdk1 with SET protein (18); as a result, the cell cycle is accelerated. GAPDH can also interact with the carboxyl-terminal of SET (18) , which may cause the release of Granzyme A (GzmA) from SET protein and induces the DNA fragmentation. Epigenetically, GAPDH is one of transcriptional factors of Histone 2B (25), which is known to condense the chromatin structural and lead to apoptosis even without any stimuli (24). **(B)** In cytosol, GAPDH is a prevalent target for oxidative attack upon stress, which consequently leads to the fragmentation of itself (6). **(D)** Furthermore, GAPDH influences the mitochondria permeability by interacting with voltage-dependent anion channel (VDAC1) and lowering the potential of mitochondrial inner membrane. Eventually, it increases the membrane permeability and causes the release of two apoptotic factors: Cytochrome c and Apoptosis-Inducing Factor (AIF) (30).

(H2BS10Ph) is essential for triggering chromatin condensation and apoptosis. Permanent and irreversible H2BS10 phosphorylation induces apoptosis, even without any additional stimuli, while dephosphorylation H2BS10 due to apoptosis is shown to inhibit the apoptotic response (24). H2B transcription is specifically activated by the gene, OCA-1 and an unknown factor called "OCA-S" which was first found in HeLa cells during S-phase, and was eventually identified as being GAPDH by MALDI-TOF peptide sequencing (25). The crucial role of GAPDH in regulating the H2B transcription machinery was confirmed by showing the physical interaction between OCA-S and the H2B promoter **(Fig. 29 Path A)** (25). GAPDH is also known to induce the expression of H2B in *in vitro* transcription assay in a dose-dependent manner. Interestingly, the GAPDH binding affinity with H2B transcription apparatus is influenced by the redox status, that is, the ratio between NAD^+ and NADH influences H2B expression (25). In another case, GAPDH has been shown to compete with NAD^+ for binding to the Sir2 protein, which is a histone H4 deacetyltransferase (H4 HDAC), and which potentially participates in the apoptotic response by using NAD^+ as a cofactor (26). NAD^+ is also a cofactor of glycolytic GAPDH activity and the apoptotic cells have been shown to preserve higher levels of oxidative stress (10). It provides a potential trigger mechanism, suggesting that GAPDH plays both a redox sensory role, as well as a trigger for the apoptotic response to heavy metals, possibly by inducing the H2B expression.

Thus, nuclear GAPDH has been reported to mediate multiple cellular responses as described above. Even though Tdh3p is only one of three isozymes of GAPDH in budding yeast, it is a specific target for oxidation and is altered in its conformation and in the proteins it associates with upon metal-induced stress. As a result, it would be interesting to determine some

of the physical parameters of the metal-induced nuclear trans-localization of Tdh3p, and potentially, the biological role of nuclear GAPDH in metal-induced apoptotic yeast cells.

Until recently, autophagy has been considered to serve merely a protective mechanism, effectively maintaining cellular homeostasis by the organized, non-specifically removal of unwanted components such as cellular wastes or redundant (or damaged) organelles. Evidence is mounting, however, which suggests that autophagy is not only specific for its targeting activity (31, 32), but is also related to the cell death mechanisms (33-36). This laboratory has been focusing on the relationship between autophagy and heavy metal-induced apoptosis in yeast cells because of the residual caspase-like activity that were found in *yca1* Δ mutant. We further inferred that Yca1p might not be the only cysteine protease harboring caspase activities in *S. cerevisiae*. In patterning the putative peptide sequences conservation of the catalytic dyad, Atg4p was considered as one of the few caspase-like candidates in the cell. This character was confirmed by showing further decreased pan-caspase-like activity in *yca1*Δ*atg4*Δ double mutant, and the absence of any cleaved Yca1p in *atg4*Δ mutant (37). These findings implicated the pleiotropic role of Atg4p in functioning beyond that of its defined cysteine proteolytic activity facilitating solely in the initial step of autophagy. Atg4p may act as another caspase, and even more, it potentiates the cleavage of Yca1p. Even so, cloned Atg4p, when expressed from either *E. coli* or *S. cerevisiae* exhibited neither caspase-like activity nor Yca1p cleavage potential (Chapter 3). Moreover, other two autophagy initiation proteins, Atg6p and Atg8p, were also shown to be necessary for any cleavage of Yca1to occur. While neither Atg6p nor Atg8p exhibit any detectable protease activities *per se*, we would suggest that they are critically involved in the process, perhaps providing a suitable environment for the Atg4p to switch between its autophagic role in cleaving Atg8 and its involvement in activation of Yca1. It was firstly inspired by

recognizing the insolubility of Yca1p, that is, *S. cerevisiae* expressed His-Yca1p was present in cell debris instead of soluble supernatant **(Fig. 30A)**. The possibility of hexahistidine tag resulting in the insolubility was excluded since the native Yca1p in *S. cerevisiae* is insoluble as well (data not shown). Yca1p molecule was absent until DTT and Tween-20 were introduced. Since Yca1p presented dramatically by introducing these two additional factors, it is interesting to know either NP-40 or DTT contribute to the Yca1 solubility. By adding NP-40 alone, Yca1 was able to be released from cell lysate **(Fig. 30B.)**. Furthermore, Yca1p, no matter if pro- or cleaved form, showed different solubility upon different concentration of NP-40 in lysis buffer. This phenomenon indicates that the Yca1p solubility may be a secondary mechanism in regulating Yca1p activities. Thus, until it is converted into a soluble form, cleaved-Yca1p cannot play its role as an executor caspase. These findings also hint that the process of Yca1p cleavage may be occurring in cell vacuoles, an insoluble cell fraction. This would explain why the mild buffers that were used, such as lysis-buffer without detergent (NP-40), were unable to dissolve Yca1p from the lysate. It also further solidifies our newly defined hypothesis that autophagic activity is required for Yca1p activation, in other words, Yca1p may be processed by other, unknown proteases in autophagosomes.

In this study, we have established the pleiotropic role that autophagy plays in cell fate decision, which is mainly determined by the temporal initiation of autophagic and apoptotic events (Chapter 3). The more delicate classification can be clearly understood by referencing potential levels of crosstalk between autophagy and apoptosis that pertain to yeast, according to

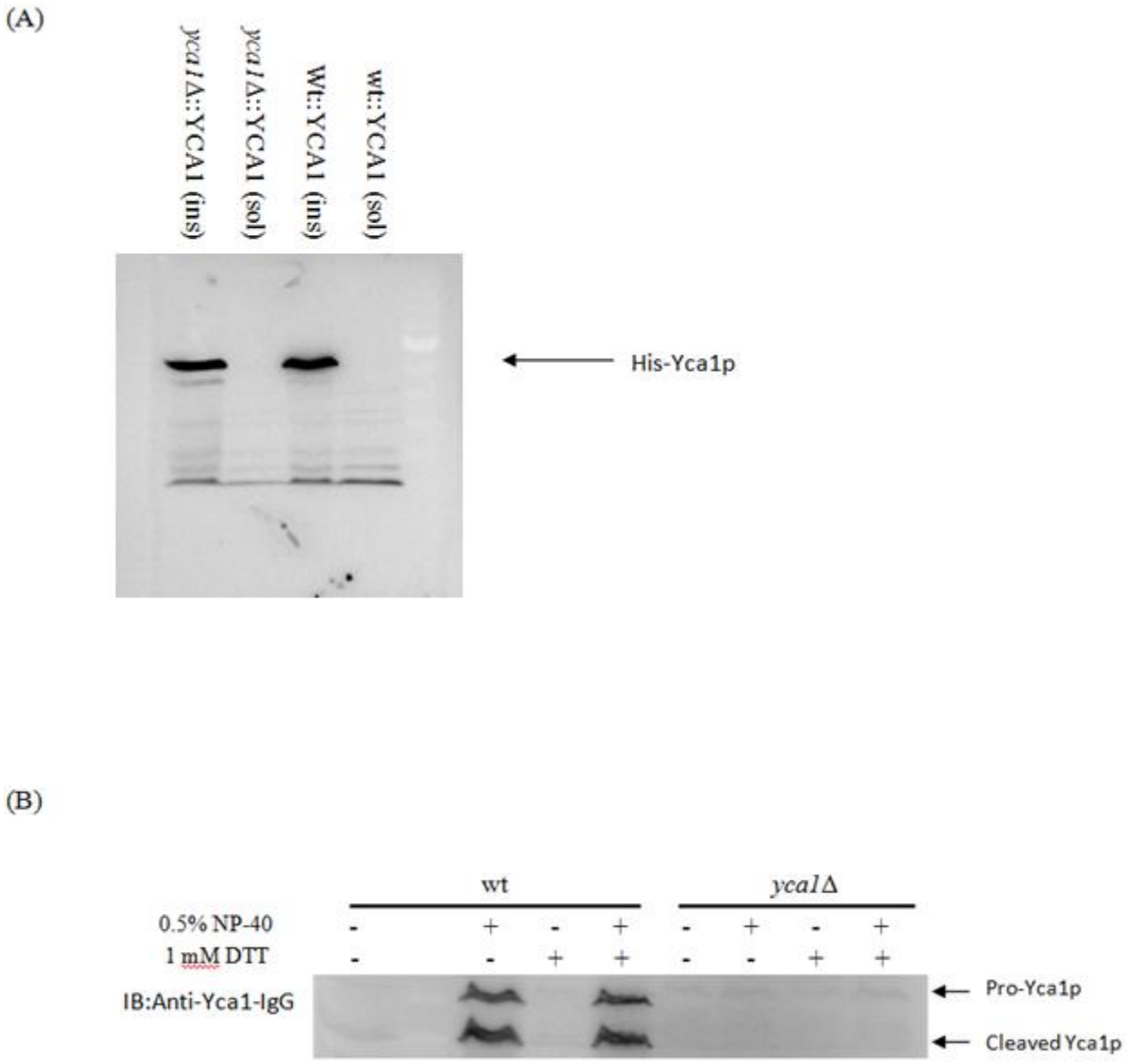

Figure 30: The insoluble character of Yca1p.

(A) Yeast-expressed His-Yca1 is insoluble. pYES2-NT.A::YCA1 was transform to wild type (wt) or *yca1*Δ host, induced by 2% galactose for 16 hours, and lysed by lysis buffer containing 2% Triton X-100. The soluble (sol) and insoluble (ins) fraction were harvested, and Western blot probed by anti-Xpress antibody was performed. **(B)** Wild type and *yca1*Δ cells were treated by 30 μM cadmium for 1 hour, following by 3 hours post-incubation. The cells were lysed by lysis buffer containing DTT, NP-40 or both.

the various potential interactive scenarios proposed by (34) and shown in **Figure 31**. In the simplest case, the cellular triggers for apoptosis, autophagy and necrosis are entirely exclusive of each other (**Fig. 31A**). Alternatively, as outlined in **Fig. 31B**, autophagy facilitates caspase-independent cell death (or Type-II cell death) by selectively degrading catalase (31), which results in diminished ROS removal from the cell, or depletion of the ATP pool as a result of DNA double strand break (38). A binary fate, without triggering environmental stress response (ESR), which is caused by exposing the cells to high dosage of stress factors, cells adapt to the environmental stress by autophagy as a homeostasis keeper while autophagic deficiencies are unfavorable to cell survival. In the more complicated scenario (**Fig. 31C**), autophagy and apoptosis can be triggered simultaneously and a number of levels cross-talk potentially exist between each other to decide the ultimate fate of the cell (**Fig. 31D**). For instance, human Beclin-1, which is a yeast Atg6p ortholog participating at the initiation step of autophagy, harbors pro-apoptotic BH3 domain. The caspase-mediated cleavage of Beclin-1 results in the exposure of BH3 domain and is favorable to trigger mitochondria-dependent apoptotic response rather than its original role to facilitate autophagy (39-41). In the opposite case, a synergistic example commonly happens in embryogenesis, where autophagic activities help to keep high level of ATP pool to ensure the sufficient removal of apoptotic cells (42).

extent, the heterogeneity of the apoptotic response within the population

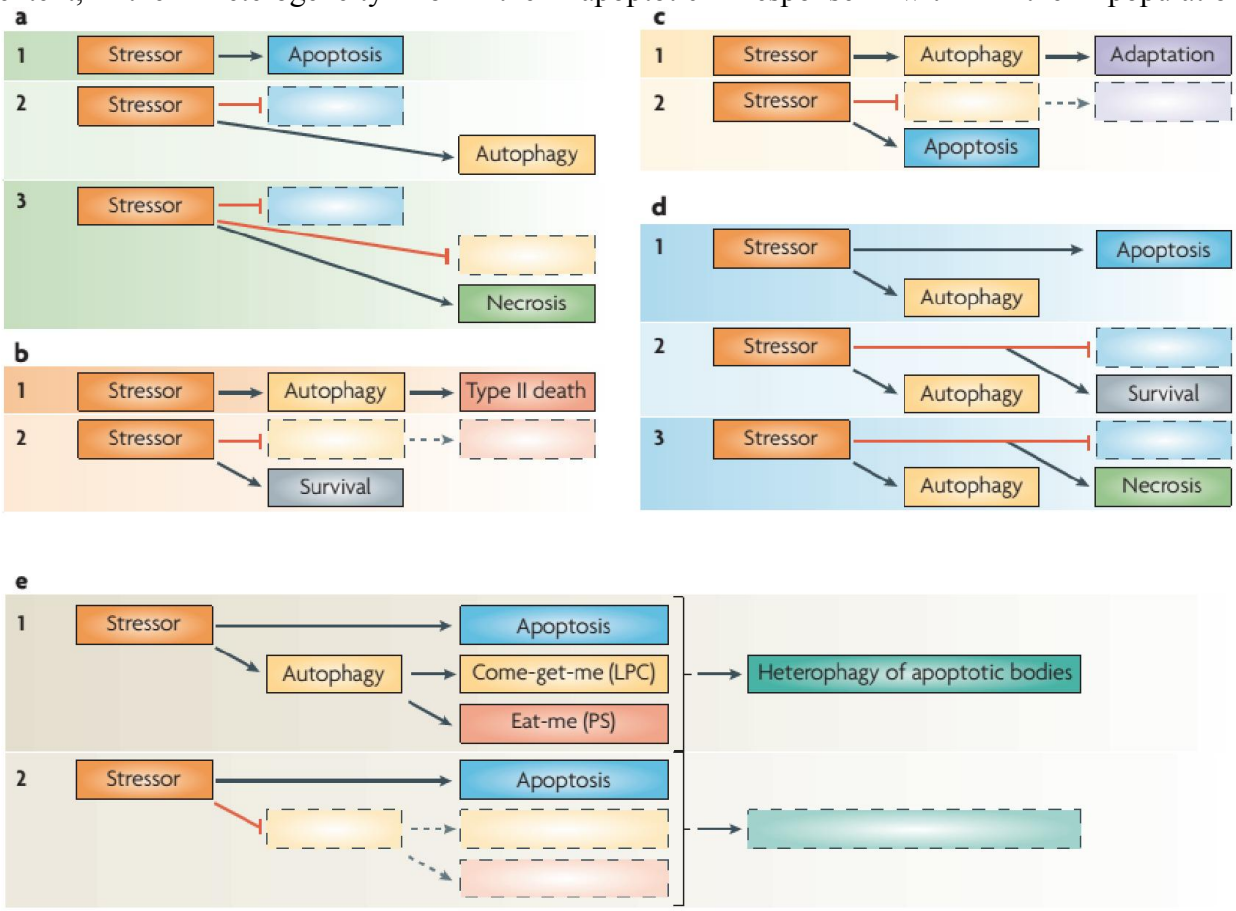

Figure 31: The cell fate decision mediated by the interconnection between apoptosis and autophagy (34).

(A) Apoptosis, autophagy or necrosis happens independently upon the stimulation of stressor. **(B)** Autophagy facilitates Type-II Cell Death, whereas other stimuli impede this death mechanism and promote the cell survival. **(C)** The classical role of autophagy helping cells to adapt to the environmental stress such as nutrient deprivation, and the depletion of this adaption consequently leads to apoptosis. **(D)** The complicated event which apoptosis and autophagy happen simultaneously, and the cell fate is decided by the pleiotypic role of autophagy. **(E)** Autophagy facilitates the clearance of apoptotic cells via the presentation of lysophosphatidylcholine (LPC) or phosphatidylserine) , which recruits the phagocytotic cells in situ.

Lastly, autophagy facilitates the presentation of lipopolysaccharide (LPS) and phosphatidylserine (PS) on the surface of cells, which are inclined to be eliminated through macrophagy (**Fig. 31E**). Upon the classification described above, yeast cells exposed to low levels of Cd behave in a similar fashion to the generic cells in the scenario presented in **Fig 31C**, which explains, to some of cells as only a small proportion of cells commit suicide, while the majority adapt to the Cd-induced stress. The cellular responses defined by **Fig. 31D** provide an additional explanation as to how cells are able to toward either autophagy (due to rapamycin) or possible apoptosis (due to their concomitant exposure to heavy metal stressors). In general, the role of autophagy as a "life saver" or "killer" is highly dependent on several factors, including the cell type, stressors, and the sequence of induction, which is introduced in this study (**Fig. 32**). No matter its duplicitous role, our study has shown reaffirmed our preliminary findings that autophagy is essential for any apoptotic response in metal-induced stress in yeast cells.

A more in-depth determination as to the mechanism(s) involved in the apparent crosstalk between apoptosis and autophagy would be the next stage of investigation. Moreover, given the nature of the two response pathways and how they are triggered what is the role do mitochondria play in such cross-talk. At the nucleation step, human Atg5, followed by LC3 (a yeast Atg8p orthologue) deposited on the outer mitochondrial membrane significantly suggests the involvement of mitochondria in the biogenesis of the autophagosomes (43). Mitochondria are also the nexus, which centralizes many of the apoptotic responses (**General Introduction, Fig. 1)** in a number of cells. In the most fundamental of responses, accumulation of ROS triggers the membrane depolarization, release of cytochrome *c* and initiation of the apoptotic cascade. Further, during the stress, impaired or hyperpermeable mitochondria are removed by mitophagy,

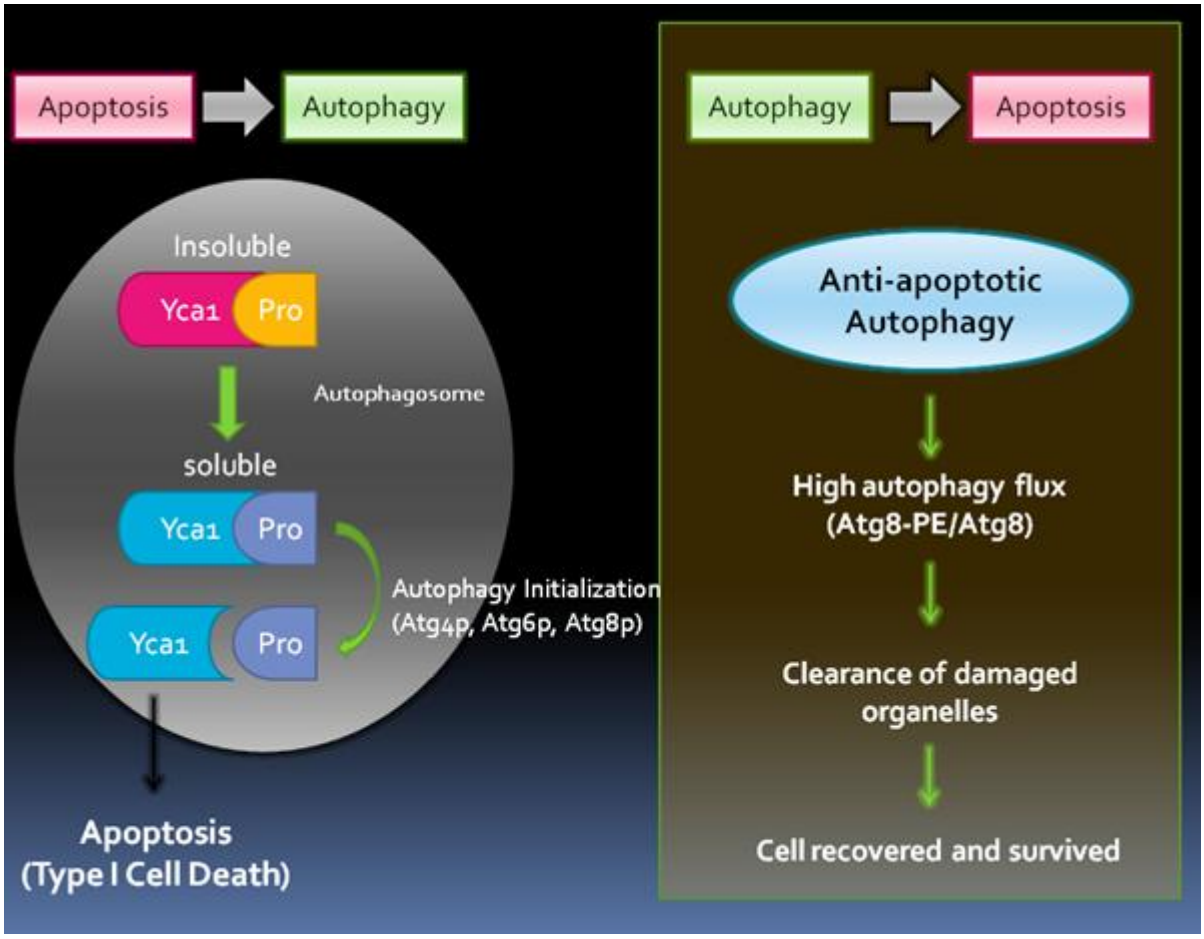

Figure 32: Proposed model of the autophagy-associated cell fate decision in heavy metal-induced apoptotic yeast cells.

The fate of metal-stressed cells is decided by the occurrence order of autophagy and apoptosis. In the scenario where apoptosis happens prior to autophagy (left), Yca1p is modified inside autophagosome, and the soluble Yca1p is able to be accessed and cleaved by other proteases. In the scenario where autophagy happens prior to apoptosis (right), autophagy plays its classical role as a adaption and survival mechanism. Augmented autophagy activity indicated by high Atg8-PE to Atg8 ratio facilitates the homeostasis in metal-stressed yeast cells, and the consequence of destruction is prevented.

a mitochondrion-specific autophagy (44-47). Given the importance of mitochondrial disintegration in apoptosis, it is possible that the mitophagic activity is directly associated with the response of cells to metal-induced apoptosis as part of a recovery mechanisms that minimizes mitochondrial damage caused by stresses. Any integral relationship between these two pathways could potentially focus on Uth1p, a mitochondrial membrane protein, which is considered to be necessary for the mitophagic response (32) and the removal of damaged mitochondria, which is abolished in *uth1*Δ mutant. These findings would indicate that a *uth1*Δ mutant would be a prime candidate for further study. Since the clearance of damaged mitochondria would be defective in these mutants, and the resulting increase in cytoplasmic cytochrome c would more likely to trigger an apoptotic cascade, this mutant strain would presumable be more prone to a concomitant apoptotic cellular response. Alternatively, mitophagy might further augment apoptotic response by disrupting the membrane integrity of mitochondria, which would promote the release of cytochrome c. In this scenario, the cytosolic cytochrome *c* would be reduced in *uth1*Δ mutant, possibly resulting in a decreased propensity for these cells to undergo apoptosis. Consequently, it would be interesting to test the difference of cytosolic cytochrome *c* concentrations between wild-type cells and *uth1*Δ mutants exposed to heavy metals, if only to confirm the likelihood of higher or lower concentrations of cytosolic cytochrome *c* resulting from the *uth1*Δ mutation and the role(s) such concentration variables might play in promoting different cellular responses.

In addition to the determination of a number of significant cellular responses within cells undergoing autophagy and metal-induced stress response, this report also includes the practical development of a technique that proved to be highly useful in detecting the progression of

autophagy in cell populations. Until now, the ratio between lipidized Atg8 (Atg8-PE) to Atg8, performed by immunoblot, presented the "gold standard" to monitor any progression in autophagic flux (48, 49). As indicated in a preceding chapter, the simpler and faster assays based on staining techniques have dubious levels of specificity (50, 51) and while the EM-based imaging assay might provide the most direct evidence of the appearance of autophagosome, the use of this technique is sufficiently constrained by the high degree of difficulty required to carry it out. We have been able to circumvent the failings of both techniques in measuring the ongoing process of autophagic flux by employing simple cytometric profiles to characterize some of the specific heterogenous attributes of cellular responses to the developing autophagosomes. This inherent cytometric heterogeneity of cells undergoing autophagy has been shown to relate well to cellular changes in cells undergoing an autophagic response. As such, in analyzing this process, we were able to reference this cytometry-based technique with the traditional Atg8p-probed immunoblot along with the samples that utilize other, different treatments (**Chapter 2**), and were able to promote its use over these techniques for certain experimental endeavours. Even so, as with many new protocols, the importance of using positive/negative controls was obviated to avoid making any false interpretations.

In summary, this study has been able to identify and analyze some of the cellular events that occur within budding yeast in response to the presence of heavy metals, including; an enhanced contribution made by Tdh3p and a more complex interplay between two of the major cellular response pathways in *S. cerevisiae* -namely, Autophagy and Apoptosis. The study has also outlined the development of a simple method to measure the autophagic flux in yeast cells using flow cytometry, which has proven to be highly reliable in the routine analysis of cellular

activities. In conclusion, the results put forward in this dissertation have proven to be significant in studies of some of the mechanisms that underlie metal-induced toxicity in yeast. As such, they may also prove to be important in our more general understanding of the harmful effects of heavy metal exposure in humans, associated with several chronic diseases, and as a result, costing enormous social resource for medical treatments (52).

References

1. Scoullos MJ (2001) *Mercury, cadmium, lead : handbook for sustainable heavy metals policy and regulation* (Kluwer Academic Publishers, Dordrecht ; Boston) pp xviii, 525 p.

2. Aleksandrowicz J, Dobrowolski JW, Balechala P, & Lisiewicz J (1982) Monitoring trace elements in cells from the blood of patients with acute myeloblastic, chronic lymphocytic and chronic granulocytic leukemia. *Haematologica* 67(3):437-441.

3. Danford DE, Smith JC, Jr., & Huber AM (1982) Pica and mineral status in the mentally retarded. *Am J Clin Nutr* 35(5):958-967.

4. Penny WJ*, et al.* (1983) Relationship between trace elements, sugar consumption, and taste in Crohn's disease. *Gut* 24(4):288-292.

5. Rieder HP, Schoettli G, & Seiler H (1983) Trace elements in whole blood of multiple sclerosis. *Eur Neurol* 22(2):85-92.

6. Shanmuganathan A, Avery SV, Willetts SA, & Houghton JE (2004) Copper-induced oxidative stress in Saccharomyces cerevisiae targets enzymes of the glycolytic pathway. *FEBS letters* 556(1-3):253-259.

7. Gasch AP*, et al.* (2000) Genomic expression programs in the response of yeast cells to environmental changes. *Molecular biology of the cell* 11(12):4241-4257.

8. Shenton D*, et al.* (2006) Global translational responses to oxidative stress impact upon multiple levels of protein synthesis. *The Journal of biological chemistry* 281(39):29011-29021.

9. Smirnova JB*, et al.* (2005) Global gene expression profiling reveals widespread yet distinctive translational responses to different eukaryotic translation initiation factor 2B-targeting stress pathways. *Molecular and cellular biology* 25(21):9340-9349.

10. Nargund AM, Avery SV, & Houghton JE (2008) Cadmium induces a heterogeneous and caspase-dependent apoptotic response in Saccharomyces cerevisiae. *Apoptosis : an international journal on programmed cell death* 13(6):811-821.

11. Shanmuganathan A (2008) An analysis of glycolytic enzymes in the cellular response of metal toxicity. Doctor of Philosophy (Georgia State University).

12. Danial NN*, et al.* (2003) BAD and glucokinase reside in a mitochondrial complex that integrates glycolysis and apoptosis. *Nature* 424(6951):952-956.

13. Boucherie H, Bataille N, Fitch IT, Perrot M, & Tuite MF (1995) Differential synthesis of glyceraldehyde-3-phosphate dehydrogenase polypeptides in stressed yeast cells. *FEMS microbiology letters* 125(2-3):127-133.

14. Mujtaba S*, et al.* (2008) Epigenetic transcriptional repression of cellular genes by a viral SET protein. *Nat Cell Biol* 10(9):1114-1122.

15. Fan Z, Beresford PJ, Oh DY, Zhang D, & Lieberman J (2003) Tumor suppressor NM23-H1 is a granzyme A-activated DNase during CTL-mediated apoptosis, and the nucleosome assembly protein SET is its inhibitor. *Cell* 112(5):659-672.

16. Fan Z, Beresford PJ, Zhang D, & Lieberman J (2002) HMG2 interacts with the nucleosome assembly protein SET and is a target of the cytotoxic T-lymphocyte protease granzyme A. *Molecular and cellular biology* 22(8):2810-2820.

17. Yamada M, Hirasawa A, Shiojima S, & Tsujimoto G (2003) Granzyme A mediates glucocorticoid-induced apoptosis in leukemia cells. *FASEB journal : official publication of the Federation of American Societies for Experimental Biology* 17(12):1712-1714.

18. Carujo S*, et al.* (2006) Glyceraldehyde 3-phosphate dehydrogenase is a SET-binding protein and regulates cyclin B-cdk1 activity. *Oncogene* 25(29):4033-4042.

19. Rathke C*, et al.* (2007) Transition from a nucleosome-based to a protamine-based chromatin configuration during spermiogenesis in Drosophila. *Journal of cell science* 120(Pt 9):1689-1700.

20. Liu JH*, et al.* (2008) Diploid parthenogenetic embryos adopt a maternal-type methylation pattern on both sets of maternal chromosomes. *Genomics* 91(2):121-128.

21. Bloushtain-Qimron N*, et al.* (2008) Cell type-specific DNA methylation patterns in the human breast. *Proc Natl Acad Sci U S A* 105(37):14076-14081.

22. Ahn SH*, et al.* (2005) Sterile 20 kinase phosphorylates histone H2B at serine 10 during hydrogen peroxide-induced apoptosis in S. cerevisiae. *Cell* 120(1):25-36.

23. Cheung WL*, et al.* (2003) Apoptotic phosphorylation of histone H2B is mediated by mammalian sterile twenty kinase. *Cell* 113(4):507-517.

24. Ahn SH, Diaz RL, Grunstein M, & Allis CD (2006) Histone H2B deacetylation at lysine 11 is required for yeast apoptosis induced by phosphorylation of H2B at serine 10. *Mol Cell* 24(2):211-220.

25. Zheng L, Roeder RG, & Luo Y (2003) S phase activation of the histone H2B promoter by OCA-S, a coactivator complex that contains GAPDH as a key component. *Cell* 114(2):255-266.

26. Matecic M, Stuart S, & Holmes SG (2002) SIR2-induced inviability is suppressed by histone H4 overexpression. *Genetics* 162(2):973-976.

27. Almeida B*, et al.* (2007) NO-mediated apoptosis in yeast. *Journal of cell science* 120(Pt 18):3279-3288.

28. Hara MR*, et al.* (2005) S-nitrosylated GAPDH initiates apoptotic cell death by nuclear translocation following Siah1 binding. *Nat Cell Biol* 7(7):665-674.

29. Bae BI*, et al.* (2006) Mutant huntingtin: nuclear translocation and cytotoxicity mediated by GAPDH. *Proc Natl Acad Sci U S A* 103(9):3405-3409.

30. Tarze A*, et al.* (2007) GAPDH, a novel regulator of the pro-apoptotic mitochondrial membrane permeabilization. *Oncogene* 26(18):2606-2620.

31. Kim I, Rodriguez-Enriquez S, & Lemasters JJ (2007) Selective degradation of mitochondria by mitophagy. *Archives of biochemistry and biophysics* 462(2):245-253.

32. Kissova I, Deffieu M, Manon S, & Camougrand N (2004) Uth1p is involved in the autophagic degradation of mitochondria. *The Journal of biological chemistry* 279(37):39068-39074.

33. Giansanti V, Torriglia A, & Scovassi AI (2011) Conversation between apoptosis and autophagy: "Is it your turn or mine?". *Apoptosis : an international journal on programmed cell death* 16(4):321-333.

34. Maiuri MC, Zalckvar E, Kimchi A, & Kroemer G (2007) Self-eating and self-killing: crosstalk between autophagy and apoptosis. *Nature reviews. Molecular cell biology* 8(9):741-752.

35. Xue L, Fletcher GC, & Tolkovsky AM (1999) Autophagy is activated by apoptotic signalling in sympathetic neurons: an alternative mechanism of death execution. *Molecular and cellular neurosciences* 14(3):180-198.

36. Zhang M*, et al.* (2012) Autophagy and apoptosis act as partners to induce germ cell death after heat stress in mice. *PloS one* 7(7):e41412.

37. Nargund AM (2010) Mechanism(s) of Metal-induced Apoptosis in Saccharomyces cerevisiae. Doctor of Philosophy (Georgia State University).

38. Xu Y, Kim SO, Li Y, & Han J (2006) Autophagy contributes to caspase-independent macrophage cell death. *The Journal of biological chemistry* 281(28):19179-19187.

39. Djavaheri-Mergny M, Maiuri MC, & Kroemer G (2010) Cross talk between apoptosis and autophagy by caspase-mediated cleavage of Beclin 1. *Oncogene* 29(12):1717-1719.

40. Maiuri MC, Criollo A, & Kroemer G (2010) Crosstalk between apoptosis and autophagy within the Beclin 1 interactome. *EMBO J* 29(3):515-516.

41. Wirawan E*, et al.* (2010) Caspase-mediated cleavage of Beclin-1 inactivates Beclin-1-induced autophagy and enhances apoptosis by promoting the release of proapoptotic factors from mitochondria. *Cell death & disease* 1:e18.

42. Qu X*, et al.* (2007) Autophagy gene-dependent clearance of apoptotic cells during embryonic development. *Cell* 128(5):931-946.

43. Hailey DW*, et al.* (2010) Mitochondria supply membranes for autophagosome biogenesis during starvation. *Cell* 141(4):656-667.

44. Abeliovich H & Klionsky DJ (2001) Autophagy in yeast: mechanistic insights and physiological function. *Microbiol Mol Biol Rev* 65(3):463-479, table of contents.

45. Elmore SP, Qian T, Grissom SF, & Lemasters JJ (2001) The mitochondrial permeability transition initiates autophagy in rat hepatocytes. *FASEB journal : official publication of the Federation of American Societies for Experimental Biology* 15(12):2286-2287.

46. Priault M*, et al.* (2005) Impairing the bioenergetic status and the biogenesis of mitochondria triggers mitophagy in yeast. *Cell death and differentiation* 12(12):1613-1621.

47. Xue L, Fletcher GC, & Tolkovsky AM (2001) Mitochondria are selectively eliminated from eukaryotic cells after blockade of caspases during apoptosis. *Curr Biol* 11(5):361-365.

48. Klionsky DJ*, et al.* (2008) Guidelines for the use and interpretation of assays for monitoring autophagy in higher eukaryotes. *Autophagy* 4(2):151-175.

49. Mizushima N (2004) Methods for monitoring autophagy. *The International Journal of Biochemistry & Cell Biology* 36(12):2491-2502.

50. Barth S, Glick D, & Macleod KF (2010) Autophagy: assays and artifacts. *J Pathol*.

51. Mizushima N, Yoshimori T, & Levine B (2010) Methods in mammalian autophagy research. *Cell* 140(3):313-326.

52. Wimo A, Jonsson L, & Winblad B (2006) An estimate of the worldwide prevalence and direct costs of dementia in 2003. *Dement Geriatr Cogn Disord* 21(3):175-181.

APPENDICES

Appendix A: Total RNA Preparation, Reverse Transcriptase (RT) PCR and expressional microarray analysis

The 30 μM $Cd(NO_3)_2$ or 0.5 mM $Cr(NO_3)_2$ treated or untreated cells were harvested and stored at -80 ^oC prior to the mechanical disruption. Around 5 x 10^7 cells along with 500 μM acid-washed glass beads (Sigma-Aldrich) and lysis buffer (see the instruction manual in kit) were mixed, followed by being bead-disrupted for 30 seconds by mini beat beater-8 (BioSPEC Product) for 4 times with cooling on ice between each disruption. The cell lysate was applied for the total RNA purification by Qiagen RNeasy^{TM} Mini Kit followed by the manufacturer's protocol. The prepared total RNA was treated by DNase I (Qiagen) at 37 ^oC for 30 minutes to remove the genomic DNA contamination then inactivated by incubated at 65 ^oC for 10 minutes. The total RNA extract was checked by PCR technique for excluding the DNA contamination. Briefly, 2 μL total RNA was added to the PCR mixture containing 2 μL 10x PCR buffer, 1 μL 10 mM dNTP, 1 μL 30 μM forward and reverse primer for metacaspase 1 (YCA1), 0.5 μL Taq polymerase (Qiagen) and 12.5 μL nuclease free water (Ambion) and followed by the thermocycling protocol: 94 ^oC for 30 seconds for denature, followed by 30 cycles of 30 seconds at 94 ^oC, 30 seconds at 55 ^oC and 1 minute at 72 ^oC. The reaction mixture was then incubated at 72 ^oC for 10 minutes, and stored at 4^oC. The amplicon was applied to 2.5 % (w/v) agarose gel. The *Saccharomyces cerevisiae* BY4741 genomic DNA was served as the positive control in PCR reaction.

The transcriptional level of metacaspase 1 (Yca1) was investigated by RT-PCR technique using β-actin as the internal control. The normalized quantity of total RNA was added to the

mixture containing forward and reverse primer for MCA1 and β-actin, nuclease free water (Ambion) and Illustra Ready-To-Go™ RT-PCR beads (GE Amersham) then subjected to the following thermocycling protocol: 42 °C for 30 minutes for reverse transcription, 95 °C for 5 minutes for denature, following by 27 cycles of 1 minute at 95 °C, 1 minute at 55 °C and 3 minutes at 72 °C. The reaction mixture was then incubated at 72 °C for 10 minutes and stored at 4°C. The amplicon was applied to 2.5% (w/v) agarose gel and the band intensity was quantified by MultiGauge™ Version 2.3 software (Fujifilm).

The Affymetrix Yeast Genome™ 2.0 Array was used to investigate the expression profile of genes in cells that were exposed to heavy metals for different amounts of time (0, 30 and 60 minutes). The procedure was undertaken according to the protocol outlined in the manual provided by Affymetrix. Briefly, the total RNA that meets the minimal requirement of the amount for target preparation was performed using the first strand cDNA synthesis by SuperScript™ RT (Life Technologies), followed by the second strand cDNA synthesis using *E. coli* DNA polymerase I (Life Technologies). The double stranded cDNA was "cleaned up" using Phase Lock Gels (PLG)-phenol/chloroform extraction and precipitated by ethanol before being re-suspended in RNase-free water (Ambion). The re-suspended cDNA was then transcribed to biotin-labeled cRNA using the RNA Transcript Labeling Kit (Affymetrix). The labeled-cRNA was purified further by 2-propanol, and upon re-suspension in RNase-free water (Ambion). The concentration was adjusted according to the manual to equate to the starting concentration of the fragmentation. The adjusted-cRNA was fragmented by 5x RNA fragmentation buffer containing 200 mM pH 8.1 Tris-acetate (Sigma-Aldrich), 500 mM potassium acetate (Sigma-Aldrich) and 150 mM magnesium acetate (Sigma-Aldrich). The cRNA fragment and 20x GeneChip™

Eukaryotic Hybridization Controls Kit (*bioB, bioC, bioD* and *cre*) (Affymetrix) was mixed and hybridized with the Yeast Genome 2.0™ Array (Affymetrix) for 16 hours. The chip was washed and stained automatically by the Fluidics Station (Affymetrix), with the fluidics program provided by Yeast Genome 2.0™ Array Manual. Finally, the chip was scanned then the raw data was processed either by GeneSpring™ GX 7.3 software (Agilent) or Office Excel™ 2007 (Microsoft) using β-actin signal intensity as the normalization baseline.

Appendix B: Data Acquisition and Comparison of cDNA Microarray Data

Two versions of yeast microarray chips with different "entries" were analyzed in this study. Some of the previous data were acquired by Amrita Nargund, Mara Maroney and Ranjith Reddy with the S98™ Yeast chip, along with data acquired in this study using the Yeast 2.0™ chip. Data acquired from the two versions of chips were made compatible through referenced to the Affymetrix™ product support website and the best matches (100%) of the probes, corresponding to various genes were chosen in order to present the most consistent results among all the data sets. The transcriptional profiles were then compared for different genes clustered in to several groups according to the gene ontology (GO). Ultimately the data were merged using Microsoft Access™ 2007 (Microsoft) using the systematic names as the primary key.

Appendix C: Quantification of GSH/GSSG

The cells were harvested in each particular time point by centrifuge at 12,000 xg, -10 ^{o}C for 2 minutes. The cell palette was washed twice by cold de-ionized water and re-suspended in 1 mL, 50 g/L metaphosphoric acid (Sigma-Aldrich). The cells were bead-disrupted for 30 seconds by mini beat beater-8 (BioSPEC Product) for 4 times with cooling on ice between each disruption. The supernatant was harvested by centrifuge at 20,000 xg, -10 ^{o}C for 5 minutes. The analytic cocktail was made by premixing 40 μL supernatant with 160 μL de-ionized water, and then subjected to P/ACE MDQ^{TM} Capillary Electrophoresis System (Beckman Coulter) for quantifying GSH/GSSG. In each assay, the capillary was filled up with Capillary Performance Sample Run Buffer A (Beckman Coulter) by 20 psi air pressure for 60 minutes, and the sample was injected into capillary by 0.5 psi pressure for 10 seconds. The sample was migrated inside the capillary under 25KV (with current around 25~29 μA) for 7 minutes. The capillary was "flushed" with 0.1N NaOH ay 10 psi pressure for 60 seconds to clean the capillary between each run. Concentrations of GSH/GSSG were determined according to the serial-diluted, GSH/GSSG standard (Sigma-Aldrich) and subsequently normalized against total protein concentrations as determined by OD280 readings.

Appendix D:

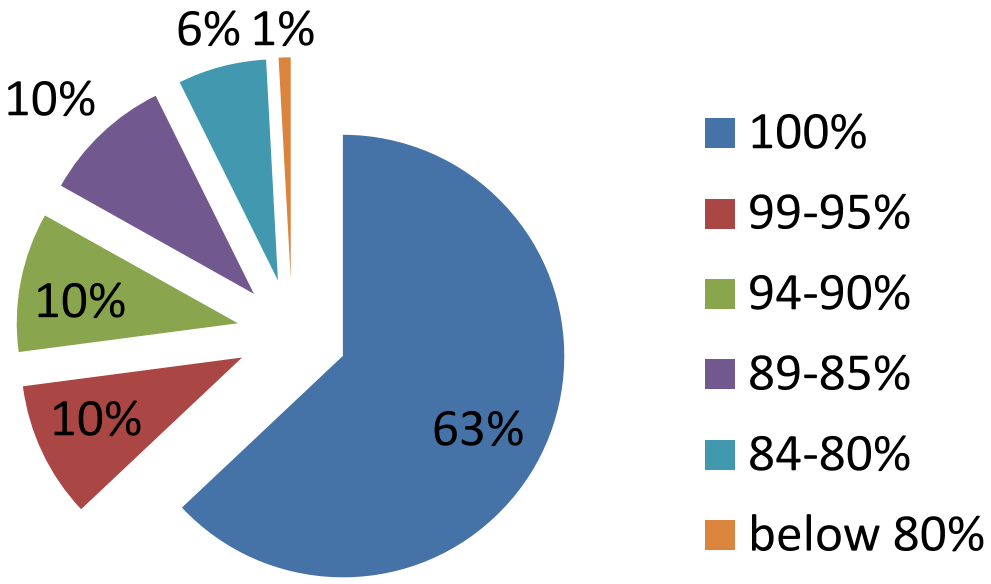

Figure 33: The probe identities between the Yeast GeneChip S98 and Version 2.0.

The identity of probe sequences between two versions of chips was compared and categorized for ensuring the compatibility between various datasets undertaken by different members of the laboratory.

Appendix E:

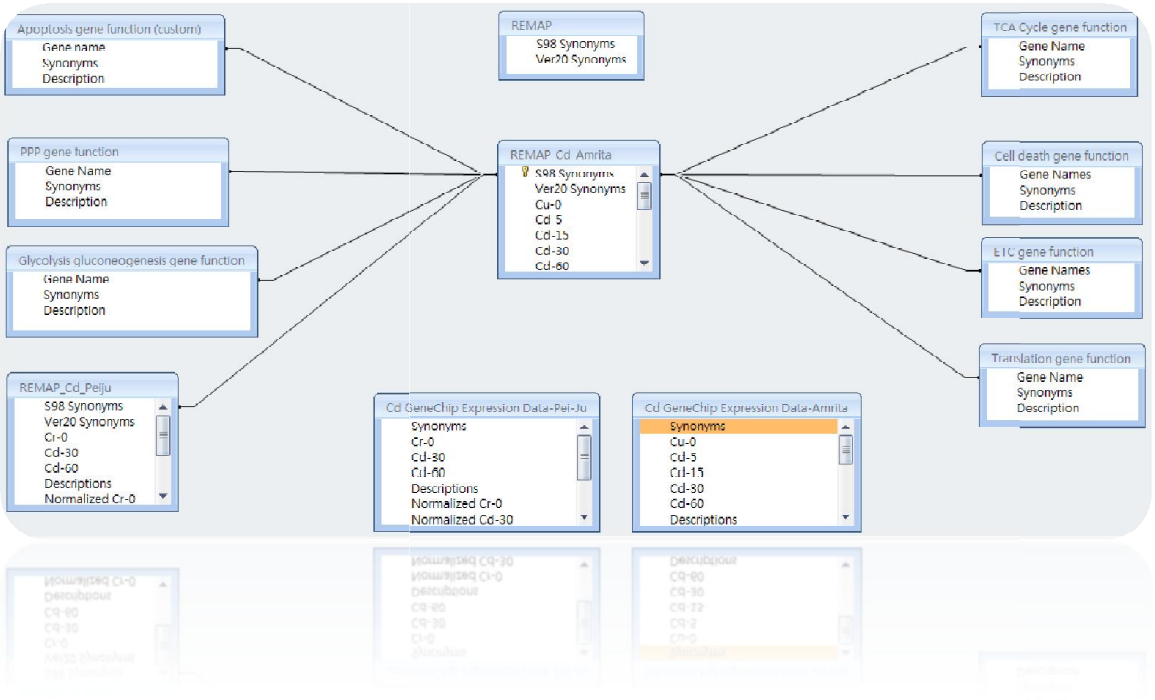

Figure 34: The conceptual data model (CDM) of the microarray database.

The conceptual data model was used for the data storage, acquisition, combination and comparison between two different versions of the yeast chip.

Appendix F:

(A)

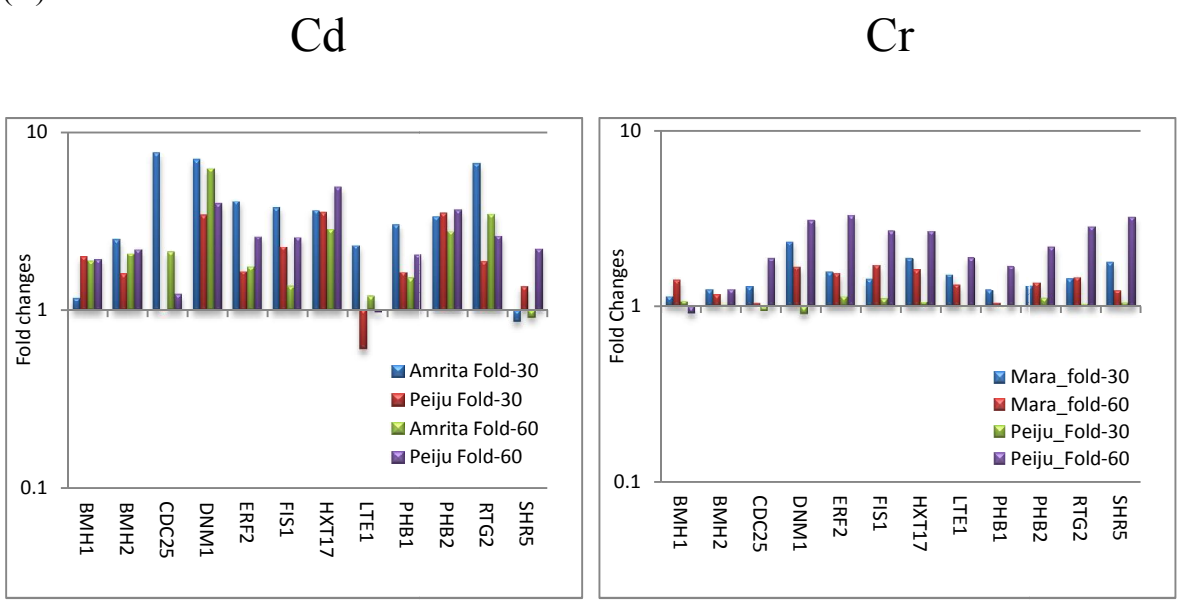

(B)

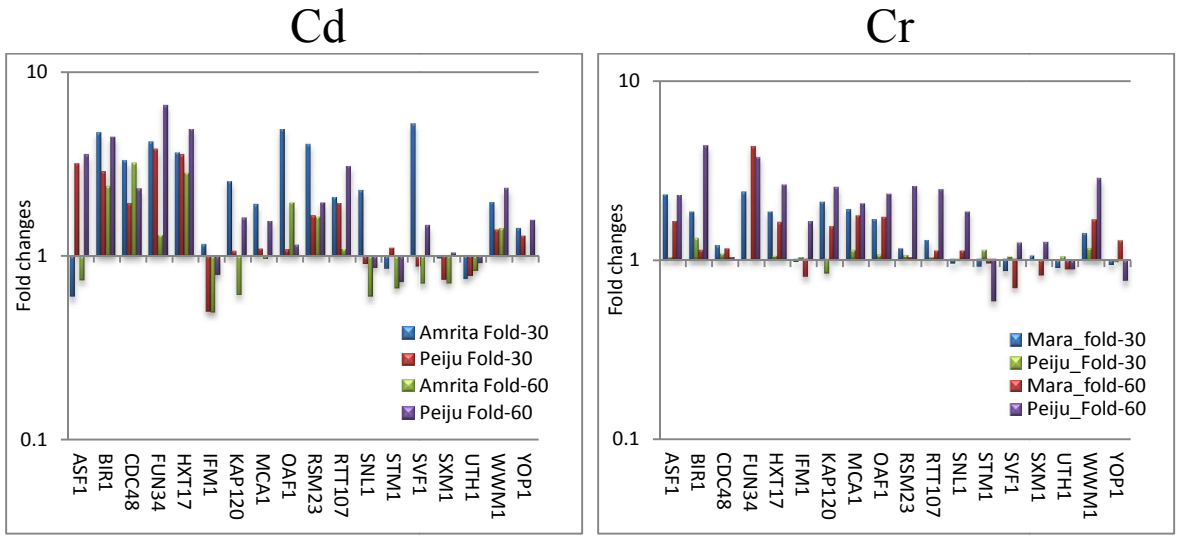

Figure 35: The fold-changes in the transcriptional expression of apoptosis and death-associated genes upon Cd and Cr exposures.

Transcriptional profiles of apoptosis **(A)** and cell death **(B)**-associated genes were displayed according to the data source (Amrita, Mara or Peiju) and the time of exposure (30 or 60 minutes)

Appendix G:

(A)

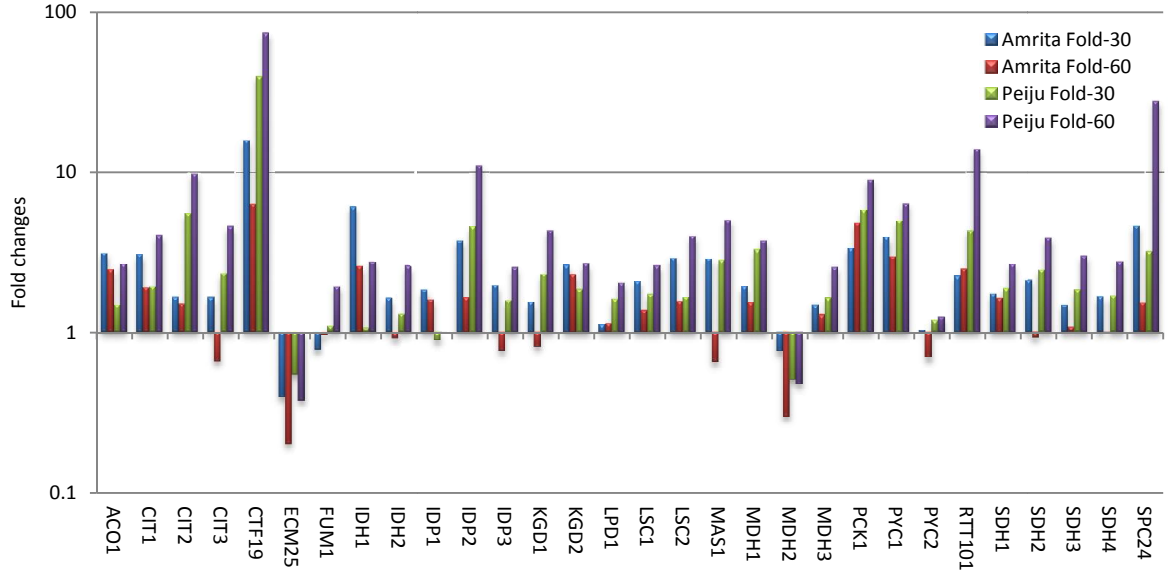

(B)

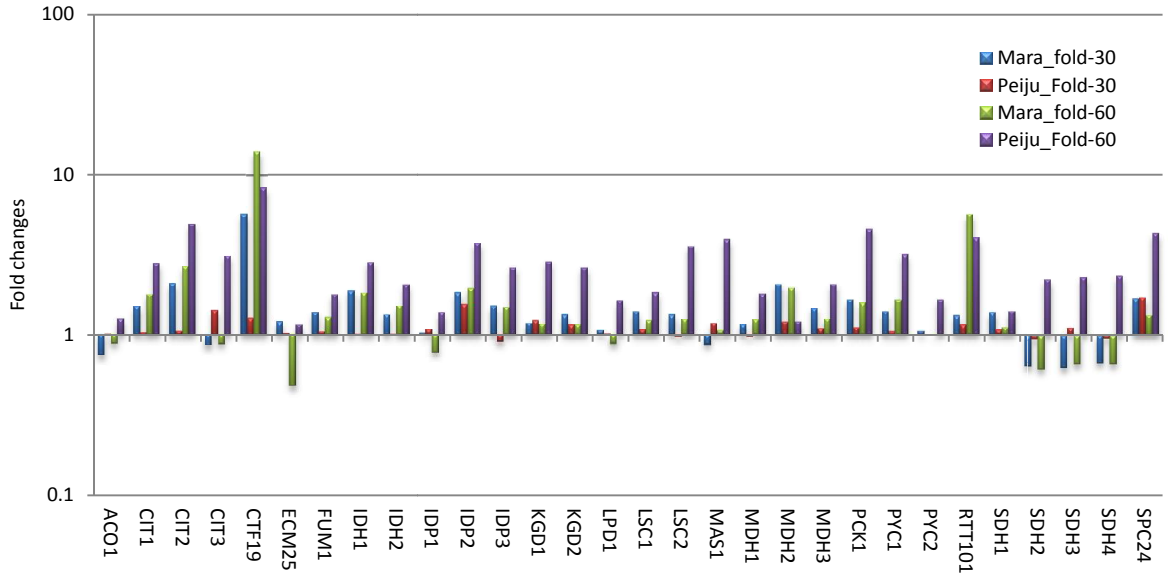

Figure 36: The transcriptional fold-change of TCA cycle-associated genes upon Cd and Cr exposures.

The transcriptional profiles of the cadmium **(A)** or chromium **(B)** exposure were displayed according to the data source (Mara or Peiju) and the time of exposure (30 or 60 minutes)

Appendix H:

(A)

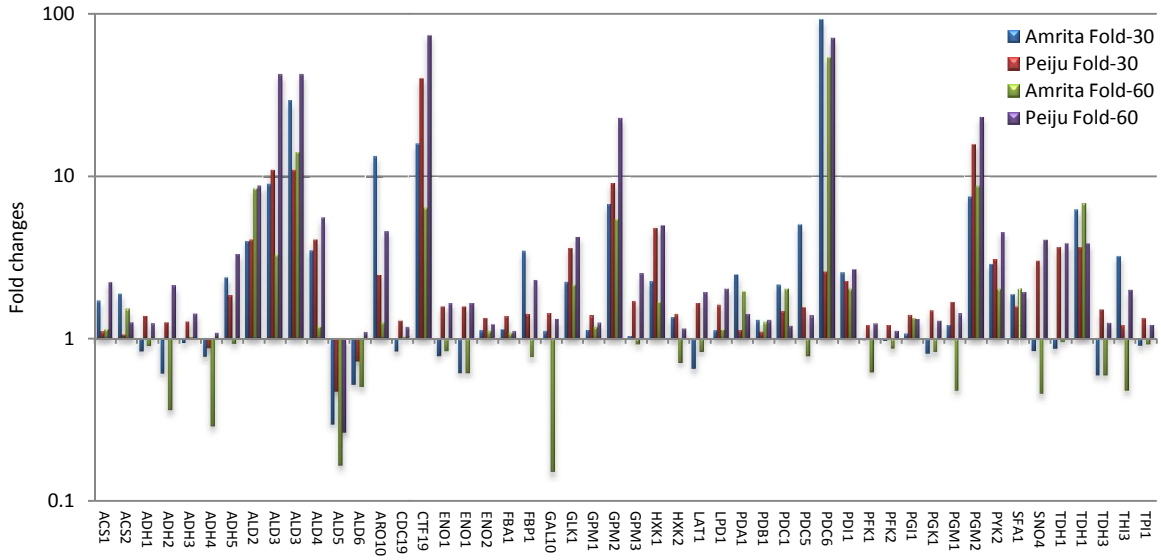

(B)

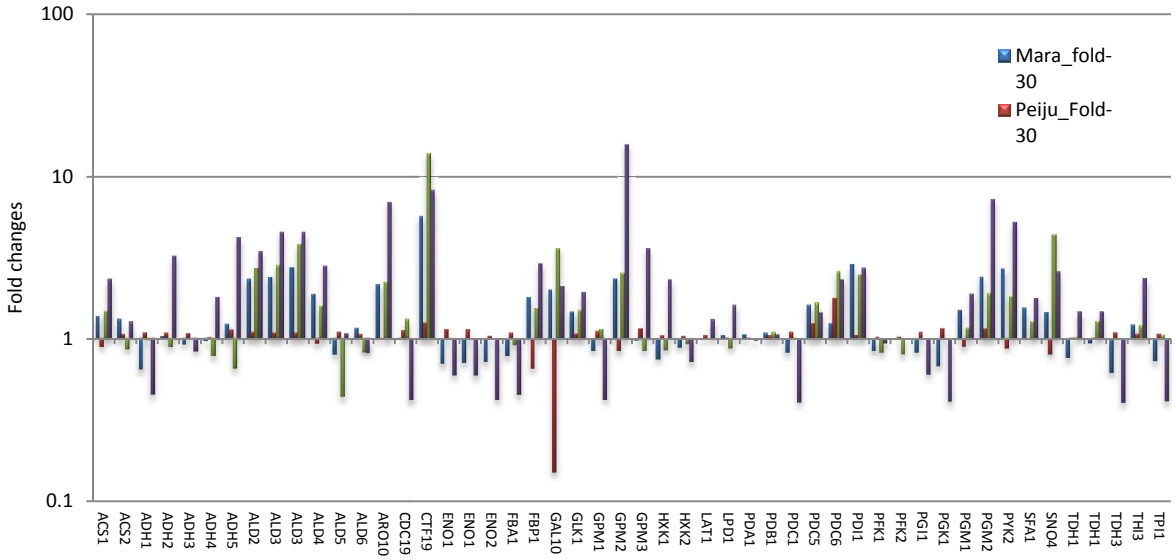

Figure 37: The transcriptional fold-change of glycolysis gluconeogenesis-associated genes upon Cd and Cr exposures.

The transcriptional profiles of the cadmium **(A)** or chromium **(B)** exposure were displayed according to the data source (Amrita, Mara or Peiju) and the time of exposure (30 or 60 minutes)

Appendix I:

(A)

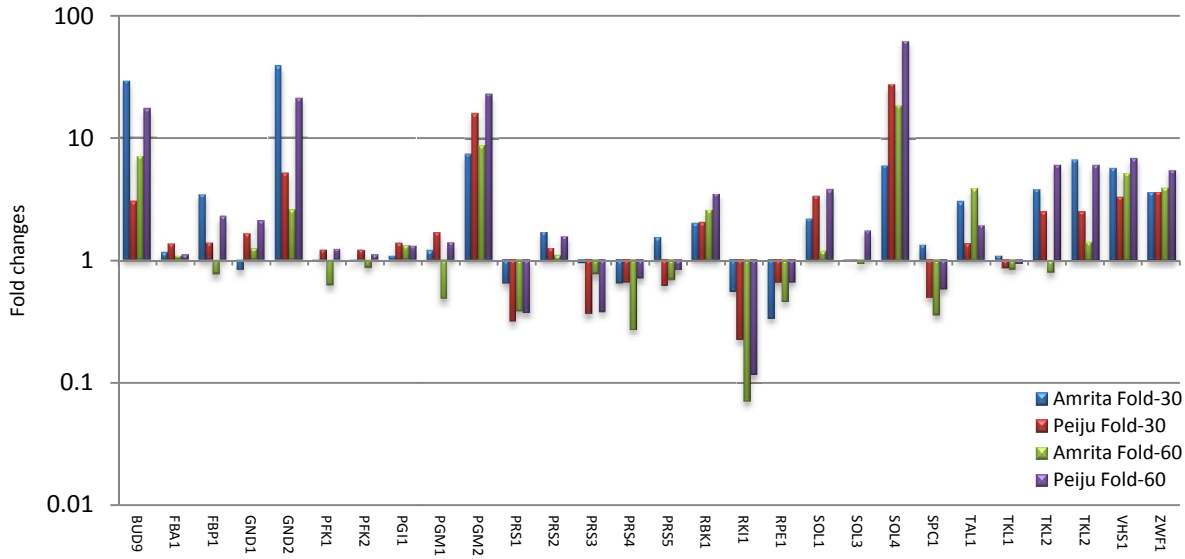

(B)

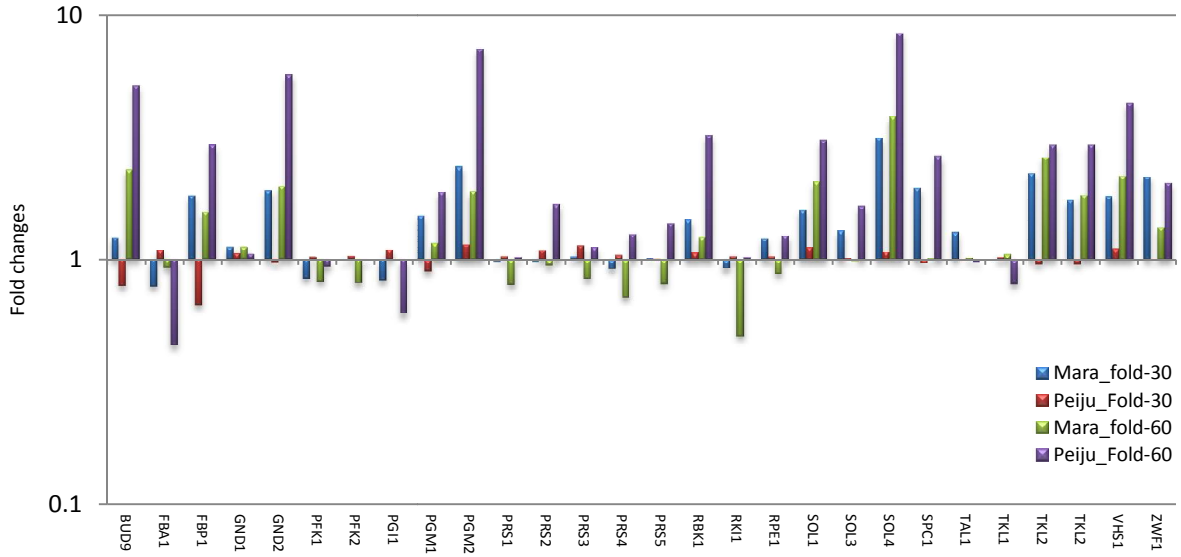

Figure 38: The transcriptional fold-change of PPP-associated genes upon Cd and Cr exposures.

The transcriptional profiles of the cadmium **(A)** or chromium **(B)** exposure were displayed according to the data source (Mara or Peiju) and the time of exposure (30 or 60 minutes)